POLITECNICO DI MILANO

Scuola di Ingegneria Industriale e dell'Informazione

Corso di Laurea Magistrale in Materials Engineering and Nanotechnology

Dipartimento di Chimica, Materiali e Ingegneria Chimica "Giulio Natta"

IN-SITU NON-DESTRUCTIVE MONITORING TECHNIQUES AND PROTECTIVE COATINGS FOR COPPER ALLOYS ARTEFACTS OF CULTURAL HERITAGE

RELATORE: Dott.ssa Sara Goidanich

CORRELATORE: Dott. Davide Gulotta

Tesi di Laurea di:

Laura Rosetti

Matricola 796440

Anno Accademico 2013 – 2014

A zio Roberto

TABLE OF THE CONTENTS

2 EXPERIMENTAL

2.1 Validation of monitoring techniques

2.1.1 Outdoor condition for copper alloys

2.1.1.1 LPR and EIS measurements

2.1.2 Indoor condition for gilded bronzes

2.2 Protective coatings for copper and bronze artefacts

2.2.1 Urban condition

2.2.2 Stressed condition, the case study of “Mi fuma il cervello (Autoritratto)” by Alighiero Boetti

2.3 Equipment

3 RESULTS AND DISCUSSION

3.1 Validation of monitoring techniques

3.1.1 Outdoor condition for copper alloys

3.1.2 Indoor condition for gilded bronzes

3.2 Protective coatings for copper and bronze artefacts

3.2.1 Urban condition

3.2.2 Stressed condition, the case study of “Mi fuma il cervello (Autoritratto)” by Alighiero Boetti

CONCLUSIONS

REFERENCES

FIGURES

TABLES

ABSTRACT

ABSTRACT

Corrosion processes are the main degradation mechanism affecting the integrity of metallic artefacts of the Cultural Heritage. They occur spontaneously when the metallic surface interacts with the atmosphere, causing the formation of visible strains, stripes and crusts.

Corrosion and conservation of historical and archaeological metal artefacts represent complex electrochemical problems, especially because the aim is to protect artefacts without altering their integrity and aesthetical appearance.

Corrosion usually leads to the formation of mineral deposits able to change the chemical properties and the surface of metals. During the period when metallic historical artefacts are exposed to atmosphere and seawater or buried in soil, a thin and compact layer, called patina, can form spontaneously on their surface; different patinas composition leads to different behavior of corrosion. Patinas not only protect the metallic substrate, but also enhance the aesthetic of art objects. Patinas are often deliberately added by artists and metalworkers. Patinas may be used to 'antique' objects, as a part of the design or decoration of art and furniture. Therefore, they should be preserved. Conservators normally use the less intrusive methods in order to maintain the original aspect of artworks and, when possible, to preserve the original patina. The use of protectives and corrosion inhibitors is one of the techniques most commonly employed to ensure long-term chemical and physical stability of the archaeological artefacts. This is because it has a reasonable cost, it is easy to apply and it can be removed for further application of the same or other products. It is not easy to find a good anti-corrosive coating that at the same time respects the strict requirements for the conservation of Cultural Heritage, first to not alter the surface. This is the reason why the perfect product has not yet been discovered. The research is still active in order to find and test advanced resistant and transparent methods of conservation.

Surface characterization methods (e.g., colour measurements, stereomicroscope, SEM) and non-destructive in-situ monitoring techniques are commonly used to obtain information about the corrosion rate and the effectiveness of applied coatings. Non-destructive in-situ monitoring methods are very important to obtain valuable information about works of art, without causing local damages to artefacts and providing reproducible measurements.

Electrochemistry offers consolidated tools for metallic surfaces monitoring, such as Linear Polarization Resistance (LPR) and Electrochemical Impedance Spectroscopy (EIS). They have been compared to gravimetric tests, to verify if they are able to estimate corrosion rate.

These traditional techniques cannot be applied on gilded bronzes. The presence of the gold/bronze galvanic couple allows the use of the macro couple current to monitor the degradation rate. This is not possible with original artefacts due to the frequent short-circuits occurring between the two metals: consequently, galvanic sensors need to be employed. They are exposed together with real gilded bronze artefacts or under different environmental conditions and provide an estimation of the corrosion rate of the process occurring on real artwork.

The present analysis intended to achieve the following goals:

- validation of LPR and EIS techniques to verify their reliability to estimate corrosion rate
- realization of improved galvanic sensors, evaluation of their ability to estimate corrosion rate and of the possibility of using them also for the monitoring of patinated, but not gilded bronzes
- evaluation of the effectiveness of protectives and corrosion inhibitors applied on quaternary bronzes in two different condition (urban condition and stressed condition), using surface characterization and electrochemical monitoring techniques.

The first part of this work allows obtaining important results about in-situ non-destructive monitoring. Electrochemical techniques (LPR and EIS) have been compared in order to assess their effectiveness and evaluate the reliability of the results in terms of polarization resistance and corrosion rate, by a comparison with mass losses. LPR and EIS cannot be applied on gilded bronzes due to the difficulties on the interpretation of results. By collecting the macro couple current flowing in the galvanic sensors, it is possible to estimate corrosion rate. Galvanic sensors confirmed to be a powerful tool for gilded bronze monitoring, giving reproducible and reliable signals. It will be possible to apply them also for non-gilded bronzes without committing a significant error.

In the second part of this work, once the monitoring techniques have been validated, electrochemical and surface characterization methods have been used to evaluate the efficiency of protective coatings and corrosion inhibitors. The work allows obtaining important information about protectives effectiveness and performances in two different condition: urban and stressed condition.

STATE OF THE ART

1.1 Copper-alloys corrosion and prevention

Copper is one of the most important metals in the history of humankind.

In prehistory, the usage of copper first and later bronze marks the transition between the Neolithic period and the first use of metals by man. Even after the coming of iron in the Iron Age, copper alloys continued to be used in different applications thanks to their unique combination of ductility, relative strength, corrosion resistance and aesthetic appearance. Besides, in the 19th century copper played a key role in enabling the electrical development because of its excellent conductivity. Even today, copper alloys constitute one of the major groups of commercial metals and are widely used in many applications (e. g., industrial machinery, building construction, electricity and electronics, coinage, medicine and decoration) (Pedeferri and Cigada 1993; Otmacic 2003; Finsgar and Milosev 2010; Brambilla 2011; Marušić, Ćurković et al. 2011; Goidanich, Gulotta et al. 2014).

Corrosion is "an irreversible interfacial reaction of a material (metal, ceramic, polymer) with its environment which results in consumption of the material or dissolution into the material of a component of the environment" according to IUPAC definition. The interaction of the metal with its environment is the basic cause of the corrosion of metallic artifacts, which leads to structural and aesthetic modifications (Pedeferri and Cigada 1993; Marušić, Ćurković et al. 2011). While corrosion of industrial metals can be expressed in economic terms, due to economic losses caused by this process, due to the cost involved in the maintenance of metallic objects or their replacement, in Cultural Heritage, every object is unique and any loss is irreplaceable.

Copper and copper alloys in humid air normally form a duplex structure of oxide layer (patina), which protects copper and its alloys from further corrosion processes. First, the inner reddish-brown patina layer, called cuprite (Cu_2O), forms and it is very adherent to the metal. This gradually oxidizes to Cu (II), producing an outer layer of cupric hydroxide in humid conditions (Finsgar and Milosev 2010). Copper corrodes at negligible rates in non-oxidizing acidic environments, since hydrogen evolution is not part of its corrosion process (copper is more noble than hydrogen evolution). On the other hand, in presence of oxygen or other oxidants such as Fe^{3+} and NO_3 ions corrosion process becomes important. Copper oxides are stable only in the pH range 8–12, but not in acidic solutions in which surface roughening can occur (Joseph, Letardi et al. 2007). In the

presence of moisture and corrosive gases (e.g., sulfur dioxide, carbon dioxide, nitrose oxides) different greenish patinas may grow, depending on the particular atmospheric conditions. For example, antlerite $Cu_3SO_4(OH)_4$ and brochantite $Cu_4SO_4(OH)_6$ are the most common compounds in sulfate-rich environments, while atacamite and/or paratacamite $Cu_2Cl(OH)_3$ are more likely to develop in chloride-rich environments (Kiele, Lukseniene et al. 2014).

When copper-based artefacts are exposed to chlorides, they may be subjected to irreversible bronze disease. It occurs mainly if metallic substrates are patinated with nantokite (CuCl). Unfortunately, bronze disease it is not reserved only for antique objects and can affect any copper bearing alloy including contemporary metals too, like modern cupro-nickel coins. Its mechanism is quite complicated and not completely clarified. Different theories are available to explain bronze disease, that is a progressive, self-sustaining and destructive process generating corrosion products, usually ugly bright bluish green or brown “growths” covering pitting areas where corrosive attack is active (Pedeferri and Cigada 1993; Finsgar and Milosev 2010).

An efficient way to reduce the degradation of Cultural Heritage metallic artefacts is to use preventive conservation measures. Since corrosion is a reaction of a material with its environment, it is possible to prevent corrosion changing either the material or the environment (Pedeferri and Cigada 1993). While the first cannot be applied to Cultural Heritage, since the physical nature of the object cannot be changed, the modification of the environment is the first choice. Preventive conservation strategies involve no action on the object itself and they are usually applied in indoor environments, where the relative humidity, temperature, oxygen and oxidant content and pollution can be controlled (Brunoro, Frignani et al. 2003). For outdoor environment, this approach is more difficult to implement, especially for economic reasons. According to IUPAC definition, preventive techniques are “all measures and actions aimed at avoiding and minimizing future deterioration or loss… These measures and actions are indirect – they do not interfere with the materials and structures of the items. They do not alter their appearance”. It is possible to act on metal surface to avoid its contact with the environment or to reduce corrosion current by controlling the cathodic and/or anodic process (Pedeferri and Cigada 1993). Many techniques belong to this group: from organic to inorganic coatings, from paints to corrosion inhibitors, that are used as protective treatments too.

1.2 Protection of Cultural Heritage

A deep understanding of the decay process is necessary for restoration purposes. It is not possible to use all the common industrial tools to improve the corrosion resistance of copper alloys artifacts (e.g., cathodic and anodic protection, change in the alloy composition, removal of damaged material). In order to preserve metallic objects from atmospheric corrosion, suitable treatments with coating substances are often required. In fact, a range of different products provides protection to the exposed surfaces forming either thick barrier layers (i. e., waxes or polymeric products) or thin films (i. e., corrosion inhibitors) on them (Beltrami 2011).

In the industrial field, metal protection is obtained by the formation of barrier effect coatings, such as anodic oxides, inorganic or ceramic coatings, organic film, conversion coatings or by corrosion inhibitors. These are usually short-term treatments (less than three years). They require the metal surface to be oxides or corrosion products free and their application frequently causes marked variations in the appearance of the metallic surface. The transfer of anticorrosive technologies from the industrial field directly to the Cultural Heritage one most of the times is not possible. Artistic objects and sculptures for outdoor expositions are usually artificially patinated, while archeological objects are covered by a layer of corrosion products, which forms over the centuries and normally must not be removed (Colledan, Frignani et al. 2005; Balbo, Chiavari et al. 2012). Treatments for the conservation of Cultural Heritage should ideally ensure long-lasting protective effects. The limit in the choice of protective agents is that it has to be possible to remove them without leaving any footprint or damage, so to apply them again or to substitute them by better products. The aim of this research and these experiments is to obtain long lasting and more efficient product respecting this requisite.

For that reason, there is a continual search for modern and improved coatings able to provide objects with a better protection, observing the peculiar principles of the conservation-restoration ethic (Sadat-Shojai and Ershad-Langroudi 2009).

While in industrial applications the protective properties of coatings are the most widely used parameter, in the protection of Cultural Heritage other properties should be taken into account such as (Sadat-Shojai and Ershad-Langroudi 2009; Goidanich, Toniolo et al. 2010; Beltrami 2011; Balbo, Chiavari et al. 2012):

- visual appearance: coatings should be transparent, with a similar gloss to the original substrate and should produce no or little change in the surface appearance
- reversibility: although it is not always possible, it should be considered; or, at least, repeatability
- respect for the original object: treatments should not modify the original material. Coatings have to be compatible with the surface of monuments, therefore the study of interaction between archaeological and new material is very important (Goidanich, Toniolo et al. 2010)
- long-term efficiency and easy maintenance, since heritage artefacts are intended to be preserved as long as possible and coatings may be eventually renovated.

These considerations impose some limitations on the selection and application of corrosion protection coatings (Sadat-Shojai and Ershad-Langroudi 2009):

- coatings should not contain pigments or colours
- coatings should be applied on variable substrates (according to material composition and state of conservation), with pre-existing corrosion products and patinas, with consequent problems of adhesion on the substrate
- coatings should be removed after many years without damaging the original surface
- coatings should be efficient, even if single or double layer (instead of the typical industrial triple layer), in order to keep the aesthetic properties of artefacts.

To guarantee an object the best protection, it is fundamental the method of application. The three main method of applications are:

- brushing
- roller
- spray.

The choice of which kind of application to use depends on:

- the size of the object (application either by roller or spray is more convenient for large surfaces; brushing would be better for smaller coating areas)
- the type of surface (spray application for curved and irregular objects while brush application for pitted surfaces)
- the ease of removal of the protective (easier when the protective is applied by brush or roller).

Usually, spray application is not recommended, since it is not easy to control the amount of applied coating. Coatings should be applied by brush.

The protection of metallic artistic surfaces by polymeric coatings has constituted a significant challenge to the surface science and technology. The major challenge concerns with the ability of combining the main features of these treatments: roughness, thickness, hydrophobic properties, transparency and durability. The protective material should have the high as possible thickness to increase hydrophobic properties and durability. However, when thickness increases, the transparency of coatings tends to reduce. Thus, a meticulous control of the thickness is required to satisfy the criteria of hydrophobicity, transparency and durability (Sadat-Shojai and Ershad-Langroudi 2009; Goidanich, Toniolo et al. 2010).

The protected surfaces that have a water contact angle higher than 150°, known as superhydrophobic ones, have attracted considerable attention due to their potential practical applications, such as self-cleaning property.

The most common protectives used for cultural heritage are:

- acrylic-based materials: they have moderate hydrophobicity and good adhesion. These applications require durability and resistance to temperature, sunlight, moisture and air pollution agents for long periods; this is why they are usually blended or copolymerized with fluorinated monomers in order to improve the protective and physical properties (Sadat-Shojai and Ershad-Langroudi 2009).
- waxes: they are polymeric, malleable and organic compounds. Waxes are insoluble in water; on the contrary, they are soluble in organic and non-polar solvents. They have a short-term durability (in fact, they should be replaced each year) and they are exposed to soiling and dust accumulation problems. Thicker layers keep their effectiveness for a longer time, nevertheless they may alter the colour and the appearance of protected surfaces (Scendo 2007; Scendo 2008).
- alkoxysilanes (or silanes): they are used especially as alkyl-modified alkoxysilanes-based coatings, that are hybrid organic – inorganic systems, having organic (alkyl groups) and inorganic (silicon backbone) components (Sadat-Shojai and Ershad-Langroudi 2009). They show a high contact angle. They are cross-linked polymers and since they form a network on the protected surfaces, they can be easily recognized.

- fluorinated polymers: they are very effective thanks to their good performances with respect to photo stability, oil and water repellency and antifouling properties (Sadat-Shojai and Ershad-Langroudi 2009). They have low surface tension and are commonly applied by spray (Beltrami 2011).
- paints: they form a protective film, which has a high adherence to the substrate (Pedeferri and Cigada 1993). They are usually transparent and glossy.

Furthermore, hybrid organic – inorganic materials (known as ceramers) are a new type of protective coatings which are a combination of different building blocks and have attracted increasing attention due to their excellent properties (Sadat-Shojai and Ershad-Langroudi 2009). In such systems, polymer blocks create good adhesion, toughness, flexibility and ease of processing, while inorganic blocks improve the mechanical properties, such as abrasion resistance, optical properties and heat resistance.

Fluorinated and hybrid polymers represent the biggest challenge in the protection of Cultural Heritage and offer a wide range of interesting applications for the future generation of materials.

1.3 Inhibitors

A corrosion inhibitor is a chemical compound that, when added to the environment in small amounts, decreases the corrosion rate of a material, typically a metal or an alloy, by acting on the cathodic and/or anodic process. The effectiveness of a corrosion inhibitor is controlled through adsorbing processes. *Cathodic inhibitors* define an increase of cathodic sovratension and a consequent reduction of corrosion potential; *anodic inhibitors* cause an increase of anodic sovratension and a consequent increase of corrosion potential and they may lead to the formation of passive films; *mixed type inhibitors* act on both cathodic and anodic processes (Beltrami 2011). A common mechanism for inhibiting corrosion involves also the formation of a coating, often a passivation layer, which prevents access of the corrosive substances to the metal.

They can be classified according to (Pedeferri and Cigada 1993):

- the chemical nature, in organic and inorganic inhibitors (as molybdates, phosphates and chromates)
- the application (for pickling, descaling and packaging)
- the condition (liquid or vapour phase)
- the electrochemical mechanism, in cathodic, anodic and mixed inhibitors
- the action, in safe and unsafe inhibitors.

The selection of a proper protective treatment should take into account (Balbo, Chiavari et al. 2012):

- exposure condition
- presence or not of corrosion products
- durability of the treatment (according to the necessity of repeated treatments, e.g. twice or three times per year)
- application ability and repeatability
- removal capability (since the removal of the protective systems usually requires delicate interventions)
- need to preserve aesthetic properties of the artefacts
- costs
- toxicity.

Inhibitors efficiency depends on (Pedeferri and Cigada 1993):

- concentration: the minimum amount of inhibitors has to be enough for the entire lifetime and surface of the material treated. It is generally assessed depending on its surface (i.e., smooth and clean surfaces need lower concentration than porous and corroded ones) and its environment composition (i.e., aggressive environments need higher concentration of inhibitors).
- nature of the metallic material: inhibitors are very specific. Their efficiency depends on the material composition and inhibitors blends can be used for alloys.
- environmental conditions: the protection is not always reliable and depends heavily on pH and temperature. When used in wrong conditions of pH or above some critical temperature values, inhibitors hence may be ineffective and cause negative effects.

Even if corrosion inhibitors are largely used, they may certain times lead to secondary and negatives effects, such as environmental pollution (in presence of phosphates, chromates and nitrates), products contamination and damages of parts that are not protected.

Along with a protective film, sometimes corrosion inhibitors are also spread with hydrophobic waxes and acrylic varnishes (copolymers of methyl- and ethyl-methacrylate) on art objects. This common protective treatments don't deface the original look of the surfaces, guaranteeing a long-lasting conservation together with avoiding that the inhibitors are washed away (Colledan, Frignani et al. 2005; Sadat-Shojai and Ershad-Langroudi 2009; Balbo, Chiavari et al. 2012).

1.3.1 BTA

Benzotriazole (BTA) and its derivatives are the most commonly used inhibitors in the area of the conservation of Cultural Heritage, as they are very effective against corrosion of copper and its alloys (Joseph, Letardi et al. 2007; Finsgar and Milosev 2010; Beltrami 2011; Marušić, Ćurković et al. 2011; Kiele, Lukseniene et al. 2014).

BTA is a heterocyclic and organic compound ($C_6H_5N_3$), in which N atoms are responsible of superficial absorption (**figure 1.1**). Many conservators have used BTA as a preventive treatment for the copper-based archaeological objects conservation, because of its capacity to form insoluble and stable polymeric complexes with Cu (I) and Cu (II) ions (Balbo, Chiavari et al. 2012).

However, BTA has proved to be less efficient when treating bronze than copper: indeed, its bond with the metal is weaker due to its low reactivity with inhomogeneities, alloy elements (Pb, Sn, Zn) and multiphasic structures (Kiele, Lukseniene et al. 2014).

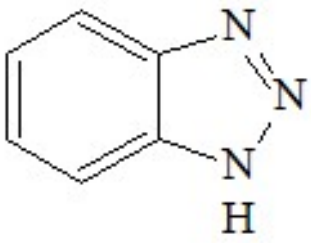

Figure 1.1 chemical structure of BTA, courtesy of wikimedia.commons.org

The BTA inhibitive action is carried out in physical way through a barrier effect, since the complexes formed on the metallic surfaces are able to slow down or stop both anodic and cathodic reactions; for this reason, benzotriazole can be considered a mixed type inhibitor, but its predominant effect is on inhibition of anodic reaction. It ensures artefacts chemical and physical stability for quite long time, without modifying the surface aspect (Marušić, Ćurković et al. 2011).
Substituted BTA derivatives were found to be effective copper alloys corrosion inhibitors when functional groups are present on the benzene ring, but not the triazole ring.
BTA and many of its derivatives may have toxic effects on plants and animals and they are supposed to be carcinogenic for humans. That is why nowadays there is an increasing interest for new harmless green inhibitors.

1.3.2 Green inhibitors

In the past two decades, the research in the field of green corrosion inhibitors has been developed using low-cost and effective molecules at low or zero environmental impact. Due to reduced impacts and good potentialities of green inhibitors, conservators are trying to extend the use of these environmentally friendly compounds (Sadat-Shojai and Ershad-Langroudi 2009; Gece 2011; Balbo, Chiavari et al. 2012; Neff 2013).

In fact green inhibitors are biodegradable and not-toxic substances, extracted from plants and renewable resources with similar properties of the traditional protective treatments (Gece 2011; Neff 2013).

At high temperature, they are chemically adsorbed, while at room temperature their adsorption is physical, whereas their efficiency decreases when their exposure time increases.

Green inhibitors can be classified in (Colledan, Frignani et al. 2005):

- organic inhibitors (extracted from fruits, oils and seeds. They are especially used for steel and stainless steel protection in acidic solutions with HCl and H_2SO_4)
- inorganic inhibitors (lanthanides salts)
- natural polymers (cellulose derivatives, as polysaccharides).

Good results have been found for amino acids and derivatives, as cysteine, momosa, tannin or isatin, which have been tested for Cu corrosion in H_2SO_4 or HCl (Balbo, Chiavari et al. 2012; Neff 2013). Their effectiveness as corrosion inhibitors is based on the presence of carboxylic ions, which contribute to prevent metal reaction and dissolution.

Good results have been found also for purine (PU) and adenine (AD) on copper corrosion in 0.5 M Na_2SO_4 solutions (pH 6.8). These organic compounds are adsorbed on copper surfaces, forming very adherent layers, and they act as mixed type inhibitors. Their inhibiting efficiency increases with an increase in their concentration (Gece 2011) (**figure 1.2**).

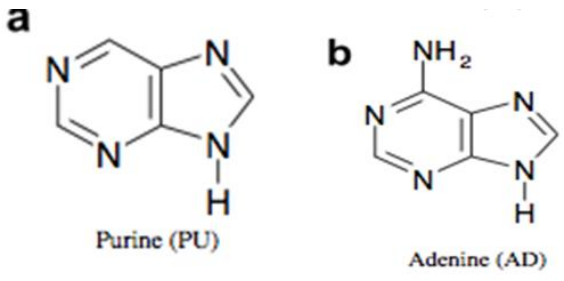

Figure 1.2 chemical structure of a) purine and b) adenine, courtesy of wikimedia.commons.org

Green inhibitors protective action is not actually completely clarified, since these substances are made of different natural organic molecules and compounds. Indeed, the research activity is still ongoing.

1.4 Corrosion monitoring

Environmental monitoring is extremely important for effective Cultural Heritage protection: from a coin inside a showcase, to a painting in a museum, from an outdoor statue or to an ancient building (Dillmann, Watkinson et al. 2013; Tidblad 2013; Watkinson 2013). The aim of monitoring is to collect all the necessary data and information to allow conservators to decide accurate conservation strategies, to ensure the artwork condition to be stable in time and the speed of decay to be low or at least acceptable.

1.4.1 Superficial characterization techniques for the study of corrosion

A large range of techniques can be used in the laboratory to study archaeological or cultural heritage metallic artefacts. Depending on what is to be studied, analysis can be carried out on the surface of the artefact in the laboratory, by using portable techniques or on micro samples collected on the studied objects. The used non-destructive techniques generally provide information on the surface of the materials (i.e., patina composition, pollution deposit, etc.), but, if information at a micrometric scale is required, it is possible to prepare the samples for cross-section observations (M. Saheb 2013; Reguer, Dillmann et al. 2013; Scott 2013).

The main micrometric techniques give data on the morphology, the elementary composition and the structure of the corrosion products formed during degradation. The first observations are performed with optical microscope or stereomicroscope and give preliminary images, with the distribution of the various phases present in the samples and with information on the thickness and on the presence of cracks and of the corrosion products (Ingo, Angelini et al. 2004; M. Saheb 2013).

Complementary observations on the morphology are obtained by using scanning electron microscope (SEM) analysis (Ingo, Calliari et al. 2000; Ingo, Angelini et al. 2004; Bracci and Morassi Bonzi 2005; Angelini, Grassini et al. 2006; Adriaens and Dowsett 2008; M. Saheb 2013; Matthiesen, Gregory et al. 2013; Reguer, Dillmann et al. 2013; Rocca and Mirambet 2013; Scott 2013). Electrons are accelerated on the surfaces of the studied samples that must be conductive in order to evacuate the charges. Two types of detector can collect SEM images. The first one

collects low energy electrons coming from the surface of the sample. They are secondary electrons (SE) and give information on the morphology of the surface (M. Saheb 2013). Due to the difficulties in localizing different areas, as metal and oxidized phases, backscattered electrons (BSE) are used: they interact with the nucleus and they are sensitive to the atomic weight. Heavier atoms appear lighter (M. Saheb 2013), so corrosion layers and metallic surfaces appear different (**figure 1.3**).

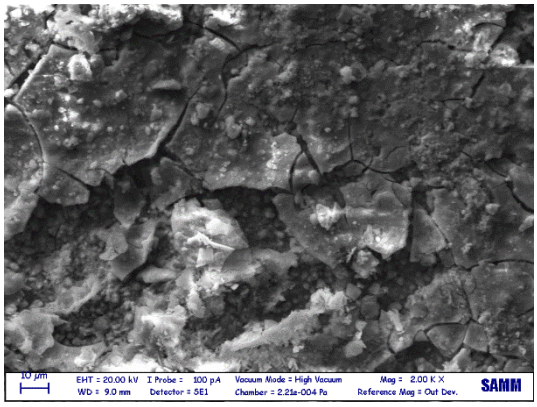

Figure 1.3 SEM image at 2000x in SE representing superficial crust of corrosion products

Elementary composition and structural analysis of the corrosion layers are carried out using energy dispersive spectroscopy (EDS), that is usually associated with SEM (Adriaens and Dowsett 2008; M. Saheb 2013; Scott 2013). The obtained spectra allow major and minor elements to be quantified and light elements up to thousand ppm to be detected in a heavy matrix. The acquisition of X-ray maps is responsible of the constitution of images of the elements distribution (M. Saheb 2013).

To decrease the detection limit, it is possible to use wavelength dispersive spectroscopy (WDS), based on analyzer crystals for specific series of elements. The detection limit is a few ppm, according to the matrix and the element (M. Saheb 2013).

X-ray fluorescence (XFR) helps to identify chemical elements and to evaluate the quantity of major, minor and trace elements of the sample (Reguer, Dillmann et al. 2013; Rocca and Mirambet 2013).

Rutherford backscattering spectroscopy (RBS) and particle-induced X-ray emission (PIXE) should also be mentioned among elementary composition techniques.

X-ray diffraction (XRD) is the most common techniques available for structural characterization (Casellato 2005; Angelini, Grassini et al. 2006; Adriaens and Dowsett 2008; Matthiesen, Gregory et al. 2013). The main advantage of this kind of analysis is that identification of the collected diagrams relies on a consolidated database, validated by the international community (International Centre for Diffraction Data) (M. Saheb 2013). When data is acquired with large diffraction angle and high resolution, quantitative information can be extracted. Moreover, since diffraction amplitude depends on the nature and position of the atoms, crystallographic structures may be determined. Finally, texture analysis can reveal thermal or mechanical effects of former treatments, according to preferred orientation of crystallites (Angelini, Grassini et al. 2006; Adriaens and Dowsett 2008; Matthiesen, Gregory et al. 2013).

Complementary structural analysis is provided by Fourier Transform Infra-Red (FTIR) spectrometry and Raman spectroscopy ((Hoffmann 2009; M. Saheb 2013; Rocca and Mirambet 2013). Raman is a technique based on an excitation of the analyzed zone by a laser beam; some limitations are encountered, since the analysis can be disturbed by fluorescence connected to the presence of polluting elements (M. Saheb 2013; Rocca and Mirambet 2013).

Morphological and structural superficial analysis can be combined to colorimetric measurements, based on the fact that human eye perceive colours as the following pairs of opposites (Diamanti 2008; Hunter 2008; EN 2010; Letardi 2013):

- light – dark
- red – green
- yellow – blue.

The CIE L*a*b* colour space is a useful system to evaluate colour differences, since it defines them by numerical values (Bacci 2005; Letardi 2013). In the CIE L*a*b* colour space, the colour coordinates are:

- L* - the lightness, that is an “attribute by which a perceived colour is judged to be equivalent to one of a series of greys ranging from black to white” (ASTM E 284). The scale for L* ranges from 0 (black) to 100 (white)
- a* - the red/green coordinate, with +a* indicating redness and -a* indicating greenness
- b* - the yellow/blue coordinate, with +b* indicating yellowness and -b* indicating blueness (Hunter 2008; Hoffmann 2009).

1.4.2 Electrochemical in-situ monitoring

Electrochemical techniques provide powerful tools for the conservation of metallic artefacts (Pedeferri and Cigada 1993; Marušić, Ćurković et al. 2011; Balbo, Chiavari et al. 2012; Goidanich, Gulotta et al. 2014). They may also be used as a treatment method to change the chemical nature of surface corrosion products and to stabilize them, to remove corrosion layers and chlorides, to deposit new protective layer or to produce deliberately specific patinas for conservation studies (M. Saheb 2013). They may be used also as analysis method: Electrochemical Impedance Spectroscopy (EIS) and Linear Polarization Resistance (LPR) have been extensively used for materials and coatings characterization, monitoring deterioration processes and evaluating the state of conservation of objects (Sadat-Shojai and Ershad-Langroudi 2009; Cano, Bastidas et al. 2010; Doménech-Carbó, Lastras et al. 2013; Letardi 2013; Kiele, Lukseniene et al. 2014). These electrochemical non-destructive in-situ monitoring methods are very important to obtain valuable information about works of art, without causing local damages to artefacts and providing reproducible measurements (Letardi 2002; Angelini, Grassini et al. 2006; Neff 2013). For both EIS and LPR it is possible to use a specially designed three electrodes contact-probe (**figure 1.4**) (Letardi 2002; Letardi 2013). It consists of a Counter Electrode and a Reference Electrode made of AISI 316 Stainless Steel, which are mechanically inserted in Teflon (PTFE). The measurement area is 2.3 cm^2. A commercial cleaning-cloth soaked with the electrolyte is fixed to the contact cell, and the system obtained is then leant on the surface to be measured (Working Electrode). This measurement method can be applied directly on Cultural Heritage metal objects and it allows to have a thin electrolyte layer on the Working Electrode (Sherif and Park 2006; Sherif, Elshamy et al. 2007). Indeed, it is possible to simulate the real outdoor condition of bronze statues: indeed, the situation is similar to rain and atmospheric humidity with pollutants (SO_2, SO_3, NO_x, Cl^-, dust) dissolved in them, which form a thin liquid layer on the surface (Sherif, Elshamy et al. 2007; Neff 2013).

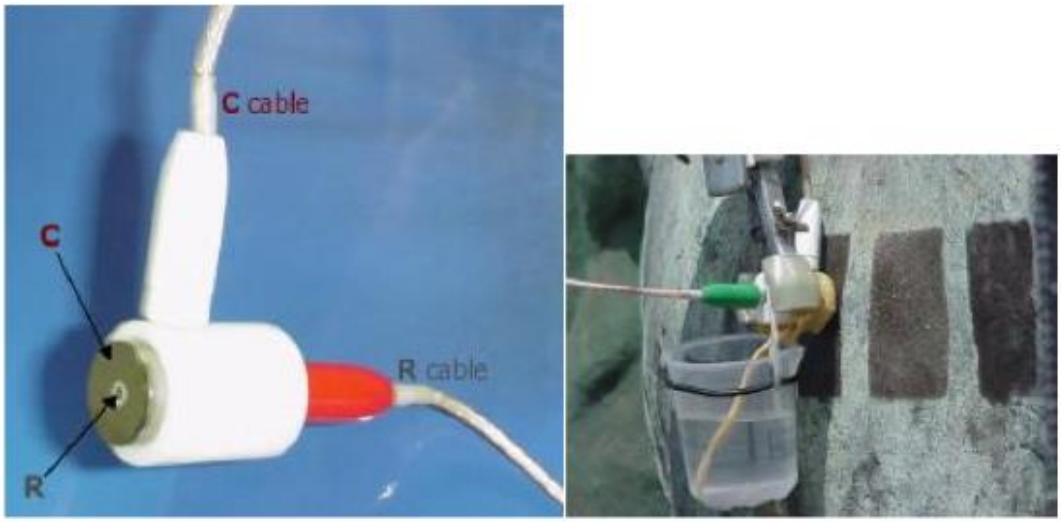

Figure 1.4 three electrodes contact-probe, courtesy of "Misure Elettrochimiche per la caratterizzazione e il monitoraggio del potere protettivo di patine e rivestimenti: la tecnica EIS" Paola Letardi, 2004

Electrolyte is usually chosen according to (Pedeferri and Cigada 1993):

- ions content
- capability of ions removal from surfaces after measurements, without damaging the metallic artefacts
- capability to resemble typical outdoor condition.

Laboratory measurements are usually carried out in 0.1M NaCl solutions, dilute Harrison's solution (0.35 wt.% $(NH_4)_2SO_4$ and 0.05 wt.% NaCl in H_2O), acid rain or mineral water (Stern and Weisert ; Sherif, Elshamy et al. 2007; Sadat-Shojai and Ershad-Langroudi 2009; Marušić, Ćurković et al. 2011). The formers are characterized by a great amount of chloride and/or sulphate ions and they are more conductive; but the latters are an easy-available option that does not destabilize the metallic artefacts.

1.4.2.1 Polarization resistance (Rp)

The polarization resistance (Rp) represents the surface resistance of metals during corrosion processes and it is strictly related to the real and instantaneous corrosion rate values (Pedeferri and Cigada 1993).

The polarization resistance of a material is defined as the slope of the potential – current density ($\Delta E/\Delta i$) curve at the corrosion potential:

$$i_{corr} = \frac{B}{Rp}$$

where Rp is the polarization resistance, i_{corr} is the corrosion current and B is a constant that can be related to the anodic βa and cathodic βc Tafel slopes, according to:

$$B = \frac{(\beta a+\beta c)}{2*3(\beta a+\beta c)}$$

Corrosion rates (in mass/time units) can be calculated from i_{corr} using Faraday's law (Finsgar and Milosev 2010).

Previous equation only applies for very small ΔE (usually 40 mV) and shows an inverse proportionality between corrosion rate and polarization resistance (corrosion rate increases, when polarization resistance decreases). For this reason, measurement of Rp permits a direct determination of corrosion current (Cano and Lafuente 2013).

The constant B is necessary to calculate i_{corr} from the experimentally determined Rp. B values can be evaluated in different ways, such as the determination of the Tafel slopes in separate experiments in the same conditions, the theoretical calculation of Tafel slopes, the use of B values already published in the literature for active metals or the empirical determination using gravimetric measurements (Cano and Lafuente 2013).

Rp values are very useful since they allow to estimate artefacts degradation, the efficacy of surface protectives and inhibitors and compare them, through a low cost, quick and non-destructive technique (Stern and Weisert ; 8044 1999; Letardi 2004; Cano and Lafuente 2013; Monnier, Guillot et al. 2013).

The main obstacles in performing Rp measurements are:

- effect of scan rate (especially for low corrosion rate systems): the rate at which the potential is scanned may have a significant effect on the amount of current produced at all values of potential. The scan rate is an experimental parameter controlled by the user. If it is not chosen properly, the scan rate can alter the analysis results, causing a misinterpretation of the features
- high solution resistance and electrolyte thickness (Monnier, Guillot et al. 2013)
- changing surface conditions: since corrosion reactions take place at the surface of metals, if the surface changes due to processing conditions or active corrosion, the potential changes

too. This may have a strong effect on the polarization curves

- difficulty in the characterization of too much insulating protective coatings
- difficulty in B constant estimation.

Corrosion rate values obtained by Linear Polarization Resistance (LPR) measurements may be higher if compared to mass loss measurements (Bartuli, Cigna et al. 1999). Indeed, this method tends to overestimate metal degradation because of the continuous surface contact with the high thickness liquid electrolyte (Sherif, Elshamy et al. 2007; Cano, Bastidas et al. 2010). The real thickness and composition of the deposit of corrosion products depend on the exposure time and on the typical climatic conditions of the exposure site. A corrosion process is active in the presence of water and it depends on the time of wetness (TOW).

As an environmental parameter, TOW is defined in terms of climatic variables, such as relative humidity and temperature. The definition of TOW presented on ISO standard 9223 is the following: “the period during which a metallic surface is covered by adsorptive and/or liquid films of electrolyte that are capable of causing atmospheric corrosion”. In addition, the new document ISO WD/9223 defines: “the wetting of surfaces is caused by many factors, for example, dew, rainfall, melting snow and a high humidity level. The length of time when the relative humidity is greater than 80% at a temperature greater than 0 °C is used to estimate the calculated time of wetness of corroding surfaces” (ISO9223:2012(E) 2012). This definition is based on the idea that above a certain humidity threshold, corrosion increases substantially due to sorption of water on the surface (D'Orazio and Cursio ; Baer, Sabbioni et al. 1989; Bartuli, Cigna et al. 1999; Corvo, Pérez et al. 2008; Schindelholz, Kellya et al. 2013; Norberg 20012).

As a surface parameter, TOW is estimated by measuring moisture on or near a surface of interest. Sensors made of arrays of electrodes separated by an insulating gap are commonly used. Reactive or noble metals are commonly used for sensors construction. Corrosion behavior of reactive electrodes is usually monitored through potential or current measurements as an indicator of wetness. Resistance across sensors is often used as a direct indicator of the presence or absence of a sufficiently conducting electrolyte. In this case, time of wetness is defined as the time during which a voltage, current or resistance threshold is exceeded (Schindelholz, Kellya et al. 2013).

A comparison between corrosion rates measured by mass loss or evaluated from Rp represents a cross confirmation of the validity of the experimental procedures. In previous researches for the Marcus Aurelius equestrian monument, the results of the two approaches do not coincide exactly.

To make a reasonable comparison of the results of the two methods, it was necessary to quantify the effective fraction of time during which a structure exposed outdoors is covered by a thin layer of water (Bartuli, Cigna et al. 1999). This corresponds to the time of wetness whose characteristic values has be collected from the standards (ISO9223:2012(E) 2012). By multiplying the values of corrosion rate calculated from Rp measurements by the fraction of wetness, the final result is closer to the real condition of the corroding surface (Bartuli, Cigna et al. 1999).

Due to the difficulties in the calculation of constant B and therefore in the estimation of the corrosion rate, normally the Rp values are used in a direct and comparative manner. It is important to validate the methodology, by using gravimetric tests on samples in the same condition, in order to be able to extrapolate correctly the corrosion rate from Rp values.

1.4.2.2 Electrochemical impedance spectroscopy (EIS)

Electrochemical impedance spectroscopy (EIS) is "an electrochemical technique based on the response of a corroding electrode to a small amplitude alternate potential or current signals at various frequencies" (Grassini 2013). It is a valuable tool in corrosion and solid-state laboratories. In fact, corrosion science was the first major scientific discipline to embrace EIS in 1980s. One of the main important features of EIS in Cultural Heritage is that this measurement is a non-destructive technique, which can provide time-dependent information about system properties and corrosion (Cano, Bastidas et al. 2010).

EIS consists in the measurement of amplitude and phase of the surface impedance of coated metallic objects at different frequencies to highlight either the protective effectiveness of a coating or the stability of a corrosion patina grown on the surface (Pons, Lemaitre et al. 2013). EIS method is usually carried out by applying an AC potential to an electrochemical cell and then measuring the current flowing in the cell.

The excitation signal is function of time:

$$E\ (t) = E_0\ \sin(\omega t)$$

where $E\ (t)$ is the potential at time t, E_0 is the amplitude of the signal and ω is the radial frequency.

In a liner or pseudo-linear system the response signal is shifted in phase (φ) and has an amplitude I_0:

$$I_t = I_0 \sin(\omega t + \varphi)$$

An expression similar to Ohm's law is used to evaluate the impedance of the system as:

$$Z = \frac{E_t}{I_t} = \frac{E_0 \sin(\omega t)}{I_0 \sin(\omega t + \varphi)} = Z_0 \frac{\sin(\omega t)}{\sin(\omega t + \varphi)}$$

The impedance is expressed in terms of magnitude, Z_0, and phase shift, φ.

In terms of Eulers relationship:

$$e^{j\varphi} = \cos\varphi + j \sin\varphi$$

so impedance can be written as a complex function:

$$Z = Z_0 e^{j\varphi} = Z_0 (\cos\varphi + j \sin\varphi)$$

$$Z(\omega) = Z_{real} + jZ_{im}$$

The impedance is typically measured in the frequency range of 1 mHz to 100 kHz, acquiring 3 to 10 points per decade and the expected impedance amplitude depends on the area of the coating that is exposed to the electrolytic solution (Pons, Lemaitre et al. 2013).

Two diagrams are available to represent impedance spectra (**figure 1.5**):

- Nyquist plots
- Bode plots.

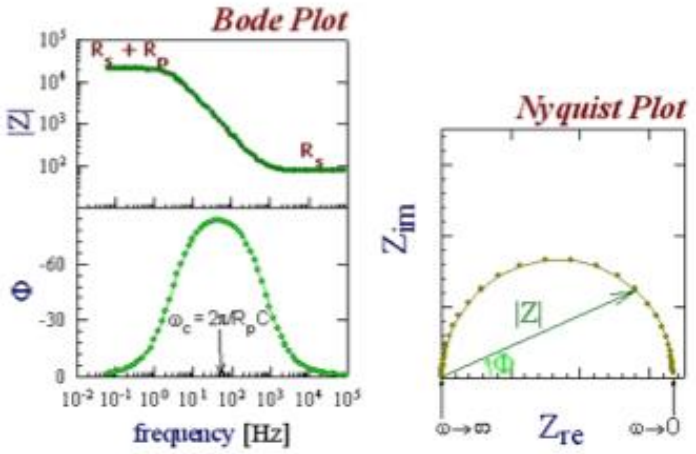

Figure 1.5 example of Nyqsuist and Bode plots, courtesy of "Misure Elettrochimiche per la caratterizzazione e il monitoraggio del potere protettivo di patine e rivestimenti: la tecnica EIS" Paola Letardi, 2004

In Nyquist plots, the real part of impedance is plotted on the x-axis and the imaginary part is plotted on the y-axis. Since the imaginary part is usually negative, the y-axis is reversed to have plots in the first quadrant. Each point in this diagram is the impedance at one frequency, even if frequency is not immediately evident. In Nyquist plot, each impedance value is a vector of magnitude $|Z|$ that forms a phase angle φ with x-axis (Li, Ma et al. 2010; Pons, Lemaitre et al. 2013).

In Bode plots, the logarithm of impedance modulus $|Z|$ is plotted versus either the logarithm of the frequency, ω, or the logarithm of the phase angle, φ. In this case frequency is directly evident in the graph (Ellingson, Shedlosky et al. 2004; Li, Ma et al. 2010; Pons, Lemaitre et al. 2013).

The Nyquist plots are used to analyse the impedance spectra in order to determine the simple electrical components (i.e., resistors, capacitors and inductors) of an equivalent circuit model, able to represent metal/solution interface (Cano, Bastidas et al. 2010; Cano, Lafuente et al. 2010; Pons, Lemaitre et al. 2013). For this reason, data fitting and electrical modelling are very important tools for EIS method. In simple systems, Nyquist plot shape analysis may also indicate how different electrical elements are combined; in complex systems (i.e., rough surfaces, patinas with variable composition, different possible interactions with the environment), the circuit, that has to be used to model the analysed situation, may not be uniquely defined (Degrigny, Guibert et al. 2010; Degrigny 2011). Since the choice of the equivalent circuit requires a deep knowledge of the corrosion system and of the electrochemical reactions, this approach is very difficult and it may lead to significant errors.

In addition to linear polarization resistance, EIS could represent another way to estimate corrosion rate values, even for high resistivity coatings thanks to the use of an alternate signal (Zhang 2002; Cano, Bastidas et al. 2010). Bode plots at high frequencies contain information on the electrolyte resistance; while at low frequencies contain information on the corrosion processes on the metallic substrates (Pons, Lemaitre et al. 2013). Therefore, it was discovered by Zhang et al. that corrosion rates could be derived with an easy method from the difference in EIS data of $|Z|$ between the low and high frequency ranges (Prosek, Kouril et al. 2013). The higher $|Z|$, the lower corrosion rate. Obviously, a more detailed analysis can provide additional information on the properties of the studied system, but the values of $|Z|$ at low frequencies are largely used to evaluate the efficiency of coatings and to compare their effectiveness on copper-alloys artefacts in both the laboratory and in-situ.

Corrosions resistance values are extrapolated graphically and they are used in a comparative and direct manner. Hence, likewise previous technique, it is necessary to validate the methodology.
The two electrochemical methods provide polarization resistance values comparable in terms of trend, but not identical. For this reason, it is important to compare them with mass loss results of standard metallic specimens exposed in-situ to estimate which of the two methodologies provides data of corrosion rate that are more reliable.
As previous technique, corrosion rate values obtained by EIS measurements may be higher if compared to mass loss measurements. By multiplying the values of corrosion rate calculated from EIS measurements by the fraction of wetness, the final result is closer to the real condition of the corroding surface (Bartuli, Cigna et al. 1999).

1.4.3 Sensors

The relationship between different climatic factors, i.e., relative humidity, temperature, concentration of pollutant gases, and the corrosion rate is complicated and a detailed knowledge on the climatic parameters is necessary. For this reason, climatic data and corrosion rates are directly measured on metal sensors (Fiorentino 2004; Leyssens, Adriaens et al. 2005; Matteini 2005; Li, Kim et al. 2007; Said, Azura et al. 2011; MacLeod 2013; Matthiesen 2013; Parvis 2013; Sjogren and Le Bozec 2013).
Implementation of on-line and real time monitoring enables operators to take immediate countermeasures if degradation increases, in order to reduce the costs of corrosion.
The goal of the researcher is to develop sensors with the following features:

- high sensitivity and reliability
- short response time
- small size and battery driven
- high stability in air, even at high temperature
- stability over a lot of scans
- easy, fast and reproducible production.

The monitoring of the corrosion rate of copper-alloys in the atmosphere commonly occurs by the means of (Li, Kim et al. 2007; Parvis 2013; Sjogren and Le Bozec 2013):

- coupon technique: a coupon of the material of interest is exposed in an environment in which the corrosivity is studied. After the exposure, quantification of mass loss is carried out.
- coulometric reduction: electrochemical reactions are useful to reduce films of corrosion products. The charge required for the reduction is a measure of the amount of corrosion products.
- quartz crystal microbalance method: it measures corrosion as changes in resonance frequency of a piezo-electric quartz crystal coated with a metal by physical vapour deposition, since the resonance frequency is a function of the mass of the crystal (Parvis 2013). The main disadvantage is that this method is equally sensitive to dust or other contaminants as to superficial corrosion products.
- electrical resistance (ER) technique (Said, Azura et al. 2011; Parvis 2013; Sjogren and Le Bozec 2013): resistance of a thin metal track is measured. This method can be only applied on metals exposed to uniform corrosion and it is not reliable in case of pitting, crevice or grain boundary corrosion. The electrical resistance of a metal is a function of its intrinsic resistivity and geometry; in fact, it is possible to use the change in geometry (i.e., thinning) of a metallic element due to corrosion and to convert this to metal loss or to corrosion rate. Electrical resistance sensors can operate in almost any environment and they are made of materials of interest with the shapes of wire, strip and tube deposited on a glass substrate. A small battery-operated corrosion logger can be used, when electricity is not available as in display cases or inside transport package.
- sensors for oxygen monitoring: they are based on amperometry where oxygen is reduced on a metal substrate at -0.8 V potential, which enables current to flow, since oxygen reduction is the main cathodic reaction in atmospheric corrosion (MacLeod 2013). These sensors may lead to some problems, since it is not completely clarified if oxygen is consumed by the studied artefact or by the amperometric sensors during measurements. For this reason, oxygen reduction on sensors is better controlled by producing very small amperometric electrodes (Fiorentino 2004; MacLeod 2013) with high spatial resolution.

No previously mentioned techniques can be applied to the monitoring of gilded bronzes, due to the bimetallic nature of these objects (**figure 1.6**). In this case, the study of corrosion behaviour

and conservation is a particularly complex topic, since unstable corrosion products form between the metal surface and the gilding, such as copper chlorides, and they cannot be completely removed without damage to the gilding. Moreover, corrosion products are very reactive in presence of nitrates and sulphates. They promote the formation of less stable compounds, responsible of volume variation. Bursting effects, cracks, progressive loss of adherence, superficial discontinuities and detachment of the gold leaf are some possible negative consequences (Oddy 2000; Goidanich, Gulotta et al. 2014). In addition, the presence of galvanic coupling between the two metals accelerates the corrosion processes.

Figure 1.6 examples of gilded bronzes: a) Porta del Paradiso, Lorenzo Ghiberti, Florence; b) detail; c) statua equestre di Marco Aurelio, Palazzo dei Conservatori, Rome; d) detail and e) cavalli di San Marco, Basilica di San Marco, Venice, courtesy of wikimedia.commons.org

Linear Polarization Resistance (LPR) or Electrochemical Impedance Spectroscopy (EIS), which allow collecting quantitative data on corroded metallic artefacts, cannot be applied to a bimetallic object due to the difficulties on the interpretation of results.

A promising alternative is the use of galvanic sensors specifically designed to simulate the stratigraphy of a corroded gilded bronze and to allow the continuous monitoring of the macro couple current density. It flows between the gilding and the bronze, it may be continuously monitored by means of a high precision multimeter and it is directly proportional to corrosion rate through Faraday's law (Brambilla 2011; Goidanich, Porcinai et al. 2013; Piccardo 2013).

Galvanic sensors are used to (Mazza, Pedeferri et al. 15-19 September 1975):

- evaluate corrosion rate in different conditions
- control the effect of environmental parameters (i.e., relative humidity, temperature and concentration of ageing species)
- check the effectiveness of eventually used inhibitors
- define the electrochemical aspects of real systems
- evaluate the type of kinetic control of the process.

The first galvanic sensors simulating gilded bronzes were designed in the late 70's by Professor Bruno Mazza of Politecnico di Milano and co-workers to evaluate new conservation strategies for the Lorenzo Ghiberti's "Porta del Paradiso" (Goidanich, Porcinai et al. 2013). The system prepared in this period consisted of a "sandwich" formed of bronze covered by its artificially obtained corrosion products on which a high porosity gold film was finally applied (Mazza, Pedeferri et al. 1977; Mathis, Salomon et al. 2013). Unfortunately, these sensors could only be used to monitor gilded bronzes for a short period, since the measured current density decreased quickly, falling below the detection limit after three months (Goidanich, Toniolo et al. 11-15 October 2010; Mazza, Pedeferri et al. 15-19 September 1975; Goidanich, Brambilla et al. 2011; Piccardo 2013; Goidanich, Gulotta et al. 2014).

Nowadays, the main request arising from conservators and museum curators is the long-term monitoring and microclimate control for the preventive conservation of restored gilded artefacts. Therefore, galvanic sensors were designed to identify the most adequate environment for the "Porta del Paradiso" conservation in the "Museo dell'Opera del Duomo" in Florence (Goidanich, Toniolo et al. 11-15 October 2010; Brambilla 2011; Goidanich, Gulotta et al. 2014). Further

experiments are necessary in order to clearly identify the most appropriate microclimate conditions for the suitable conservation of gilded bronzes with unstable corrosion products (Cagnini, Porcinai et al. 2012; Cagnini, Porcinai et al. 2012).

Galvanic sensors proved to be a powerful tool for simulating and monitoring the corrosion rate of gilded bronzes. For this reason, new sensors have now been realized, to control microclimate influence on their behaviour and to try to apply them also on patinated, but not gilded bronzes.

The research on the exact fabrication of galvanic sensors is still ongoing (Aldrovandi, Lalli et al. 2005; Squarcialupi and Burrini 2005). Thus, further improvements are necessary to obtain more reproducible, reliable and durable sensors.

EXPERIMENTAL

2.1 Validation of monitoring techniques

Electrochemical and continuous monitoring techniques provide powerful tools for the characterization of the real state of health of metallic artefacts. Traditional techniques are normally setup for application in solution. To make their use reliable also for in-situ measurements, it is necessary a confirmation of the validity of their experimental procedures. Indeed, it is important to validate the methodology using mass loss tests on analogous samples in the same exposure condition.

2.1.1 Outdoor condition for copper alloys

Linear Polarization Resistance (LPR) and Electrochemical Impedance spectroscopy (EIS) are non-destructive in-situ monitoring techniques. An intense bibliographic research and a preliminary experimental activity have been done in previous works to define equipment settings and the proper electrolytic solution (Letardi 2002; Letardi 2004; Beltrami 2011; Brambilla 2011).

They have been extensively used for materials and coatings characterization, monitoring deterioration processes and evaluating the state of conservation of objects.

Due to the difficulties in the calculation of constant B and therefore in the estimation of the corrosion rate according to the Stern-Geary formula, normally the Rp values are used in a direct and comparative manner. For this reason, it is important to validate the experimental methodology using gravimetric tests on samples exposed in the same conditions.

The following materials have been used for electrochemical techniques validation (**table 2.1**): they are copper-based alloys exposed in outdoor conditions.

Table 2.1 outdoor Copper and Bronze

material	sample name	alloy composition	exposure condition	area (cm^2)
Copper	Cu X	99.99% Cu	Outdoor, 45° South, Milano	34.73
	Cu Y			34.43
Bronze	Bronze X	88.35% Cu, 5.66% Sn, 3.50% Zn, 1.58% Pb, 0.57% Ni, 0.12% Fe, 0.03% P, 0.02% Sb		51.11
	Bronze Y			51.00
	Bronze Z			50.85

Copper and bronze samples have been exposed at 45° from the horizontal facing South in not-sheltered conditions. Exposure went on for 7 months at an urban site in Milan. The samples were mounted on a Plexiglas support.

Before exposure, all the specimens underwent to ultrasonic cleaning for two minutes in acetone. Bronze samples have been additionally polished with abrasive paper (100) to remove undesired superficial alteration and macroscopic defects resulting from the fabrication processes, which may act as preferential pathways for corrosion. The sandpaper polishing has not been applied on copper samples.

Electrochemical results from LPR and EIS have been validated and compared to gravimetric measurements. Periodic LPR and EIS measurements were performed on the same samples subjected to gravimetric measurements. The mass of the specimens has been recorded after the following procedure that was repeated at least 5 times per each sample:

- two minutes in HCl 37% solution (500 ml of hydrochloric acid and reagent water to make 1000 ml)
- two minutes in demineralized water
- two minutes in ethanol.

2.1.1.1 LPR and EIS measurements

The type of electrode and the characteristics of the electrolytic solution are key factors affecting LPR and EIS efficiency.

According to previous results (Beltrami 2011; Brambilla 2011), in this work the following three electrodes contact-probe has been used (**figure 2.1**). Reference and counter electrodes are made of stainless steel AISI 316. They are concentric and they have been embedded into Teflon to achieve electrical insulation. The total contact area is 2.3 cm^2.

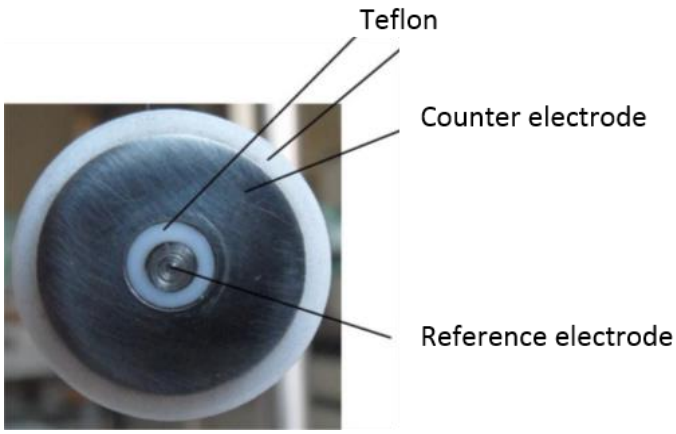

Figure 2.1 three electrodes contact-probe used for electrochemical measurements

No standards about chemical composition of electrolytic solutions simulating atmospheric corrosion of metallic surfaces are available. The actual composition and concentration of atmospheric pollutants may vary significantly according to geographical area and meteorological conditions. The use of mineral water is an easy-available option since it has suitable conductivity values for the electrochemical measurements and it does not destabilize the metallic artefacts (Letardi 2002; Letardi 2013). Furthermore, it solubilizes the deposits cumulated over the surface. Chemical-physical properties and substances dissolved in water (mg/l) are listed in the following tables (**table 2.2** and **table 2.3**).

Table 2.2 chemical-physical properties of mineral water

temperature (°C)	15.4
Hydrogen ions concentration	7.42
fixed residual at 180 °C	272
conductivity at 25 °C (µS/cm)	415
hardness (°F)	not available
free CO_2	8
dissolved O_2 (mg/l)	6.3
oxidability (mg/l)	not available

Table 2.3 substances dissolved in water (mg/l)

Ca^{2+}	48.6	**F^-**	0.15
Mg^{2+}	29.4	**Li^+**	not available
Na^+	5.8	**Sr^{2+}**	not available
K^+	1	**NO_2^-**	not available
HCO_3^-	301	**$NH4^+$**	not available
SO_4^{2-}	4.1	**I^-**	not available
Cl^-	2.4	**SiO_2**	15.2
NO_3^-	8.5	**H_2S**	not available

A commercial cleaning-cloth wetted with the electrolyte is fixed to the contact cell, and the system obtained is then applied on the metal surface to be measured (Working Electrode). This measurement method can be applied directly on Cultural Heritage metal objects, being totally non-invasive (Sherif, Elshamy et al. 2007; Sadat-Shojai and Ershad-Langroudi 2009; Marušić, Ćurković et al. 2011; Letardi 2013). The wet cloth provides the presence of a thin layer of the electrolyte on the Working Electrode during the measurement (**figure 2.2**).

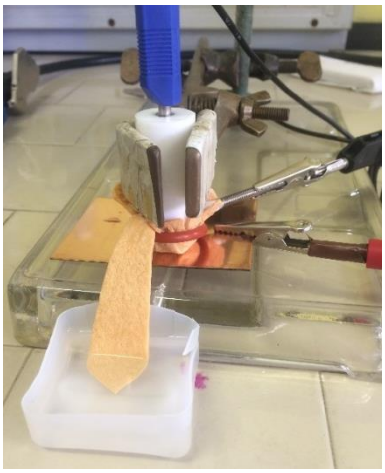

Figure 2.2 three electrodes contact-probe during measurements on copper sample

LPR and EIS tests have been repeated after different exposure time (before exposure, after fifteen days, one month, four months and seven months) and the resulting corrosion resistance values are strictly related to the actual instantaneous corrosion rates.

An inverse proportionality between corrosion rate (i_{corr}) and corrosion resistance (R_p) is defined by the Stern-Geary formula:

$$i_{corr} = \frac{B}{R_p}$$

where B is a constant related to the anodic βa and cathodic βc Tafel slopes, according to:

$$B = \frac{(\beta a + \beta c)}{2 * 3(\beta a + \beta c)}$$

Corrosion rates (in mass/time units) can be calculated from i_{corr} using Faraday's law (Finšgar and Milošev 2010; Cano and Lafuente 2013). The B constant can be used to calculate i_{corr} from the experimentally determined Rp, but its evaluation can be difficult especially for copper (it can be Cu^{+} and Cu^{2+}). Therefore, in many case the only option is to make direct comparison with corrosion resistance values.

Both LPR and EIS measurements use a portable potenziostatic device: Ivium Technologies CompactStat with Ivium® software (**figure 2.3**).

Figure 2.3 images of Ivium equipment, courtesy of Ivium Technologies (www.ivium.ne)

- *EIS*

Electrochemical Impedance Spectroscopy is an electrochemical test based on the response of a corroding electrode to a small amplitude alternate potential at various frequencies (Grassini 2013). By applying an alternate potential $E(t)$ to a metallic sample, surface response is the current $I\ (t)$, according to:

$$Z(\omega) = \frac{E(t)}{I(t)}$$

$Z(\omega)$ is system impedance, depending on angular frequency (Grassini 2013; Pons, Lemaitre et al. 2013).

Measurements have been carried out after 30 minutes of immersion of the commercial cleaning-cloth in electrolytic solution and after 10 minutes of system stabilization. Frequencies vary from 100 KHz to 10 mHz, the maximum potential amplitude is 10 mV with respect to OCP (Open Circuit Potential) and no equilibration time has been applied.

Resistance values have been calculated from Bode plots (Zhang, He et al. 2002; Cano, Bastidas et al. 2010): at high frequencies, they provide information on the electrolyte resistance, while at low frequencies, they provide information on the corrosion processes on the metallic substrates (Pons, Lemaitre et al. 2013). Therefore, it was discovered by Zhang et al. that corrosion rates could be derived from the difference in EIS data of $|Z|$ between the low and high frequency ranges (Prosek, Kouril et al. 2013). The higher $|Z|$, the lower corrosion rate.

- *LPR*

The polarization resistance of a material is defined as the slope of the potential – current density curve $^{\Delta E}/_{i_{ext}}$, where $\Delta E = E - E_{corr}$ (E is the applied potential and E_{corr} is the free corrosion potential) and i_{ext} is the external measured current. Polarization resistance can be evaluated after cathodical or anodical polarization of the material (Cano and Lafuente 2013).

Measurements have been carried out after 30 minutes of immersion of the commercial cleaning-cloth in electrolytic solution and after 10 minutes of system stabilization. After E_{corr} evaluation, ΔE = ± 20 mV is applied with a 10 mV/min scanning rate.

Polarization resistance is calculated according the following formula:

$$R_p = \frac{E - E_{corr}}{i_{ext}} = [\Omega \cdot m^2]$$

where E [V] is the working electrode potential with respect to reference one, E_{corr} [V] is the free corrosion potential (or Open Circuit Potential, OCP) and i_{ext} [A/m^2] is the measured current density. Rp value is the slope of the curve obtained by plotting on y-axis applied potential and on x-axis collected current density values. Higher Rp values means lower corrosion rate.

2.1.2 Indoor condition for gilded bronzes

Traditional electrochemical techniques such as Linear Polarization Resistance (LPR) or Electrochemical Impedance Spectroscopy (EIS) cannot be applied to a bimetallic object, like a gilded bronze (see previous chapter). Galvanic sensors are a suitable alternative technique for corrosion monitoring, since they simulate corroded gilded bronzes (**figure 2.4**).

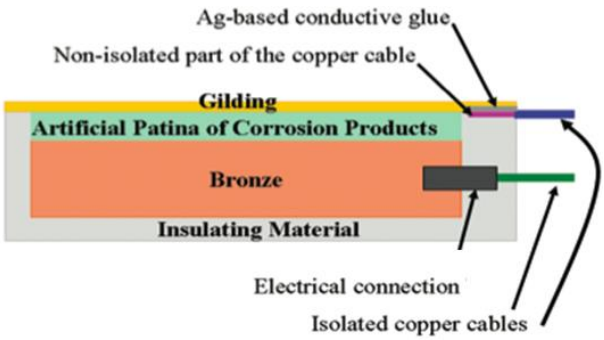

Figure 2.4 example of prepared galvanic sensors

Mazza and co-workers first developed them in the late 70's at the Politecnico di Milano (Mazza, Pedeferri et al. 15-19 September 1975; Mazza, Pedeferri et al. 1977; Brambilla 2011; Goidanich, Porcinai et al. 2013). Galvanic sensors were used by the same research group to evaluate the efficacy of a conditioning system that may allow to maintain of the "Porta del Paradiso" in its original location outdoor in Florence (Mazza, Pedeferri et al. 15-19 September 1975; Mazza, Pedeferri et al. 1977). Because of the initial and promising results, in previous projects other sets of galvanic sensors have been developed and used for the monitoring of corrosion rate in different environments (Goidanich, Toniolo et al. 11-15 October 2010; Brambilla 2011; Goidanich, Brambilla et al. 2011; Goidanich, Gulotta et al. 2014).

In this work of thesis, new double layer gold leaf sensors have been realized for the monitoring of the "Porta del Paradiso". The sensors will be soon installed in the new showcase where the "Porta del Paradiso" will be exposed. The galvanic sensors allow monitoring the macro couple current flowing between the gilding and the bronze that is directly correlated to corrosion rate by Faraday's law. Galvanic sensors simulate the real stratigraphy of the gilded bronzes. The main challenge was to produce more durable sensors, with more reproducible and reliable signals. Furthermore, to verify their reliability on monitoring actual corrosion rate, the galvanic current recorded has been compared to mass loss measurements of identical samples exposed in the same conditions. In addition, some non-gilded samples were prepared in order to evaluate the possibility of using the galvanic sensors also for the monitoring of patinated or heavily corroded non-gilded bronzes.

- *galvanic sensors preparation*

The galvanic sensors have been prepared according to the following procedure:

1. polishing with abrasive paper (100) of the surface to eliminate oxidation products and to obtain a rough, plane and reproducible surface
2. cleaning of the surface with ethanol
3. realization of electrical connection by applying a conductive silver-based glue between copper cable and metallic substrate
4. application of an epoxy resin coating on the electrical connection, on the four sides and on the back of the sensor to ensure a complete electrical insulation of the entire system with the exception of the upper surface
5. patination of the upper surface

6. gilding by applying a gold leaf on the artificial patina, before it gets completely dry, by leaning the wet surface of the patina directly on the gold leaf (**figure 2.5**). The humid condition of the patina provides an adequate adhesion so no additional adhesive is necessary.

Figure 2.5 brush, spatula and gold leaf used for gilding

- *patination of galvanic sensors*

The realization of artificial patinas with specific and reproducible characteristics in terms of thickness, porosity, cohesion and composition is a crucial point for the setup of suitable galvanic sensors, since patina acts as the electrolytic layer. The methodology for patination was developed during previous works (Brambilla 2011; Goidanich, Gulotta et al. 2014) that had to face some problems, such as:

- thickness: the thickness of the patina influences the durability, the performances of the galvanic sensors and the macro couple current. The applied paste must be thick enough to avoid short circuits between gold and substrates. A thin layer of patina is preferred to prepare both durable sensors and with high macro couple current.
- homogeneity: the patina has to be homogeneous on the whole surface of the sample to avoid formation of holes that can be the cause of short circuits.
- adhesion to the substrate: patinas must be adherent to obtain more durable and reproducible sensors. For this reason, metallic substrates are treated with abrasive paper (100) to remove oxidation products. This approach is tested in this work for the first time with the aim of increasing patinas adhesion, instead of the use of cuprite layer.

- resistance: the patina must offer a quite high resistance to the current flow to allow the measurement of the macro couple current. On the other hand, if the resistance is too high (e.g., too thick patina or too dry), the galvanic coupling could not work properly.

The patinas composition used in the present work have been chosen according to previous researches (Brambilla 2011; Goidanich, Brambilla et al. 2011; Goidanich, Gulotta et al. 2014), in which several tests have been carried out to define the following parameters:

- the best water/powder ratio
- thickness of the patinas
- methodology for gold leaf application
- the adequate relative humidity of the environment during the curing period.

Several chemical and electrochemical patination methodologies have been tested in previous researches (Brambilla 2011) without any satisfactory results. These methods have not been used due to problems of reproducibility. Indeed, the artificial patina has been prepared according to the "applied paste" method (Hughes and Rowe 1997) that allows the preparation of artificial patina with a wide range of different compositions representative of the condition of ancient gilded bronzes. The patination of the substrate has been made by applying a paste made of copper salts. Salts have been selected according to previous researches (Brambilla 2011; Goidanich, Gulotta et al. 2014) and in order to be representative of the specific stratigraphy and corrosion products of the "Porta del Paradiso".

Solid ingredients of the paste have been ground to a fine consistency using a pestle and mortar (**figure 2.6**).

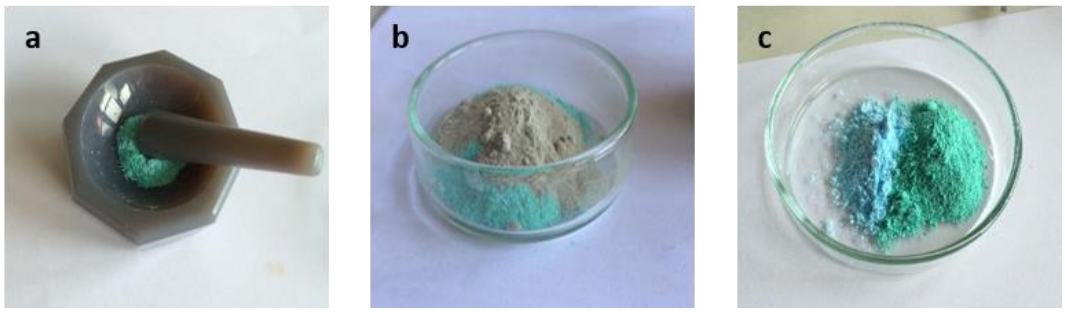

Figure 2.6 a) pestle and mortar; b) and c) mixing of the solid ingredients of the patina

Demineralized water is then added to the powder until the proper fluidity is achieved. It is possible to obtain patinas with different thickness, varying the amount of powder per cm^2 of substrate,

changing the demineralized water/powder ratio and overlapping additional layers (up to three overlapped layers have been tested in previous works) (Brambilla 2011; Goidanich, Gulotta et al. 2014). In this work, the desired thickness has been reached by overlapping two layers.
Patinas composition, mass/area and water/powder ratio used for this thesis work are listed in the following table (**table 2.4**).

Table 2.4 list of used patinas

name of the patina	**mass/area (g/cm^2)**	**H_2O/powder (g/g)**
Classic patina (S&C = sulfates and chlorides) $CuSO_4$-$5H_2O$ + CuCl + $CuCl_2$-$2H_2O$ (4: 3: 1)	0.025	1
Atachamite (BCC = basic copper chlorides) $Cu_2(OH)_3Cl$	0.01	2
Brochantite + Nantokite (1:1) Brochantite $Cu_4SO_4(OH)_6$ Nantokite CuCl	0.025	1
Brochantite + Chalcanthite (1: 1) Brochantite $Cu_4SO_4(OH)_6$ Chalcanthite $CuSO_4$-$5H_2O$	0.025	1

After the mixing with water, the past has been applied on the surface of the sensors with a spatula, worked with it to obtain a smooth surface and then left to dry in laboratory. The application of the second layer of the paste takes place 24 hours after the first application and then gilding takes place after a variable time (30-45 minutes), according to patina composition and amount of water.
Two different set of galvanic sensors have been prepared.

- *first set*

The first set of galvanic sensors has been prepared to verify their reliability through mass loss measurements and to try to apply them also on patinated bronzes without gilding.

Eighteen galvanic sensors have been realized (**table 2.5**); they have been continuously monitored for 7 months and subjected to cycles of low and high humidity.

Table 2.5 first set of galvanic sensors

	number of Cu sensors	**number of Bronze sensors**
BCC	3	2
S&C	3	3
brocchal	2	-
brocnan	3	2

Twenty-eight samples have been realized and used for mass loss measurements (**table 2.6**); they have been exposed in the same condition of the galvanic sensors. They are thirteen gilded and intentionally short-circuited samples and fifteen non-gilded samples useful to evaluate the possibility of using the galvanic sensors also for the continuous monitoring of patinated or heavily corroded non-gilded bronzes.

Table 2.6 intentionally short-circuited sensors

	Cu sensors		**Bronze sensors**	
	gilded	**not gilded**	**gilded**	**not gilded**
BCC	2	3	1	1
S&C	3	2	2	2
brocchal	2	3	-	-
brocnan	2	3	1	1

Sensors made of copper (Cu 99.99 %) and bronze substrates have been prepared. The following table describes bronze composition (**table 2.7**).

Table 2.7 bronze substrate composition

Cu	Pb	Sn	Fe	Al	Ni	Mn	Sb	P	Si	Zn
88.35	1.58	5.66	0.12	0.00	0.57	0.00	0.02	0.03	0.00	3.50

As previously mentioned, the measured galvanic current is directly correlated to the corrosion rate. However to calculate corrosion rate from galvanic current, the following assumptions must be made:

- the bronze and the gilding have the same surface area
- the cathodic process (i. e., oxygen reduction) occurs mainly over the gold surface
- only copper is oxidised ($Cu \rightarrow Cu^{2+} + 2e^-$)
- corrosion is generalised.

Galvanic sensors have been put into a climatic chamber, periodically varying relative humidity (from 20% to 65%). A constant temperature has been maintained during monitoring (T = 25 ± 3 °C).

The macro couple current is continuously monitored by means of a high precision multimeter. The validation occurs by comparing the obtained results to mass loss tests (by using the same pickling cycles described before). They have been carried out on metallic samples with the same substrate composition of the sensors that were intentionally short-circuited to simulate corrosion conditions and exposed in the same indoor conditions of the galvanic sensors.

- *second set*

The second set of galvanic sensors has been prepared for corrosion monitoring of the “Porta del Paradiso”, a masterpiece of Italian Renaissance, created by Lorenzo Ghiberti, between 1425 and 1452 (**figure 2.7**).

1. Adam and Eve
2. Cain and Abel
3. Noah
4. Abraham
5. Isaac with Esau and Jacob
6. Joseph
7.Moses
8. Joshua
9. David
10. Solomon and the Queen of Sheba

Figure 2.7 ten panels of the Porta del Paradiso, courtesy of work of thesis of Laura Brambilla

It is a gilded bronze artwork made using the technique of indirect lost-wax casting and then gilded. The "Porta del Paradiso" was the main entrance of the Baptistery of Florence and it was located in front of the Duomo of Santa Maria del Fiore. The artworks is constituted by 10 panels representing different episodes of the Bible, 24 friezes with small statues of biblical personages and 24 medallions with heads and small busts.

The metal used for the casting is a quaternary alloy constituted by copper, zinc, tin and lead. The average chemical composition (wt. %) of three panels (Moses, Adam and Eve and David) is reported in the following table (**table 2.8**).

Table 2.8 composition of three panels of the "Porta del Paradiso"

	Cu	Sn	Pb	Zn	Fe	Ni	Ag	Co	Sb
VII (Moses)	93.51	0.13	1.14	3.78	0.13	0.14	0.06	0.00	0.13
I (Adam and Eve)	91.12	2.09	1.37	3.43	0.47	0.22	0.05	0.03	0.44
IX (David)	95.19	0.70	0.84	1.10	0.38	0.17	0.05	0.02	0.50

Alloys of quite similar composition have been used as substrates for the preparation of galvanic sensors (**table 2.9**). Sensors made of copper substrates (Cu 99.99 %) have also been prepared.

Table 2.9 bronze substrate composition

Cu	Pb	Sn	Fe	Al	Ni	Mn	Sb	P	Si	Zn
88.35	1.58	5.66	0.12	0.00	0.57	0.00	0.02	0.03	0.00	3.50

Sixteen galvanic sensors have been realized (**table 2.10**). They will be soon installed in the new showcase where the "Porta del Paradiso" will be exposed. Conditioning period and continuous monitoring of their macro couple current are now ongoing.

Table 2.10 second set of galvanic sensors

	number of Cu sensors	number of Bronze sensors
BCC	-	-
S&C	3	3
brocchal	2	3
brocnan	2	3

2.2 Protective coatings for copper and bronze artefacts

Laboratory tests have been performed to evaluate the efficiency of protective coatings in two different condition: urban condition and stressed condition.

2.2.1 Urban condition

Bronze samples have been studied after more than two years exposure time (27 months, from July 2012 to October 2014).

They have been exposed at 45° from the horizontal facing south at an urban site in Milan to test the effectiveness of different protective treatments.

The alloy composition is Cu 88.3 %, Sn 5.7 %, Zn 3.9 %, Pb 1.6 % and it is representative of the real copper-alloys used during XIX century for bronze artefacts production.

Both not-patinated and patinated bronzes have been studied; the composition of the artificial patina was obtained in foundry by combining K_2S and NH_4Cl.

The application has been made by brush by OPD specialists. Protective treatments have been applied in combination with corrosion inhibitors to valuate any synergic effect (**figure 2.8**). Moreover, double and triple layer of different protective have been tested (**figure 2.9**)**.**

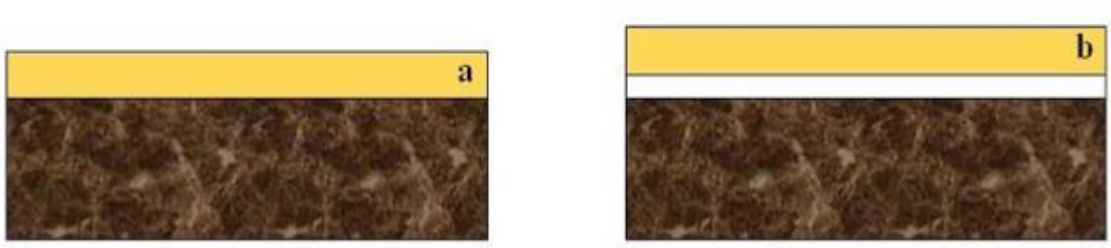

Figure 2.8 a) bronze sample (brown) with a single layer protective (yellow); b) synergic use of inhibitor (white) and protective (yellow) on a bronze sample (brown)

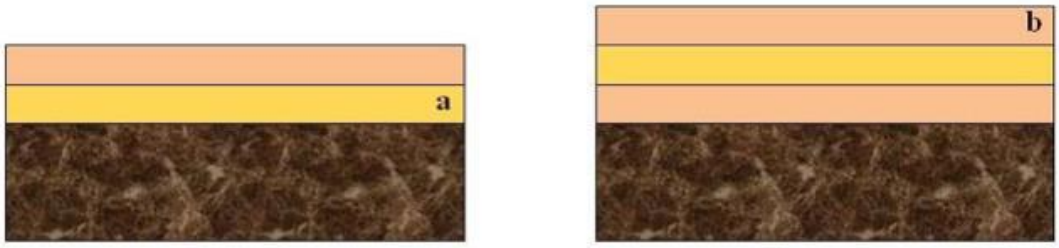

Figure 2.9 a) double layer protective (yellow and pink) on a bronze sample (brown); b) triple layer protective (pink, yellow and pink) on a bronze sample (brown)

The chemical structure and properties of the selected protectives and inhibitors have been studied in previous works (Beltrami 2011; Brambilla 2011).

The protectives are listed below:

- Soter wax
- Incral 44
- Resvax wax
- Fluoline
- Polysiloxane
- Polylactic acid.

The corrosion inhibitors are listed below:

- BTA
- Mercaptobenzothiazole
- Sodium Oleate
- Tolyltriazole.

Incral 44, Soter wax and BTA are commercial products widely employed for the conservation of copper-alloys artefacts. Resvax wax and Fluoline have been chosen according to previous scientific researches of OPD laboratories. Polysiloxane is commonly used for stone protection and its action

on the protection of bronze artefacts has been studied. Polylactic acid has been synthetized by Chemical Department of Florence University. Mercaptobenzothiazole, Sodium Oleate and Tolyltriazole have been chosen according to their lower toxicity with respect to BTA.

The list of the samples according to the different surface characteristics (patination) and applied products is reported in **table 2.11**.

Table 2.11 samples exposed in urban condition

treatments	inhibitors	patination	extended name
-	-	No	NNNTNIA
		Yes	PNNTNIA
Resvax	-	No	NNCRNIA
		Yes	PNCRNIA
	BTA	No	NNCRBZA
		Yes	PNCRBZA
	Mercaptobenzothiazole	No	NNCRMEA
		Yes	PNCRMEA
	Sodium Oleate	No	NNCROLA
		Yes	PNCROLA
	Tolyltriazole	No	NNCRTTA
		Yes	PNCRTTA
Soter	-	No	NNCSNIA
		Yes	PNCSNIA
	BTA	No	NNCSBZA
		Yes	PNCSBZA
Fluoline	-	No	NNFLNIA
		Yes	PNFLNIA
	BTA	No	NNFLBZA
		Yes	PNFLBZA
	BTA	No	NNFLMEA
		Yes	PNFLBZA
	Sodium Oleate	No	NNFLOLA
		Yes	PNFLOLA
Polysiloxane	-	No	NNSINIA
		Yes	PNSINIA
	BTA	No	NNSIBZA
		Yes	PNSIBZA
Polylactic Acid func. BTA	-	No	NNPFNIA
		Yes	PNPFNIA
Polylactic Acid mix. BTA	-	No	NNPMNIA
		Yes	PNPMNIA
Double Layer	-	No	NNDSNIA
		Yes	PNDSNIA
	BTA	No	NNDSBZA
		Yes	PNDSBZA
Triple Layer	-	No	NNTSNIA
		Yes	PNTSNIA

The durability of the protective coatings and the protection performances have been studied using electrochemical techniques (LPR and EIS that have been validated, as previously mentioned). Colorimetric measurements have been performed to evaluate colour alteration after two years of natural ageing. SEM-EDX and stereomicroscope analysis have been used to study surface morphology and elemental composition. This characterization has been useful to observe exposure effect on protected surfaces and to define the best protective performances.

Experimental tests before exposure were performed during previous works of thesis (Beltrami 2011; Bressan 2011).

The surface characterization has been performed on a small area of each sample (a hole of 12mm diameter) by using a special mask to monitor the same area during time.

2.2.2 Stressed condition, the case study of "Mi fuma il cervello (Autoritratto)" by Alighiero Boetti

"Mi fuma il cervello" is an iconic self-portrait of Alighiero Boetti (Turin, December 16, 1940 – Rome, April 24, 1994), made of bronze.

The artist represents himself standing up and holding a copper hose, which conveys demineralized water; as water hits the sculpture's head, steam rises at about 300° C (**figure 2.10**). The working conditions of the statue are thus very critical.

Figure 2.10 front and back view of "Mi fuma il cervello"

The artwork was originally designed in the 70s and completed few months before the artist's death, in 1990. Ugo Vismara, an artisan who still works in the foundry (**figure 2.11**), realized the sculpture at Fonderia Artistica Battaglia in Milan.

Figure 2.11 Alighiero Boetti and Ugo Vismara during statue fabrication, courtesy of Fonderia Artistica Battaglia (www.fonderiabattaglia.com)

The work of art depicts a fountain, nevertheless its meaning alludes to a representation of the thought process, in line with Boetti's conceptual poetics. To achieve this purpose, the sculpture's

head contains a pump and an electrical box; these produce water vapor, which spreads in the air creating a striking effect on the observer. Therefore, “Mi fuma il cervello” represents the flow of thoughts. Limescale continually forms on the sculpture’s head because of residual water (Modrone 2008).

Recently, the artwork has been brought to the restoration workshops of the Fonderia Battaglia to limit its deterioration and to restore it for future expositions.

The removal of limescale is necessary to preserve vapor emission, legibility and appearance. Currently, the statue is exposed at the exhibition “Alighiero Boetti, tra sé e sé abbracciare il mondo”: a retrospective in memory of the artist on the 20th anniversary of his death, edited by Francesca Franco and Sergio Risaliti and organized by Christian Stein Gallery, Milan.

The restoration, made by Fonderia Artistica Battaglia, has allowed to remove the carbonate patina that largely covered head and shoulders, by using ultrasound and mechanical tools (**figure 2.12**). These tools have allowed the abrasion of calcareous deposits without damaging the bronze’s patina, which was formed on the head because of a prolonged heat exposure.

Figure 2.12 statue and head detail during restoration

One of the major problems concerns with the fact that this restoration is not a definitive solution. In fact, when the artwork is exposed again, carbonate crusts will form once more, deteriorating the patina of the bronze substrate.

The research has been conducted in collaboration with the restorers of Fonderia Artistica Battaglia laboratories, in order to identify a protective able to create a resistant surface layer that helps the future removal of carbonates without altering the bronze below and acting as sacrificial layer.

The surveys have focused on three types of siliconic commercial paints (Talken, Dupli-Color, Saratoga), resistant to very high temperature (up to 600 °C). They have been subjected to an accelerated ageing process in order to test their thermal resistance, ability to maintain the aesthetic properties, chemical physics compatibility and reversibility under prolonged stress.

The samples used have the same composition of the statue. They have been treated to create a patina made of ammonium sulfide, which simulates the one of the statue. The commercial paints have been applied according to the indications of the suppliers. The samples have been exposed to similar conditions of the statue that is pouring rain and heat. The water used is not demineralized: in fact, the purpose was to simulate the worst conditions helping the formation of carbonate deposits on the surface to test their removal from the painted surface.

The samples have been provided by Fonderia Battaglia; they have dimensions of about 6 cm x 6 cm and the same composition of the statue (**table 2.12**).

Table 2.12 composition of bronze samples

Cu	Pb	Sn	Fe	Al	Ni	Mn	Sb	P	Si	Zn
88.22	1.81	5.57	0.10	0.00	0.21	0.00	0.04	0.03	0.00	3.91

The protectives have been tested by using non-destructive in-situ electrochemical techniques (LPR and EIS that have been validated, as previously mentioned) and colorimetric measurements. The photo documentation of the samples has been achieved by using the Canon Power Shot A2100 IS device and the Leica M250C stereo microscope equipped with a Leica DFC290 digital camera for image acquisition at different magnification.

Fonderia Battaglia has provided two sets of samples. The first one has been subjected to a thermal ageing of two different durations (twenty-five hours and fifty hours); it is described in the following table (**table 2.13**). **Figure 2.13** shows the bronze samples.

Table 2.13 first set of samples

sample	protective	ageing	hours
0	-	-	0
1	Talken	-	0
1S1	Talken	T = 400 °C and continuous H_20	25
1S	Talken	T = 400 °C and continuous H_20	50
2	Dupli-Color	-	0
2S1	Dupli-Color	T = 400 °C and continuous H_20	25
2S	Dupli-Color	T = 400 °C and continuous H_20	50
3	Saratoga	-	0
3S1	Saratoga	T = 400 °C and continuous H_20	25
3S	Saratoga	T = 400 °C and continuous H_20	50

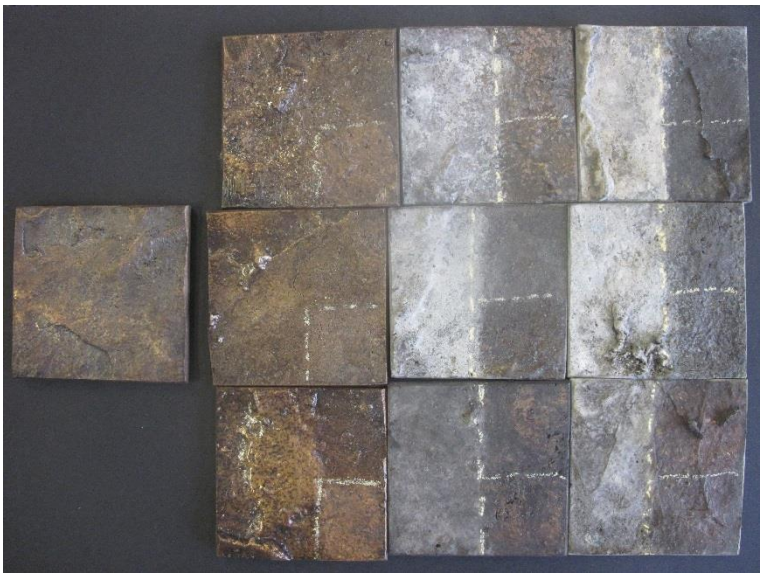

Figure 2.13 first set of samples

In the second set of samples, the treatment has lasted longer than in the previous one (one hundred hours), since during an exhibition the statue is exposed to heat and pouring rain for at least 8 hours per day. To make the ageing process as similar as possible to the real conditions of the statue, it has been chosen a temperature of 300 °C.

The ageing procedure details are shown in the following table (**table 2.14**). **Figure 2.14** shows the bronze samples not treated surfaces.

Table 2.14 second set of samples

sample	protective	ageing	hours
A	Talken	T = 300 °C and continuous H_20	100
B	Dupli-Color	T = 300 °C and continuous H_20	100
C	Saratoga	T = 300 °C and continuous H_20	100

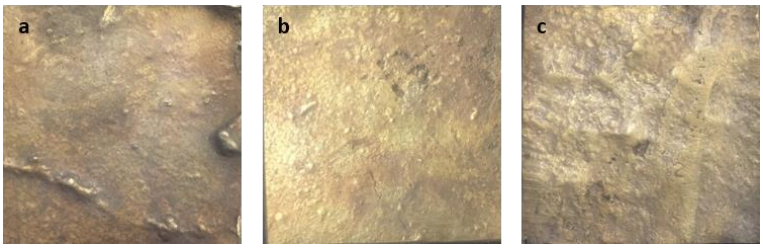

Figure 2.14 second set of samples before treatments

Before use, the silicone paints need a heat-treatment, in order to have a proper curing of the coating itself. This process has been applied only to the second set of samples, those exposed to the one hundred ageing procedure. Indeed, in the Cultural Heritage field, it is not always possible to subject an artwork to this kind of heat treatment in stove, due to the size of the piece or the location where the treatment has to be done. For these reasons, it seems reasonable to check also the efficiency of these paints without previous curing. Indeed, the first set of samples has been subjected to a shorter ageing procedure of twenty-five and fifty hours without previous heat-treatment.

2.3 Equipment

- *photographic documentation*

A Canon Power Shot A2100 IS ha been used for documentation.

- *stereomicroscope*

A stereomicroscope type Leica M250C, equipped with a Leica DFC290 digital camera for image acquisition (**figure 2.15**) has been used for the Alighiero Boetti "Mi fuma il cervello" specimens documentation. A specific setting of the illuminant has been defined in order to acquire all the images in the same conditions.

Figure 2.15 stereo microscope type Leica M250C

Documentation of the bronze samples exposed to urban condition took place in reflected light by using the Microscope Zeiss Mod. Stemi 2000-C with a halogen lamp source at Opificio delle Pietre Dure. Magnification is 32x. Images were acquired before and after exposure in the same reference area (a hole of 12mm diameter), localized by using a special mask.

- *SEM*

Scanning Electron Microscopy with Energy Dispersive Spectroscopy (SEM-EDS) was performed by using Zeiss EVO 50 EP instrument equipped with a LaB6 source and X-ray Oxford INCA 200-Pentafet LZ4 spectrometer to characterize surface morphology and determine elemental composition (**figure 2.16**).

Figure 2.16 Zeiss EVO 50 EP instrument, courtesy of Zeiss (www.zeiss.com)

- *colorimetric measurements*

Colorimetric measurements have been performed by using two different types of spectrophotometer. A Konica Minolta CM600D device has been used for the replicas of the Alighiero Boetti statue. A Konica Minolta CM2500D device with a D65 light source at 10° has been used for colour characterization of samples exposed in urban conditions (**figure 2.17**).

Figure 2.17 a) Konica Minolta CM600D; b) Konica Minolta CM2500D, courtesy of Konica Minolta (www.konicaminolta.com)

In this work of thesis the values were registered in the CIE L*a*b* colour reference space. A variable number of measurements were performed over each sample, following a regular and repeated pattern for all the specimens:

- 20 measurements in the first set of Alighiero Boetti replicas
- 10 measurements in the second set of samples

- 5 measurements in the bronze samples studied at Opificio delle Pietre Dure, by using the special mask with the hole of 12 mm.

Average values of the measurements have been calculated for L*, a* and b* parameters, which describe univocally the real colour of an object by a point in the colour space (L* value is represented on the central and vertical axis of the colorimetric sphere; a* and b* are on the horizontal plane) (**figure 2.18**).

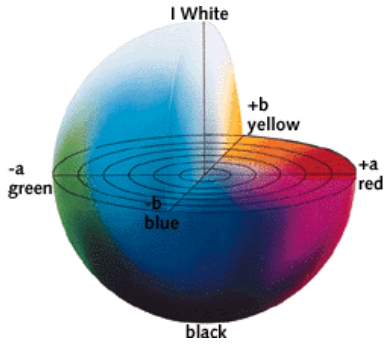

*Figure 2.18 CIE L*a*b* sphere, courtesy of commons.wikimedia.org*

In this uniform space, colour difference corresponds to the real difference perceived by the human eye. Colour variation is mathematically expressed by the following formula (EN 2010):

$$\Delta E = \sqrt{(\Delta L^2 + \Delta a^2 + \Delta b^2)}$$

where ΔE is the total colour variation, ΔL the brightness variation, Δa and Δb the chromatic coordinates variation.

For bronzes exposed in urban conditions, L*, a* and b* parameters acquisition occurs in SCI (Specular Component Included) modality, according to previous researches (Bressan 2011). Both SCI and SCE (Specular Component Excluded) have been used for the characterization of Alighiero Boetti replicas. In this casa also spectra values have been collected (400 nm < λ < 700 nm).

- *electrochemical measurements*

Linear Polarization Resistance and Electrochemical Impedance Spectroscopy measurements used a portable potenziostatic device: Ivium Technologies CompactStat with Ivium® software. Both techniques are described in the previous paragraphs (see 2.1 and 2.1.1).

- *climatic chamber and multimeter*

The macro couple current has been continuously monitored by using a high precision Keithley 3706 multimeter. Driving force for the galvanic corrosion and electrical resistance of the artificial patina, which acts as electrolyte, have been recorded too. The resolution of the multimeter is 0.01 – 100 µV in the 100 mV – 300 V range, 0.1 µΩ – 10 Ω in the 1 Ω – 100 MΩ range and 1 pA – 1 µA in the 10 µA – 3 A range.

Galvanic sensor have been kept in a climatic chamber in the laboratory (**figure 2.19**). Temperature and relative humidity monitoring occurs by the means of ELR200 LSI Lastem T - RH sensors (-20 – 60 °C range, 0 – 100% relative humidity range, ± 0.5 °C temperature accuracy, ± 2% relative humidity accuracy).

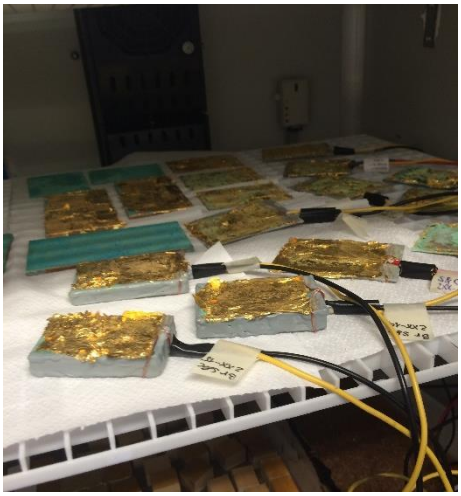

Figure 2.19 sensors in climatic chamber

RESULTS AND DISCUSSION

3.1 Validation of monitoring techniques

Environmental monitoring is extremely important for effective Cultural Heritage protection: from a coin inside a showcase, to a painting in a museum, from an outdoor statue or to an ancient building. The aim of in situ non-destructive monitoring is to collect all the necessary data and information to allow conservators to decide accurate conservation strategies without altering surfaces integrity, to ensure the artwork condition to be stable in time and the speed of decay to be low or at least acceptable.

3.1.1 Outdoor condition for copper alloys

Electrochemical monitoring techniques provide powerful tools for the characterization of the real state of health of metallic artefacts. To improve their reliability, it is it is important to evaluate the validity of their experimental procedures. A traditional and consolidated way for validating electrochemical methods is based on the comparison of corrosion rates measured by mass loss and those obtained by electrochemical tests.

As previously mentioned, an inverse proportionality between corrosion rate, i_{corr} (A/m^2), and polarization resistance, Rp (Ω·m^2) exists. It is expressed by the Stern-Geary formula:

$$i_{corr} = \frac{B}{R_p}$$

where B is a constant related to the anodic βa and cathodic βc Tafel slopes, according to:

$$B = \frac{(\beta a + \beta c)}{2 * 3(\beta a + \beta c)}$$

The B constant is necessary to calculate i_{corr} from the experimentally determined Rp, but its evaluation can be difficult especially for copper because it can be oxidized both to Cu^+ and Cu^{2+}. This is the reason why often it is preferable to use the Rp values in a direct and comparative manner. Indeed, polarization resistance values are very useful since they allow the estimation of the artefacts degradation and the evaluation of the efficacy of surface protectives and inhibitors.

However, it may be very useful to obtain also a good estimation also for i_{corr} values, since this parameter can be more easily used and understood in the Cultural Heritage field and by restorers. As previously mentioned, constant B evaluation from the Tafel slopes is often difficult (Goidanich,

Ormellese et al. 2006), as an alternative it is possible to use B values already published in the literature for active metals or to evaluate them empirically from gravimetric measurements.
According to literature (Pedeferri and Cigada 1993), the B values related to a generic monoelectronic or bielectronic process are represented in the following table (**table 3.1**).

Table 3.1 common B values from literature for Cu

		B (mV/decade)
$Cu = Cu^{+} + e^{-}$	monoelectronic	120
$Cu = Cu^{2+} + 2e^{-}$	bielectronic	60

Using mass loss values obtained through gravimetric tests ($g/m^2 \cdot y$), corrosion rate is calculated (A/m^2) by using the Faraday's law. Constant B is estimated according to the Stern-Geary formula for copper and bronze samples. This experimental procedure aims at defining a methodology that allows calculating reliable values of i_{corr} from experimental Rp.
Since corrosion attack varies significantly, especially in the first period of exposure, a set of Rp measurements has been repeated during time on the same samples used for mass loss, which procedure is accurately described in previous chapter.
In **figures 3.1** and **3.2**, Nyquist and Bode plots obtained through EIS technique are represented for copper and bronze samples. They have been exposed at 45° from the horizontal facing South in not-sheltered conditions. Exposure went on for 7 months at an urban site in Milan. After exposure, gravimetric tests have been carried out.

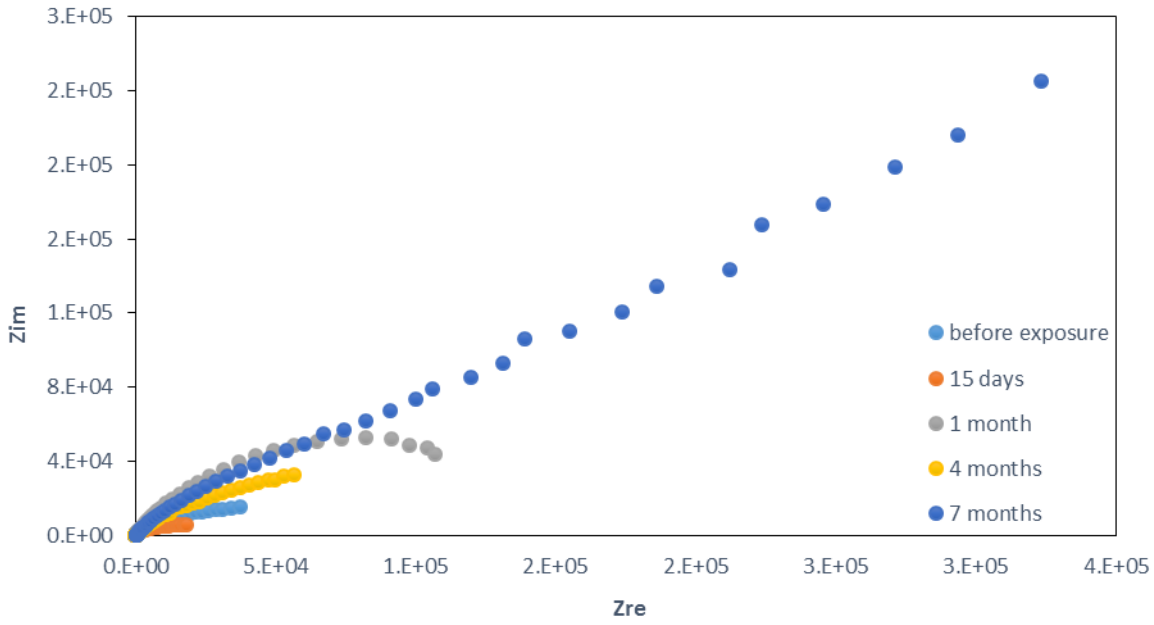

Figure 3.1 Nyquist plot of Bronze Y during 7 months outdoor exposure

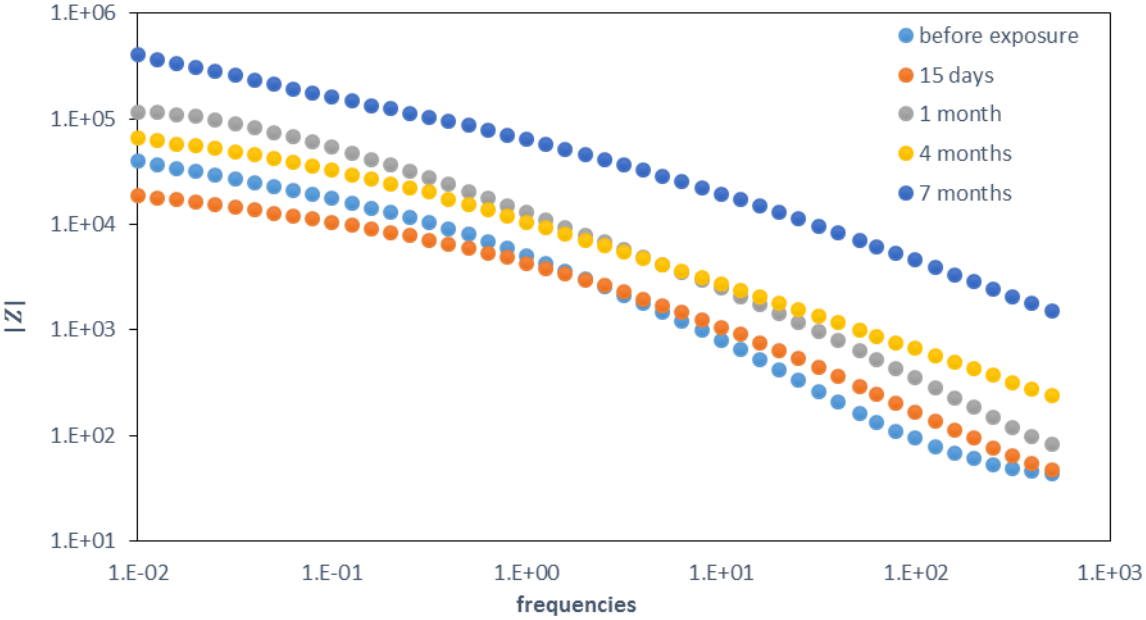

Figure 3.2 Bode plot of Bronze Y during 7 months outdoor exposure

The Nyquist plots may be used to analyze the impedance spectra in order to determine the simple electrical components (i.e., resistors, capacitors and inductors) of an equivalent circuit model, able to represent metal/solution interface. All the most common equivalent circuits proposed in the literature have been tested (GUILMINOT, RAMEAU et al. 2000; Afshari and Dehghanian 2010;

Beltrami 2011), but unfortunately data fitting with electrical modelling have not been able to give reliable results due to the high error associated.

Only Bode plots have thus been used to obtain Rp values. Indeed, at high frequencies, Bode plots contain information on the electrolyte resistance; while at low frequencies, they contain information on the corrosion processes on the metallic substrates. According to Zhang et al. studies, corrosion rates have been derived with an easy method from the difference in EIS data of $|Z|$ between the low and high frequency ranges. The higher $|Z|$, the lower corrosion rate (Zhang 2002; Cano, Bastidas et al. 2010; Cano, Lafuente et al. 2010; Pons, Lemaitre et al. 2013; Prosek, Kouril et al. 2013).

In **figures 3.3** and **3.4**, average Rp values and standard deviations (Ω/m^2) obtained through LPR and EIS are plotted as function of time for copper and bronze samples.

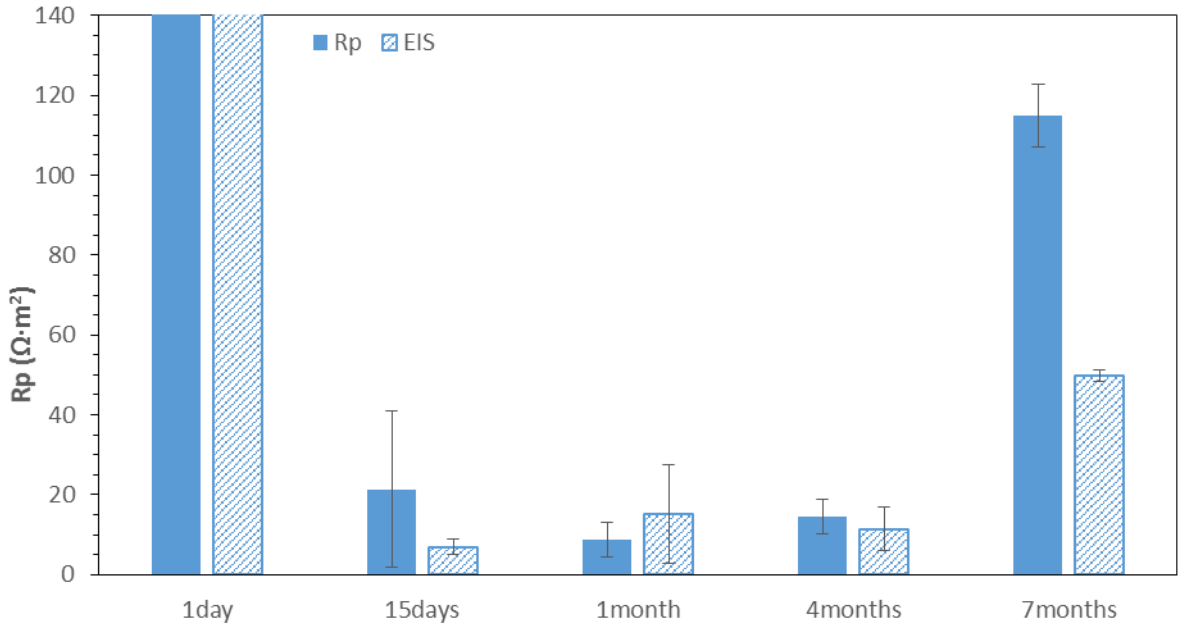

Figure 3.3 average Rp values and standard deviations (Ω·m2) for Cu

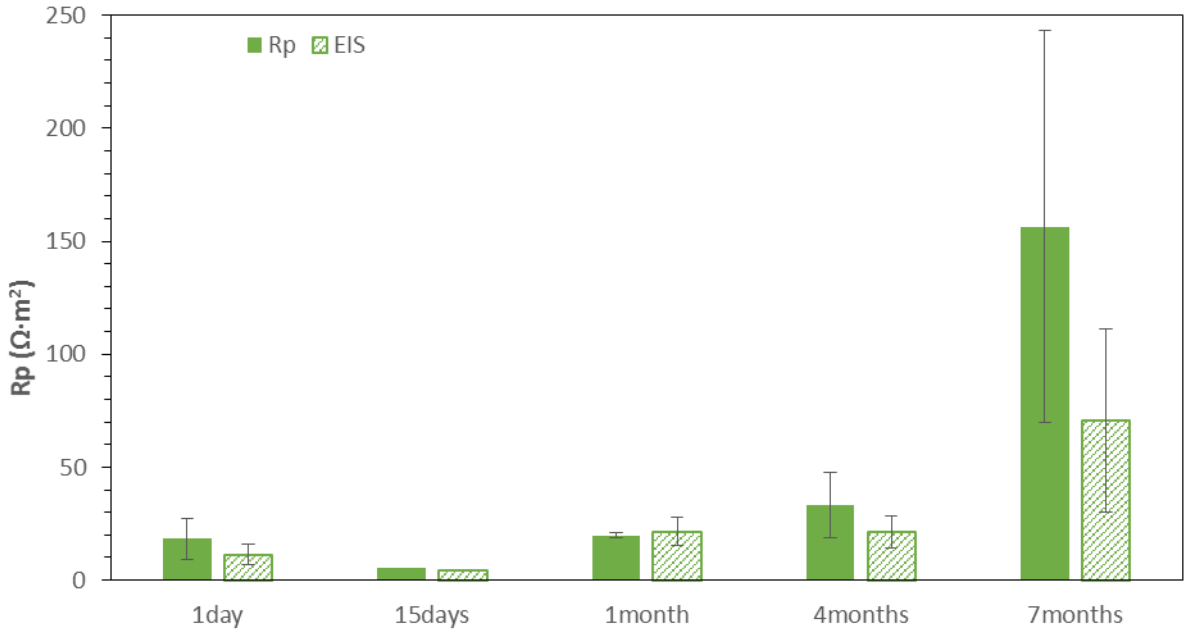

Figure 3.4 average Rp values and standard deviations (Ω·m2) for bronze

High Rp values calculated for Cu samples on the first day of exposure are ascribed to the presence of a superficial protective coating that was not removed by the degreasing procedure performed with acetone before exposure. This is confirmed by the fact that if the surface is polished, Rp values are significantly lower (**table 3.2** and **figure 3.5**).

Table 3.2 Rp values (Ω·m2) for polished and not-polished Cu samples

	Rp (Ω·m²) from LPR	**standard deviation (Ω·m²)**	**Rp (Ω·m²) from EIS**	**standard deviation (Ω·m²)**
polished Cu	4.01	-	2.54	-
not-polished Cu	578.75	48.31	313.07	43.19

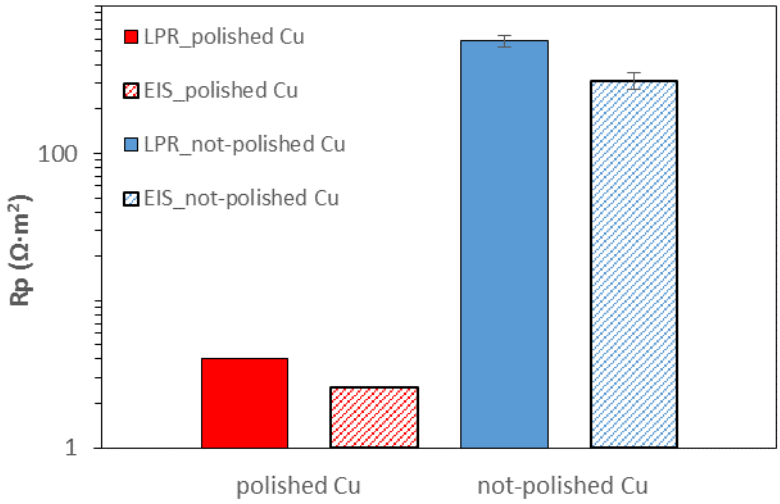

Figure 3.5 effect of surface protective on Rp values (Ω·m2) of Cu (logarithmic scale)

By observing **figures 3.3** and **3.4**, it is possible to note that in the first stage of exposure Rp values are low, with the only exception for copper on the first day. Due to the inverse proportionality defined by the Stern-Geary formula, it means high corrosion rate. By increasing the exposure time, Rp increases and corrosion rate decreases because of the formation of protective corrosion patinas on the surfaces of exposed samples.

When i_{corr} is high and Rp is low, LPR and EIS techniques give similar values; for lower i_{corr} and higher Rp, LPR gives higher results than EIS, in the presence of a protective coating or of a superficial protective patina.

Previous results (Odnevall Wallinder and leygraf 1997; Odnevall Wallinder 2002; Odnevall Wallinder, Bertling et al. 2004; Odnevall Wallinder, Bertling et al. 2004; Odnevall Wallinder, Hedberg et al. 2009; Brambilla 2011) indicate that normally in urban condition bronze corrosion rate values are lower with respect to copper ones, but in this case, they have similar value, with slightly higher values for bronze. This has most probably to be ascribed to the initial presence of a protective coating over the Cu samples. This is most probably the reason why the obtained Rp values of copper and bronze are very similar. By contrast, previous experimental studies shows that the Rp values of bronze are one order of magnitude higher than those of copper.

Table 3.3 shows the average values and corresponding standard deviations of corrosion rates from gravimetric tests ($g/m^2 \cdot y$), the calculated corrosion current (A/m^2), Rp ($\Omega \cdot m^2$) and constant B (mV/decade) for Cu^+ and Cu^{2+} hypothesis in copper and bronze samples. Polarization resistance

values are obtained with LPR and EIS. For Bronze it was supposed for simplicity that only copper was corroded.

Table 3.3 average values and standard deviations of v_{corr}, i_{corr}, Rp and B for copper and bronze

	Copper		**Bronze**	
	average value	**standard deviation**	**average value**	**standard deviation**
v_{corr} (g/m²·y) from weight loss	5.14	0.45	6.76	0.86
Rp (Ω·m²) from LPR	56.10	1.22	51.29	22.09
Rp (Ω·m²) from EIS	30.98	1.37	31.86	10.66
1) MONOELECTRONIC HYPOTHESIS ($Cu = Cu^+ + 1e^-$)				
i_{corr} (A/m²) from weight loss	2.47E-04	2.14E-05	3.25E-04	4.15E-05
B (mV/decade) experimental from LPR	13.86	0.90	16.35	6.19
B (mV/decade) experimental from EIS	7.64	0.33	10.44	3.78
i_{corr} (A/m²) from LPR (B = 120 mV/decade)	2.14E-03	4.64E-05	2.62E-03	1.01E-03
i_{corr} (A/m²) from EIS (B = 120 mV/decade)	3.88E-03	1.72E-04	4.10E-03	1.52E-03
2) BIELECTRONIC HYPOTHESIS ($Cu = Cu^{2+} + 2e^-$)				
i_{corr} (A/m²) from weight loss	4.94E-04	4.29E-05	6.51E-04	8.30E-05
B (mV/decade) experimental from LPR	27.71	1.81	32.70	12.38
B (mV/decade) experimental from EIS	15.50	0.71	21.00	7.81
i_{corr} (A/m²) from LPR (B = 60 mV/decade)	1.07E-03	2.32E-05	1.31E-03	5.04E-04
i_{corr} (A/m²) from EIS (B = 60 mV/decade)	1.94E-03	8.58E-05	2.05E-03	7.59E-04

It is possible to note that LPR and EIS give similar Rp trends and values. Weight losses confirm similar corrosion rates for both Cu and bronze, with slightly higher values for bronze.

Experimental B values are significantly lower than the theoretical ones from literature that in solutions are supposed to be 60 and 120 mV/decade for bielectronic and monoelectronic respectively.

Corrosion rate values obtained using electrochemical measurements are about one order of magnitude higher if compared to gravimetric measurements. This is due to the fact that the conditions of the electrochemical measurements simulate a constantly wet surface, due to the continuous surface contact with the liquid electrolyte and therefore it does not represent the real condition during outdoor exposure, as shown in previous works (Bartuli, Cigna et al. 1999; Schindelholz, Kellya et al. 2013).

It is important to remember that the conditions of the electrochemical measurements simulate a continuously wet surface, which is not the real situation for the exposed samples that are subjected to T and RH variations.

To obtain more reliable results of corrosion rate by using Rp data and B from the literature, one should quantify the effective period of time during which a structure exposed outdoors is covered by a thin layer of water (time of wetness). The wetting of the surfaces is caused by many factors, for example dew, rainfall, melting snow and a high humidity level. The time of wetness (TOW) as environmental parameter can be calculated as the hours per year characterized by a relative humidity higher than 80% and a temperature above 0°C (Baer, Sabbioni et al. 1989; Bartuli, Cigna et al. 1999; Corvo, Pérez et al. 2008; ISO9223:2012(E) 2012; Schindelholz, Kellya et al. 2013; Norberg 20012).

According to the ISO 9223:2012, exposure tests should start in the spring or autumn and last one year. In this work, 7 months exposure has been considered for reason of time. By using the meteorological data from Arpa Lombardia (www.arpalombardia.it), the fraction of wetness has been calculated about 0.24 for the 7 months exposure for the city of Milan, which is not a very dissimilar fraction of wetness about 0.28 for one-year exposure. As it is written in the standard ISO 9223:2012, the fraction of wetness should have a general validity, since the corrosion attack can vary from year to year, depending on the natural variation in climate. Among the five categories described in the ISO 9223:2012, Milan belongs to C3 category with medium corrosivity; the corresponding fraction of wetness may vary from 0.029 to 0.29.

Corrosion rate values have been recalculated by multiplying the values of corrosion rate evaluated from electrochemical measurements by the fraction of wetness and they have been expressed in µm/y. Results are shown in the **table 3.4** and **figure 3.6**.

Table 3.4 comparison of corrosion rate values as measured by means of different techniques, considering TOW for LPR and EIS

	Copper		Bronze	
	average value	**standard deviation**	**average value**	**standard deviation**
µm/y from weight loss	0.58	0.05	0.76	0.10
µm/y for Cu^+ from LPR	1.20	0.03	1.47	0.57
µm/y for Cu^+ from EIS	2.18	0.10	2.30	0.85
µm/y for $Cu2^+$ from LPR	0.30	0.01	0.37	0.14
µm/y for $Cu2^+$ from EIS	0.54	0.02	0.58	0.21

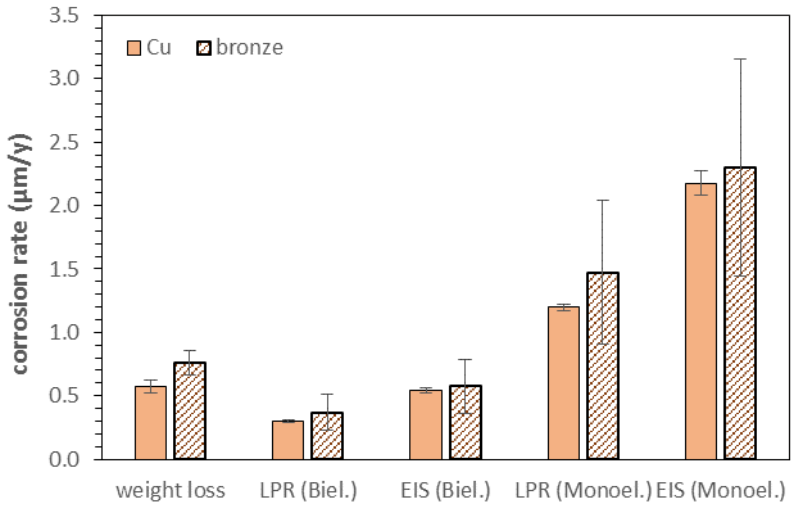

Figure 3.6 comparison of corrosion rate values as measured by means of different techniques and considering the TOW for LPR and EIS

The values obtained by supposing a bielectronic behaviour for the specimens are slightly lower than the data from weight losses; results for Cu^+ tend to significantly overestimate corrosion rate. Indeed, copper alloys show an intermediate electronic behaviour between Cu^+ and Cu^{2+} with normally prevailing Cu^{2+} copper among the corrosion products. Percentage error are represented in the following table (**table 3.5**).

Table 3.5 percentage error of corrosion rate with respect to mass loss

	% Copper	% Bronze
Cu^+ from LPR	108.76	93.62
Cu^+ from EIS	278.31	202.70
$Cu2^+$ from LPR	47.81	51.59
$Cu2^+$ from EIS	5.42	60.92

These values are in good agreement with the results of Bartuli et al. (they have the same order of magnitude). They aimed to investigate the corrosivity of the atmosphere on the Capitoline Hill in Rome where LPR has been used to evaluate the real condition of patinated bronze sculptures (especially the Marcus Aurelius equestrian monument) in terms of corrosion rate values. The results were compared to mass loss results of standard metallic specimens exposed in situ.

- *final considerations*

In the literature, LPR and EIS are not usually used simultaneously for in-situ measurements. The present analysis has intended to:

- compare the two techniques in order to assess the reliability of in-situ measurements
- provide an evaluation of the reliability of the results not only in terms of polarization resistance but also of corrosion rate.

LPR presents undoubted advantages, for example it allows a simple and fast measurement and a higher reproducibility of results (in fact, the standard deviations are lower); however, it cannot be applied when highly insulating coatings are present. On the other hand, EIS provides more information, but only if a proper equivalent circuit is individuated, and it can be applied even with highly insulating coatings. Nevertheless, it is difficult to find an equivalent circuit in the case of complex systems like the surfaces of metallic artefacts, so that its application is often limited to calculate the Rp values by using the Bode curves.

The two techniques provide similar results, which are coherent with the mass losses. In order to estimate the corrosion rate of copper alloys exposed to the atmosphere, it is suggested to considerate an oxidation of bivalent copper (B = 60 mV/decade) and to multiply the result by the fraction of wetness. In this way, underestimated values of corrosion rate with an error of 47.81 %

for Cu and 51.59% for bronze from LPR and 5.42 % for Cu and 60.92 % for bronze from EIS are obtained.

Nevertheless, a larger validation campaign with a greater number of alloys, during longer periods of exposure and in multiple exposition sites is required to confirm these results.

3.1.2 Indoor condition for gilded bronzes

LPR and EIS have been validated for in-situ measurements and they can provide important information. These electrochemical monitoring techniques give corrosion rates representative of a continuously wet surface during tests. Such measurements imply the wetting of surfaces that originally may be dry. After wetting, an initial acceleration of the corrosion process can occur: normally it is not dangerous but it may lead to an incorrect interpretation of the artefact state.

Furthermore, in the case of gilded bronzes, LPR and EIS cannot be applied due to the difficulties on the interpretation of results. A promising alternative is the use of galvanic sensors (Mazza, Pedeferri et al. 1977; Goidanich, Gulotta et al. 2014) specifically designed to simulate the stratigraphy of a corroded gilded bronze and to allow the continuous monitoring of the macro couple current density that flows between the gilding and the bronze and that is directly proportional to corrosion rate through Faraday's law. Therefore, the galvanic sensors overcome all the drawbacks of LPR and EIS and they can be used as replica of the original artefact in order to test new protective treatments, to study the degradation mechanisms and to monitor the impact of the environment.

The artificial patina is a key factor for the realization of galvanic sensors with good durability and reliability (Brambilla 2011; Goidanich, Brambilla et al. 2011). Thickness and adhesion to the metallic substrates are very important factors: the patina should be thick enough to avoid short circuits between the gilding and the substrate, but when the thickness increases, the overall durability tends to be reduced due to the presence of hygroscopic compounds, as chlorides, that tend to blister and detach from the metallic substrate.

The characteristics of the artificial patinas that have been set up for the preparation of galvanic sensors were summarized in **table 2.4**. The types of patinas have been chosen according to their relevance in the conservation and study of the gilded bronze artefacts (Goidanich, Toniolo et al. 11-15 October 2010; Fiorentino, Marabelli et al. 1982; Fiorentino 1994; Goidanich, Brambilla et al. 2011; Goidanich, Porcinai et al. 2013; Goidanich, Gulotta et al. 2014).

In order to increase the durability and the reproducibility of these sensors, their setup has been improved with respect to the sensors realized in previous works (Goidanich, Toniolo et al. 11-15 October 2010; Goidanich, Brambilla et al. 2011; Goidanich, Gulotta et al. 2014) with the main purpose of reducing the most affecting factors of degradation. Indeed, the use of the cuprite layer has been replaced by the polishing of metallic substrates with abrasive paper (100) to remove

oxidation products and to obtain a rougher surface. This approach was tested in this work for the first time with the aim of increasing patinas adhesion. Results confirmed that the elimination of the cuprite layer and the polishing of the surface lead to an improvement of the quality of the sensors in terms of reproducibility and reliability, compared to the previous sets used for the conservation of the "Porta del Paradiso" (Goidanich, Toniolo et al. 11-15 October 2010; Goidanich, Gulotta et al. 2014).

Eighteen galvanic sensors have been realized (see **table 2.5**); they have been put into a climatic chamber, periodically varying relative humidity (from 20% to 65%). A constant temperature has been maintained (T = 25 ± 3 °C). The macro couple current has been continuously monitored for seven months by means of a high precision multimeter.

In this work, macro couple current data (A/m^2) have been collected and corrosion rates (μm/y) calculated. Faraday's law allows the evaluation of the corrosion rate from macro couple current density.

However, in order to calculate corrosion rate from galvanic current, several assumptions are required:

- the bronze and the gilding have the same surface area
- the cathodic process of oxygen reduction occurs mainly on the gold leaf
- the anodic process of oxidation occurs only on Cu with the formation of mainly bimetallic corrosion products: $Cu = Cu^{2+} + 2e^-$
- corrosion is generalized.

Figure 3.7 represents RH trend during seven months exposure.

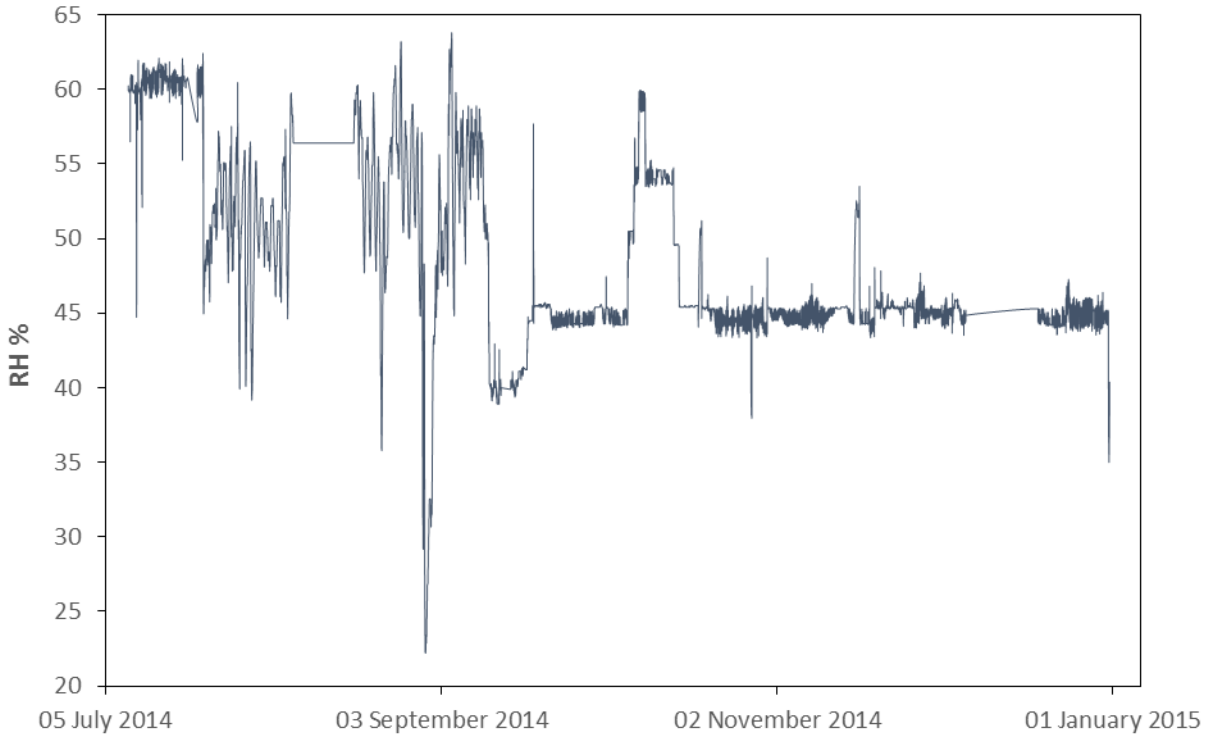

Figure 3.7 RH trend during exposure

The following figures (**figure 3.8**, **3.9**, **3.10** and **3.111**) represent current density trends plotted in logarithmic scale versus monitoring time. Each graph refers to a specific patina composition for both Cu and bronze substrates.

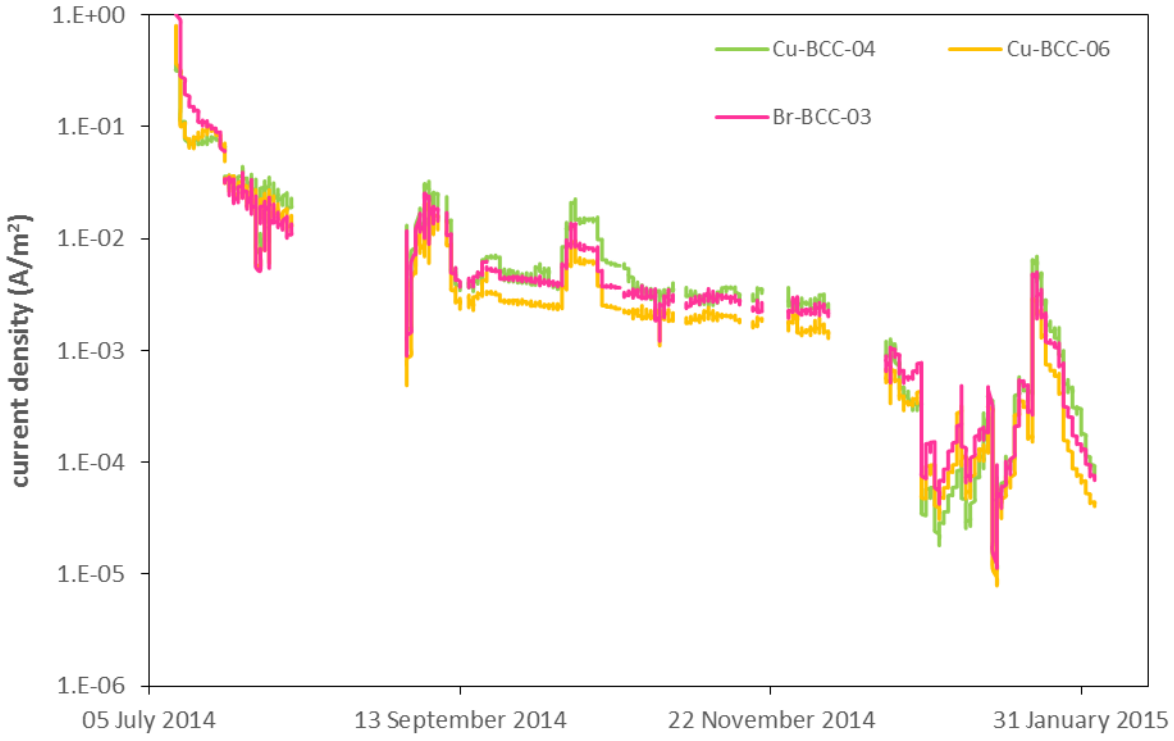

Figure 3.8 macro couple current as a function of time for galvanic sensors with Cu and bronze substrate and double layer of Basic Copper Chlorides (BCC) patina

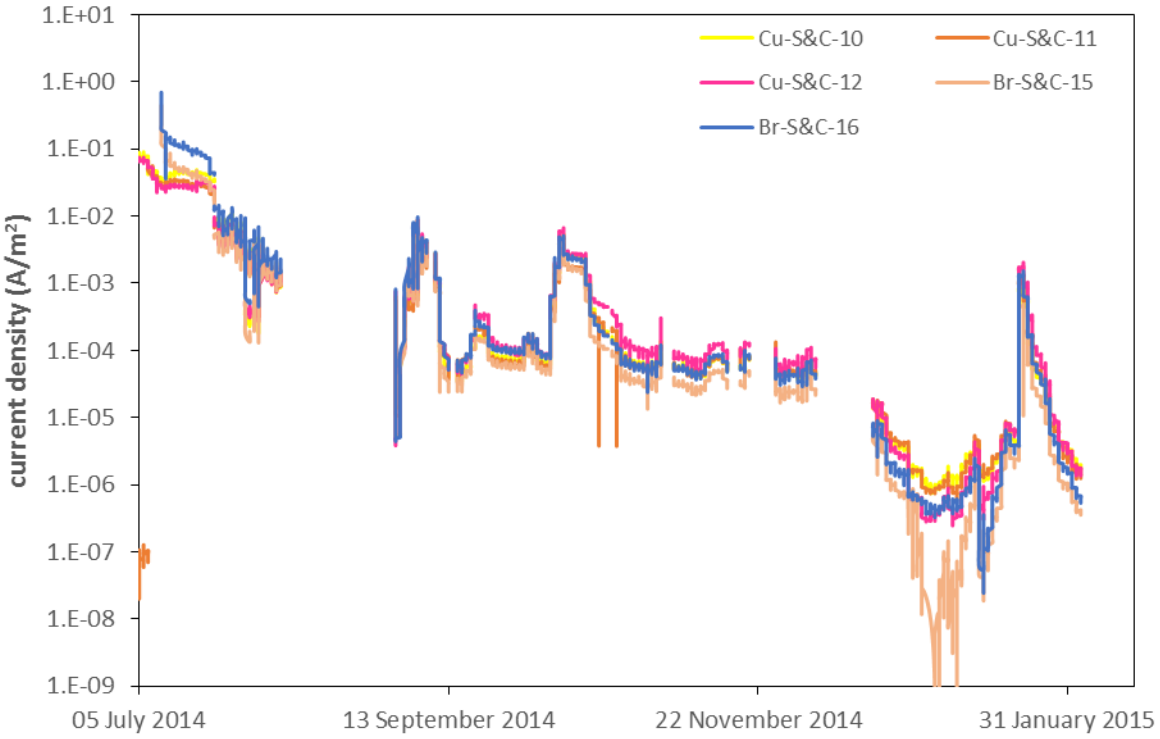

Figure 3.9 macro couple current as a function of time for galvanic sensors with Cu and bronze substrate and double layer of Sulfates & Chlorides (S&C) patina

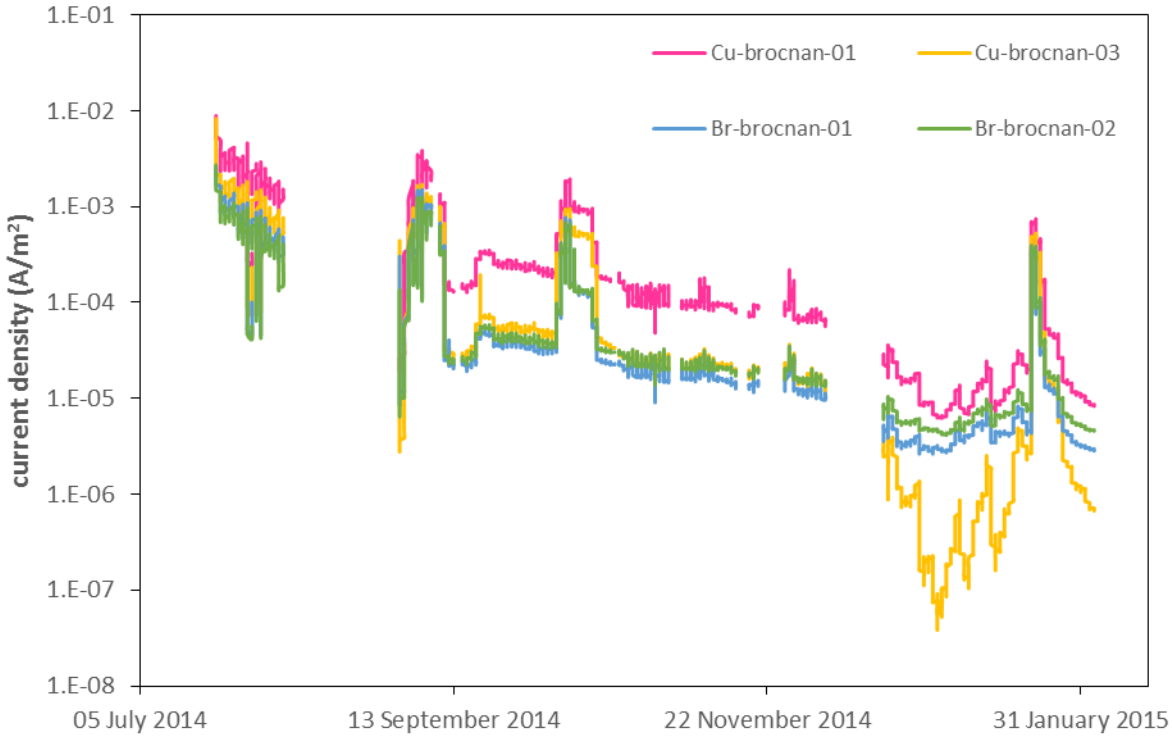

Figure 3.10 macro couple current as a function of time for galvanic sensors with Cu and bronze substrate and double layer of Brochantite and Nantokite (brocnan) patina

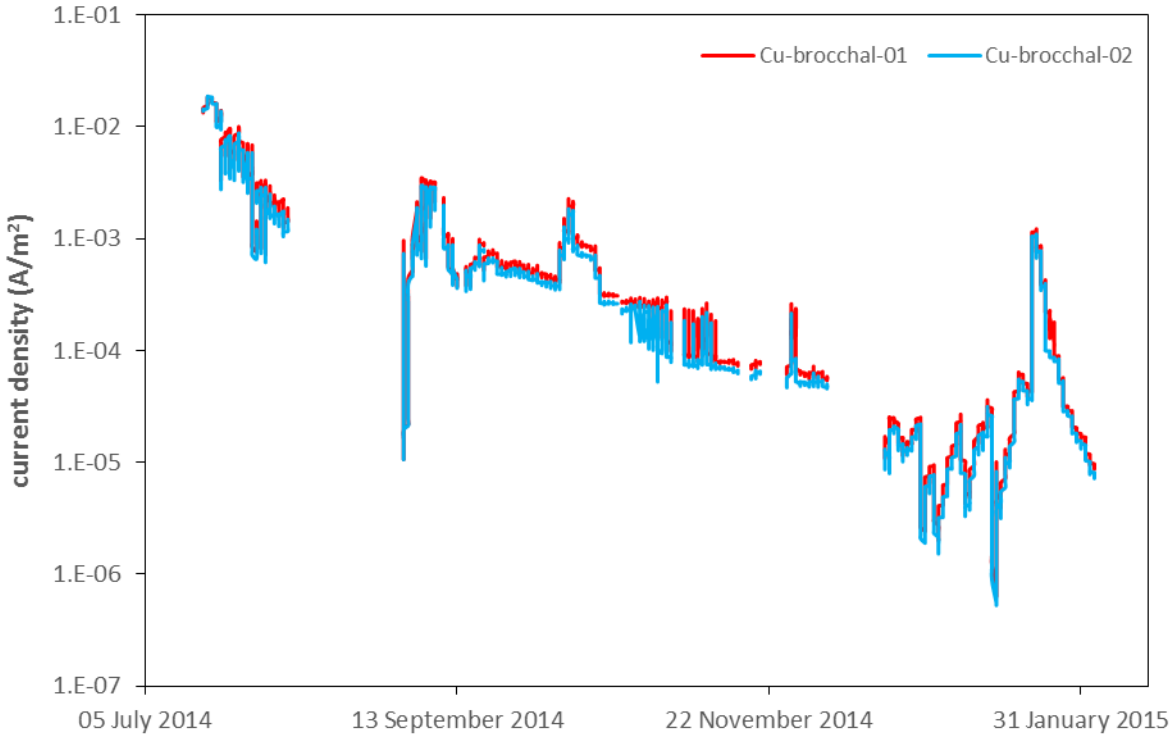

Figure 3.11 macro couple current as a function of time for galvanic sensors with Cu substrate and double layer of Brochantite and Chalcanthite (brocchal) patina

Some data are missing due to data acquisition problems during monitoring. Both relative humidity and current densities data are not available for the first days of December. After that period a general decrease of current density, if the same RH is considered, was observed for all the sensors. Unfortunately, due to the lack of data, it is not possible to give an explanation about the current density decrease after that period.

By observing previous figures, it is possible to observe that sensors with patinas of the same type show very similar behaviour with highly improved reproducibility of the macro couple signal. However, there are few exceptions represented for example by Br-S&C-15 in the last period of exposure in **figure 3.9** or by Cu-brocnan-03 in **figure 3.10**. Current density values seem to have a good reproducibility among sensors treated with the same patina, being brocnan the one with the worse reproducibility of signal

Galvanic sensors preparation is a laborious and handmade procedure, even if it has been standardized as much as possible thanks to previous laboratory researches. The check-up of the sensors is part of the procedure it is almost unavoidable to have to discard some of them after a period of preconditioning. They are also very delicate and sometime they need to be replaced. With the new improved procedure, the number of sensor that, on average, has to be discarded has been significantly reduced and their durability has significantly improved.

In general, initial current density values are higher due to the high moisture content of the patina and then they tend to reduce with time, even at the same RH values. Current density is strongly correlated with RH variations.

In **figure 3.12** and **3.13** average current density values and standard deviations (A/m^2) are reported. They refer to Cu and bronze sensors, which values have been calculated during the first four weeks monitoring at 55% RH.

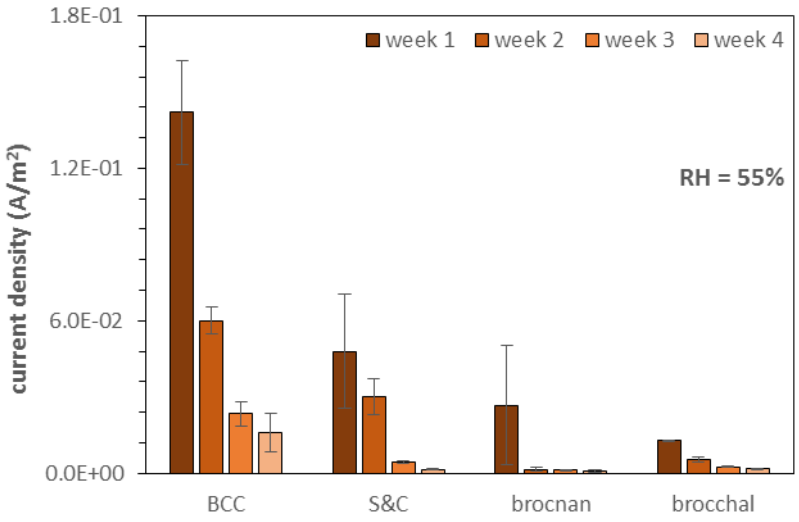

Figure 3.12 average current density values and standard deviations (A/m²) in the early stage of exposure for Cu sensors, RH = 55%

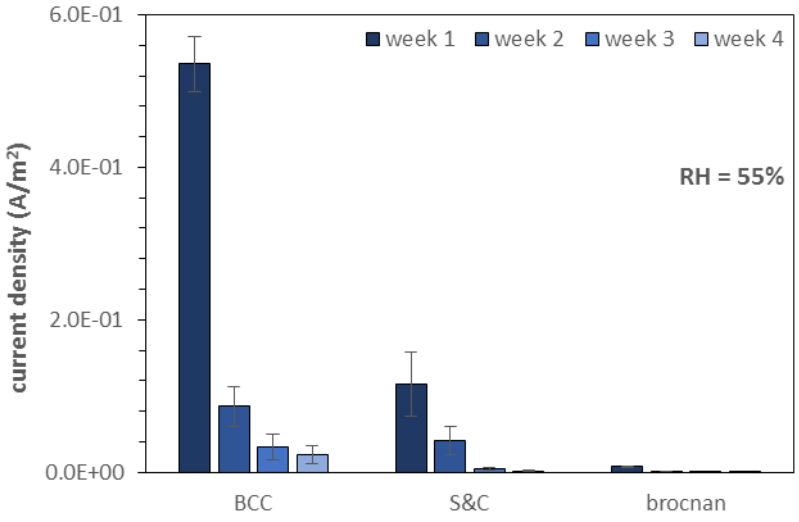

Figure 3.13 average current density values and standard deviations (A/m²) in the early stage of exposure for bronze sensors, RH = 55%

As it can be observed current density decreases significantly during the first weeks for all the type of patinas. This is because patination produces highly moistened corrosion layers. For this reason, the patinas are more conductive in the early stage of sensors exposition, the macro couple current is higher and the galvanic corrosion is enhanced. Therefore, it is necessary a conditioning period to allow the galvanic sensors to reach more stable values of corrosion rates before using them for monitoring.

During the conditioning period, a higher macro couple current density is recorded. As it can be observed, for the first week, current density reaches the highest values for all the patinas in both

copper and bronze sensors due to the higher water content, while it tends to attest at lower values in the later weeks, when moisture evaporation occurs. In addition, standard deviations decrease for increasing observation time, since they are calculated with respect to lower current density values.

Indeed, the effect of the conditioning period is confirmed in the following graphs. In **figure 3.14** and **3.15**, average monthly current density values and their standard deviations (A/m^2) are reported in a logarithmic scale for the first six months of exposure for all patina composition, for both Cu and bronze substrates and when RH = 45%.

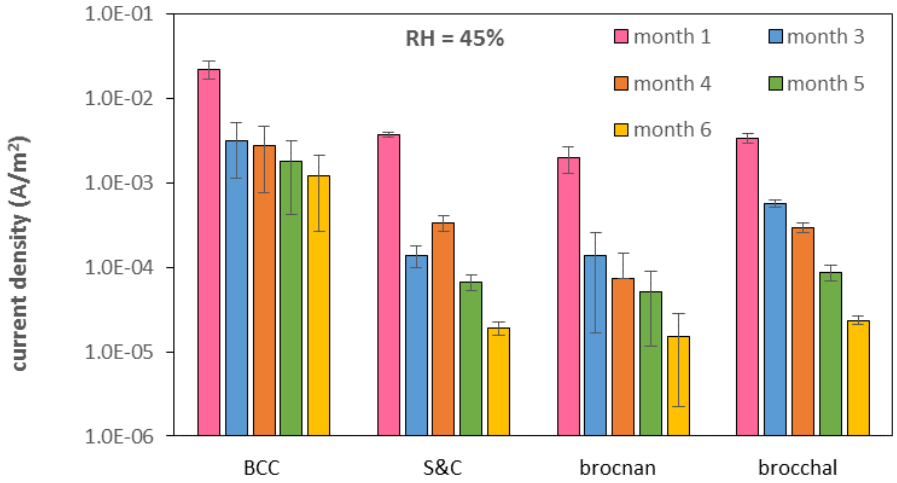

Figure 3.14 comparison among average current density values and their standard deviations (A/m^2) of Cu galvanic sensors during the first six months of exposure, RH = 45%

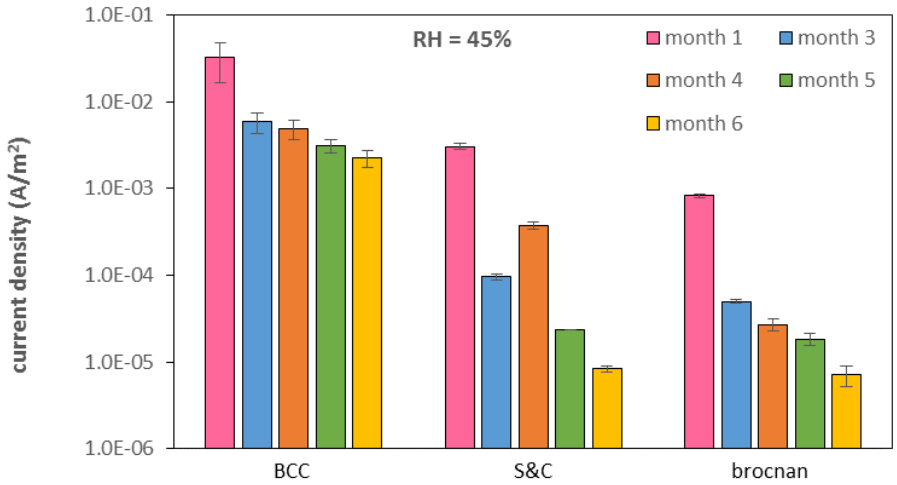

Figure 3.15 comparison among average current density values and their standard deviations (A/m^2) of bronze galvanic sensors during the first six months of exposure, RH = 45%

During the first month of exposure, current density values are one order of magnitude higher than in the following months.

The composition of the artificial patina is very important. Significant variations in terms of average current density (A/m^2) have been observed for different composition during different months of life at RH = 45%. BCC is the most corrosive patina with the highest current density, confirming previous results (Goidanich, Gulotta et al. 2014). It shows the highest current density values during the whole exposure time.

As previously mentioned, these graphs confirm that in general, current density values in the early steps of exposure are higher due to the high moisture content of the patina and then they tend to reduce with time, even at the same RH values. The only exception is S&C patina that during the fourth month of life shows a small current density increase on both Cu and bronze substrate with respect to the other months plotted in **figures 3.14** and **3.15**.

Galvanic sensors with the same artificial patina composition have a quite reproducible macro couple current density. Generally, deterioration of the sensors leads to a decrease of collected current density with the exposure time. Until now, just those containing chlorides in the patina composition show some small cracks and detachments as consequences of the cycles of high and low humidity to which they were subjected (**figure 3.16**).

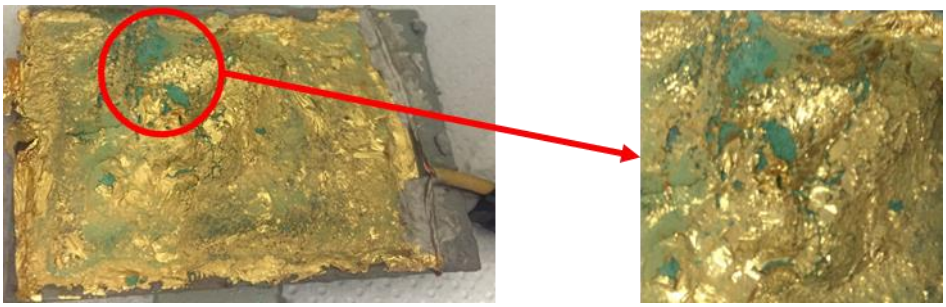

Figure 3.16 degradation on Cu-S&C-12 surface

- *mass losses and comparison with galvanic current results*

A set of mass loss tests has been performed and the obtained results have been compared with those obtained from galvanic sensors. The purpose was to evaluate how precisely corrosion rate can be estimated by using galvanic sensors. As previously mentioned, the measured galvanic

current is directly correlated to the corrosion rate; however, some assumptions are required to convert current into corrosion rate.

Twenty-eight samples have been realized and used for mass loss measurements (they have been previously described in **table 2.6**); they have been exposed in the same condition of the galvanic sensors. They are thirteen gilded and intentionally short-circuited samples with the same substrate composition of the galvanic sensors. In addition, fifteen non-gilded samples have been realized with the purpose of evaluating the feasibility of using the galvanic sensors also for the continuous monitoring of patinated or heavily corroded non-gilded bronzes.

It is important to underline that the patination process is highly corrosive and this should be considered while comparing mass losses and corrosion rates obtained by galvanic current monitoring. Indeed, the highest current density values are collected during the early stage of indoor exposure, as previous graphs (**figure 3.12 – 3.15**) have shown for all patina compositions, when the moisture of the patina is still high. The patinas have a high water content and they are more conductive in the first period of exposure. The collected current density values are higher and corrosion is enhanced. Indeed, a conditioning period must be considered to reach more stable values of corrosion rates and lower macro couple current density.

Therefore, preliminary tests were performed in order to estimate the mass loss after twenty-four hours from the patination procedure.

Any lack of reproducibility or errors associated to this kind of tests will affect significantly the following results and comparisons with galvanic sensors, especially in the case of sensors that have lower current densities and therefore corrosion rates.

Average values and standard deviations of mass loss related to patination (g/m^2) and average values and standard deviations of mass loss related to seven months exposure (g/m^2) of both gilded and not gilded specimens are reported in the following table (**table 3.6**) for different patinas composition and for both Cu and bronze substrates.

Table 3.6 average values of mass losses and standard deviations (g/m²) associated to patination and to seven months exposure for Cu and bronze substrate

COPPER						
	Cu 24 h		**Cu not gilded 7 months**		**Cu gilded 7 months**	
	average (g/m²)	**standard dev. (g/m²)**	**average (g/m²)**	**standard dev. (g/m²)**	**average (g/m²)**	**standard dev. (g/m²)**
BCC	14.49	1.63	45.81	4.17	51.79	6.74
S&C	26.31	1.31	58.43	1.60	63.39	1.84
brocnan	6.82	-	12.82	2.10	13.34	0.59
BRONZE						
	Bronze 24 h		**Bronze not gilded 7 months**		**Bronze gilded 7 months**	
	average (g/m²)	**standard dev. (g/m²)**	**average (g/m²)**	**standard dev. (g/m²)**	**average (g/m²)**	**standard dev. (g/m²)**
BCC	16.07	0.10	48.51	-	51.57	-
S&C	31.70	5.18	64.51	0.95	64.37	2.10
brocnan	7.09	-	10.79	-	17.20	-

By subtracting mass losses due to patination after twenty-four hours to the values obtained after seven months indoor exposure, the following average corrosion rates and standard deviations (µm/y) have been estimated for both gilded and not gilded samples (**figure 3.17**).

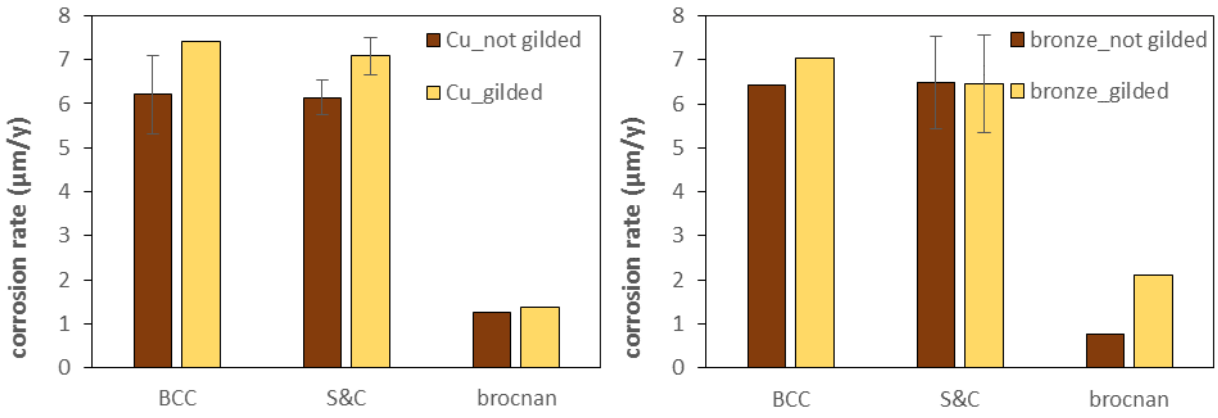

Figure 3.17 average corrosion rates and standard deviations (µm/y) for gilded and not gilded sensors by considering mass losses due to patination procedure: Cu substrate (left), bronze substrate (right)

By considering mass losses due to patination procedure in **table 3.6**, it is possible to observe that quite similar values are obtained for both Cu and bronze substrates for different patina composition.

S&C seems to be the most aggressive patina procedure on both substrates. Indeed, its values are about twice BCC mass losses. After twenty-four hours, S&C mass loss represents about 50% of the total value estimated after seven months exposure (see **table 3.6**), while average values of corrosion rates reported in **figure 3.17** are almost the same for both BCC and S&C patinas on both substrates. In addition, by observing previous graphs obtained from the monitoring of the galvanic sensors for both BCC and S&C (**figures 3.8** and **3.9**), the two patinas have quite similar current density values for high RH, while, if RH is low, S&C sensors seem to be less corroded. Thus, lower average corrosion rates for S&C samples were expected according to galvanic sensors trends and current density evaluation. It has to be considered that the first hours of monitoring are very crucial, especially for BCC and S&C patinas, and any delay may affect the estimated cumulated corrosion. Indeed, even few hours of asynchrony between mass losses and galvanic sensors monitoring may significantly affect the final comparison between the two techniques. In addition, the patination procedure contribute to the total mass loss is very high. Therefore, it would be useful to perform further tests with an improved experimental methodology in order to verify if really BCC and S&C provide a similar corrosion rate for all relative humidity conditions. It is suggested to extend to one week the time for the evaluation of the mass loss related to the patination technique and then start monitoring with galvanic sensors after one week from the realization of the sensors. It is also suggested to prepare two sets of samples to be kept at two different and constant values of relative humidity and for longer exposure time, in order to identify the real influence of RH on patina aggressiveness and corrosivity.

In **figure 3.17**, gilded and not gilded samples average corrosion rates and standard deviations have been compared. Average corrosion rates of gilded samples are just slightly higher than the not gilded ones due to the effect of gold/bronze galvanic couple. The only exception is represented by S&C patina applied on bronze substrates, since the values are almost the same.

There are not high differences between corrosion rates evaluated for the same patina applied on different substrates. The differences between corrosion rates of gilded and not gilded samples with both substrates with the same patina are not relevant, with the exception for brocnan patina applied on bronze substrate: corrosion rate is estimated 0.77 μm/y for not gilded bronze substrate and it is one order of magnitude lower than the gilded one. This may be related to some localized

corrosion process due to the presence of chlorides that is enhanced on bronze substrate and in the presence of galvanic coupling. However, this may also be associated to errors on the evaluation of the patina procedure mass loss, which, as previously discussed, has a high impact on the result. A more correct comparison between gilded and not gilded samples can be obtained by comparing the total mass losses, including the one related to the patination procedure (**figure 3.18**).

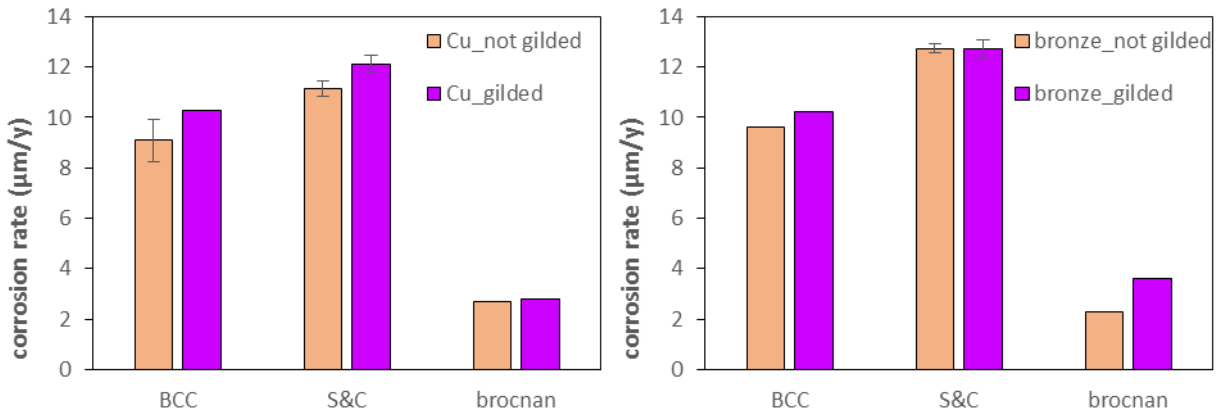

Figure 3.18 average corrosion rates and standard deviations (µm/y) for gilded and not gilded sensors without considering mass losses due to patination procedure: Cu substrate (left), bronze substrate (right)

Previous observations are confirmed: indeed, the differences between corrosion rates of gilded and not gilded samples with both substrates with the same patina are not relevant. Without considering mass losses due to patination procedure, brocnan average corrosion rates differences on bronze substrate are reduced, even if they are still higher with respect to the other samples.

Since average corrosion values are not significantly different for gilded and not gilded samples, it is possible to use the galvanic sensors also for the continuous monitoring of patinated or heavily corroded non-gilded bronzes.

The following figure (**figure 3.19**) shows the average values and corresponding standard deviations of corrosion rates from gravimetric tests (µm/y) and galvanic sensors for Cu^{2+} hypothesis in copper and bronze samples. Indeed, copper alloys show an intermediate electronic behaviour between Cu^{+} and Cu^{2+} with normally prevailing Cu^{2+} copper among the corrosion products. Corrosion rates from galvanic sensors have been calculated by using Faraday's law.

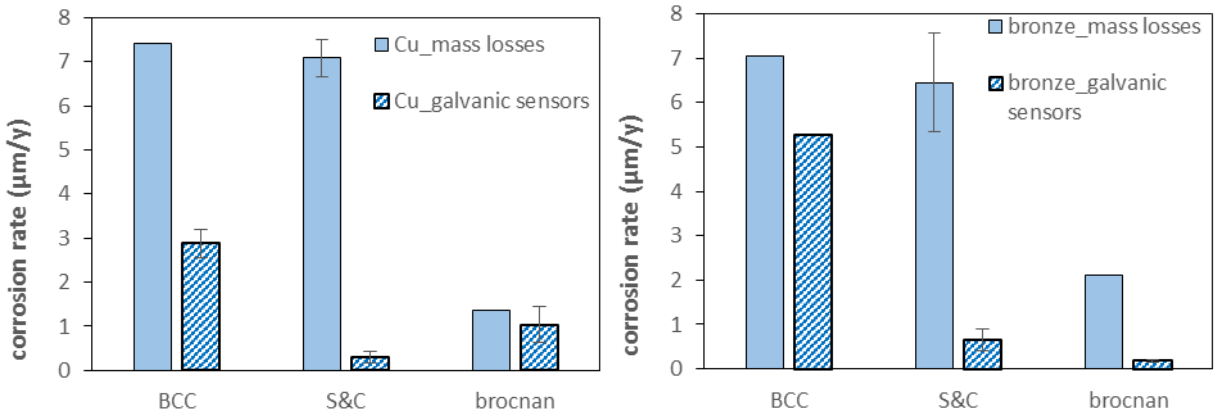

Figure 3.19 comparison of average corrosion rates (µm/y) from galvanic sensors and mass losses

It can be observed that galvanic sensors underestimate corrosion rate values with respect to mass losses. Indeed, the values calculated from galvanic sensors are not the real and exact corrosion rates because some current is lost during acquisition and significant approximations and assumptions are made (same surface area for gold and bronze, oxygen reduction only on the gold, Cu^{2+} bielectronic behaviour for copper and hypothesis of generalized corrosion). However, the obtained results are in good agreement for BCC patina on bronze substrate and for brocnan patina for Cu substrate, while the main differences can be observed for S&C patina on both Cu and bronze.

The direct comparison does not provide very reproducible results in term of errors between the two different techniques. Indeed, by considering brocnan patina, underestimation is lower for Cu sensors (24.27 %) with respect to bronze ones that underestimate corrosion rates with a 91.20 % percentage error. The highest error is calculated for S&C patina: 95.58 % for Cu galvanic sensors and 89.86 % for bronze galvanic sensors. As previously discussed, further improved experiments are required in order to confirm these results and better interpret them.

- *final considerations*

Since non-destructive in-situ electrochemical techniques cannot be applied on gilded bronzes, galvanic sensors can be considered a suitable alternative technique for corrosion monitoring, because they simulate the stratigraphy of corroded gilded bronzes.

The present analysis has intended to:

- produce more durable sensors, with more reproducible and reliable signals

- compare mass loss and continuous monitoring of galvanic sensors in order to verify their capability on providing corrosion rate values
- prepare some non-gilded samples in order to evaluate the possibility of using the galvanic sensors also for the monitoring of patinated or heavily corroded non-gilded bronzes.

The new and improved sets of galvanic sensors that have been prepared for this work of thesis have a strong signal and a quite reproducible macro couple current density for the same patina composition on both Cu and bronze substrates and higher durability compared to previous ones.

Corrosion rates have been evaluated from mass losses in order to verify the reliability and the error associated to galvanic sensors and to try to extend the use of these sensors also for continuous monitoring of not gilded copper alloys artefacts.

Since mass losses provide similar results for both gilded and non-gilded samples, it is possible to use galvanic sensors also for not gilded Cu and bronze artefacts, considering that galvanic sensors tend to underestimate the real current density flowing between the gilding and the bronze since some current is lost during acquisition.

Corrosion rates underestimation based on so far collected data does not represent a systematic percentage error for the different patinas and some problems have been associated to S&C mass losses. Therefore, a larger validation campaign with longer monitoring time and various sets of samples at different RH values are required in order to test again each patina and understand how much RH variations affect mass losses due to patination and if galvanic sensors use implies some significant limitations in corrosion rates estimation.

3.2 Protective coatings for copper and bronze artefacts

Laboratory tests have been performed to evaluate the efficiency of protective coatings in two different conditions: urban condition and stressed condition.

Coatings efficacy and compatibility with the monuments should be evaluated according to electrochemical protection that they ensure and the chromatic alteration that they induce. It is reasonable to think that a protective works properly from the electrochemical point of view if no corrosion products form.

The respect for the original object it is very important: indeed, treatments should not alter the original aesthetic aspect of the material. Protectives should produce no or little change in the surface appearance. However, significant colour variations may be ascribed to protectives yellowing after ageing. For this reason, it is also possible to find very effective protectives with respect to their ability to control corrosion process, but that cannot be used in the field of Cultural Heritage due to their tendency to turn yellow.

SEM-EDX and stereomicroscope analysis have been used to study the surface morphology and to investigate the elemental composition of the samples.

Colorimetric measurements have been performed to evaluate colour alteration.

The durability of the protective coatings and the protection performances have been studied using LPR and EIS.

3.2.1 Urban condition

Bronze samples have been studied after 27 months exposure. They have been exposed outdoor to the urban environment of Milan with a 45° orientation and facing south to test the effectiveness of different protective treatments. The treatments have been chosen by Opificio delle Pietre Dure (OPD) according to a critical analysis of the scientific literature, the results of previous researches, and the evaluation of safety issues such as toxicity and environmental impact.

The samples are quaternary bronzes, both patinated and not patinated (see previous chapter), whose composition is representative of the real copper-alloys used during XIX century for the production of bronze artefacts. The applied patina is obtained in foundry by combining K_2S and NH_4Cl.

The samples characteristics as alloy composition and superficial finishing have been defined during previous studies which were focused on the characterization and evaluation of the protective treatments before exposure (Beltrami 2011; Bressan 2011).

- *superficial characterization*

After a two-year exposure, the visual observation of the not patinated samples does not reveal significant differences in terms of colour and superficial morphology. Indeed, all the samples show a rather compact aspect.

The patinated samples appear generally darker than the not patinated ones. Only in the case of 1N and 1P, where no protective treatments have been applied before exposure, also not patinated sample appear dark as the not patinated one (**figure 3.20**).

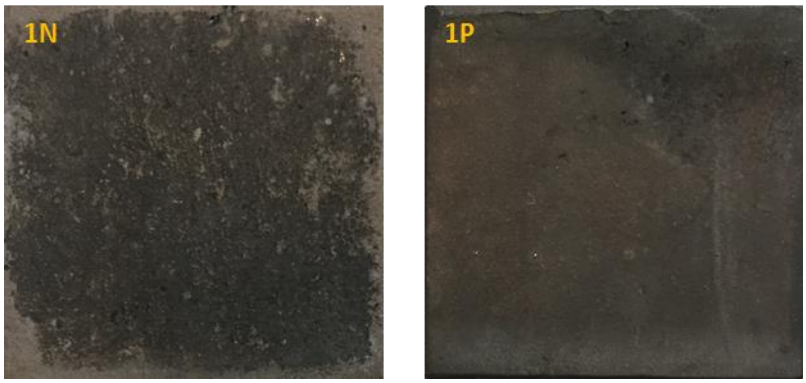

Figure 3.20 dark surfaces of not treated reference samples

On such patinated and treated samples, a visible deposition of green coloured compounds can be observed as a result of the exposition. In particular, the colour alteration of Soter wax (applied as single, double and triple layer) forms a continuous patina, which covers the entire surface of the specimens, while the most of the samples shows a more irregular presence of the green alteration (**figure 3.21**).

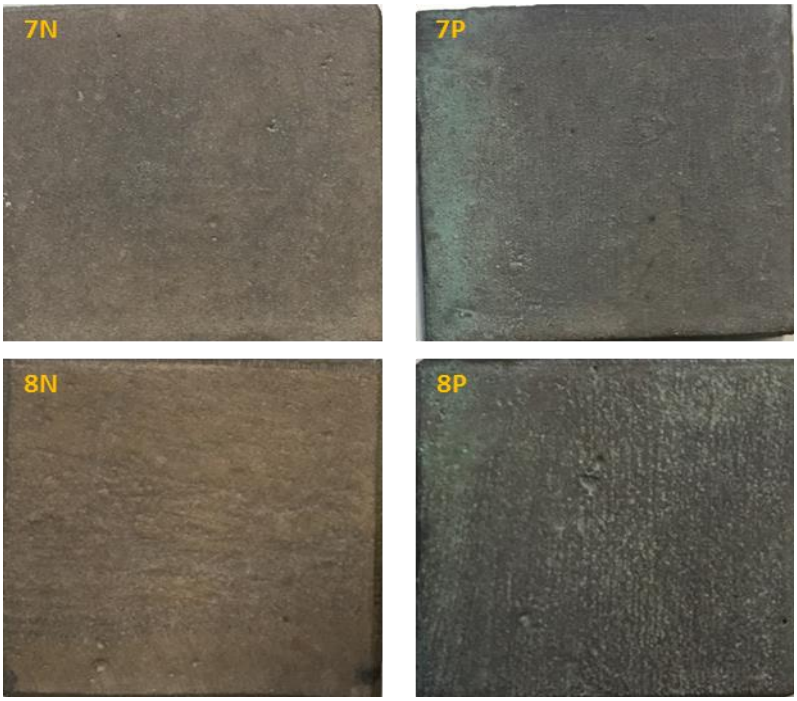

Figure 3.21 greenish patina formation on samples treated with a single layer of Soter: not patinated specimens on the left and patinated specimens on the right

In addition, in both 18N and 18P, where the synergic effect of double layer of Incral and Soter wax and BTA corrosion inhibitor has been tested, and in 19N and 19P, with triple protective layer, the surface is covered by a stripe-like pattern, which probably derives from the repeated application by brush of the overlapped protective layer.

Greenish deposits are less homogeneously diffused on the other surfaces and have a more intense green hue in samples treated with Fluoline or Resvax wax (**figure 3.22**).

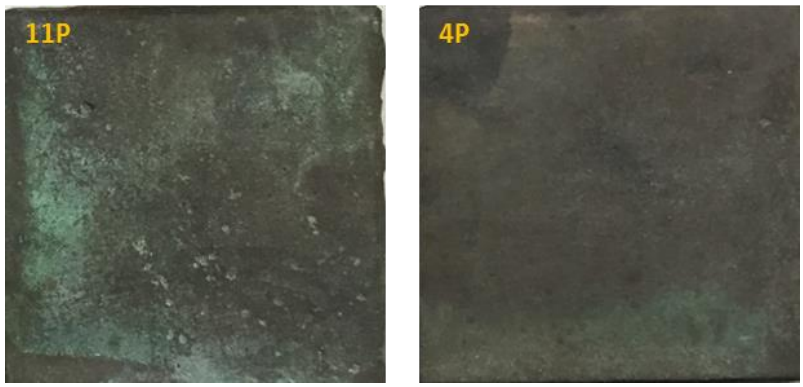

Figure 3.22 greenish deposits on patinated samples treated with Fluoline (11P) and Resvax wax (4P)

A different superficial aspect can be observed as a result of the application of the Polysiloxane coating (**figure 3.23**). Indeed, a particularly evident glossy effect is observed in samples 13N, 13P, 14N and 14P. Moreover, the Polysiloxane coating appears damaged after the exposure with several cracks and partial detachment of the protective layer.

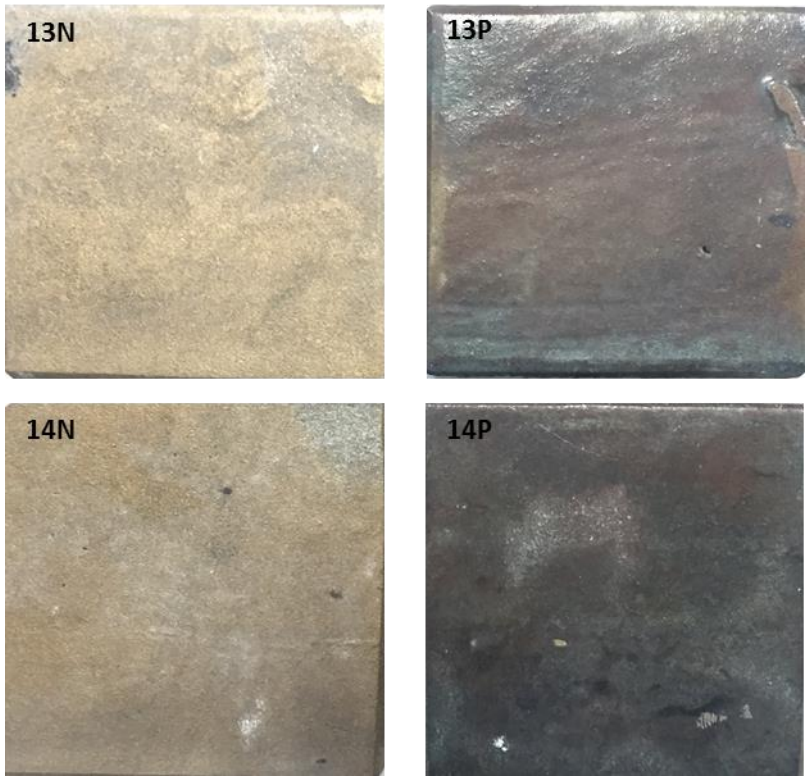

Figure 3.23 samples treated with Polysiloxane showing a particularly evident gloss appearance (not patinated on the left, patinated on the right)

The stereomicroscope observation of the specimens confirms the general observation previously reported for the aesthetic differences between not patinated and patinated samples.

The exposure has led to the deposition of particulate matter and soil deposits within the voids and irregularities of the surface (**figure 3.24**).

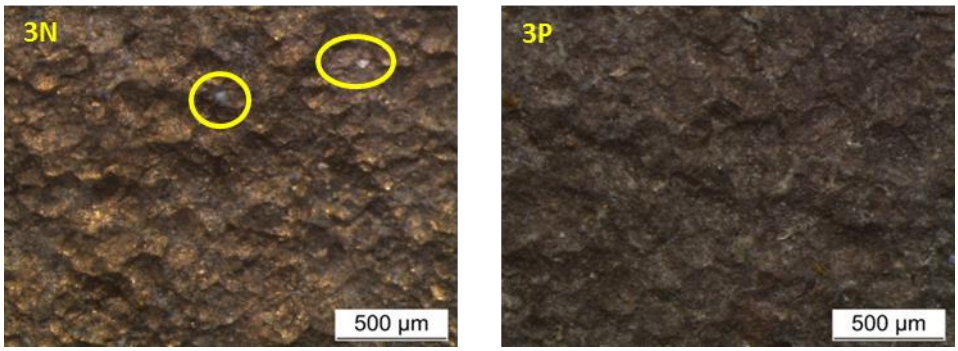

Figure 3.24 darker patinated surface and particulate matter deposition

The observation of the green corrosion products confirms that they are particularly diffused on patinated samples treated with Fluoline protective (**figure 3.25**). They form a discontinuous superficial crust that is diffused over the entire surface and becomes more compact, when the Fluoline protective is coupled with inhibitors, as for 11P specimen with Mercaptobenzothiazole.

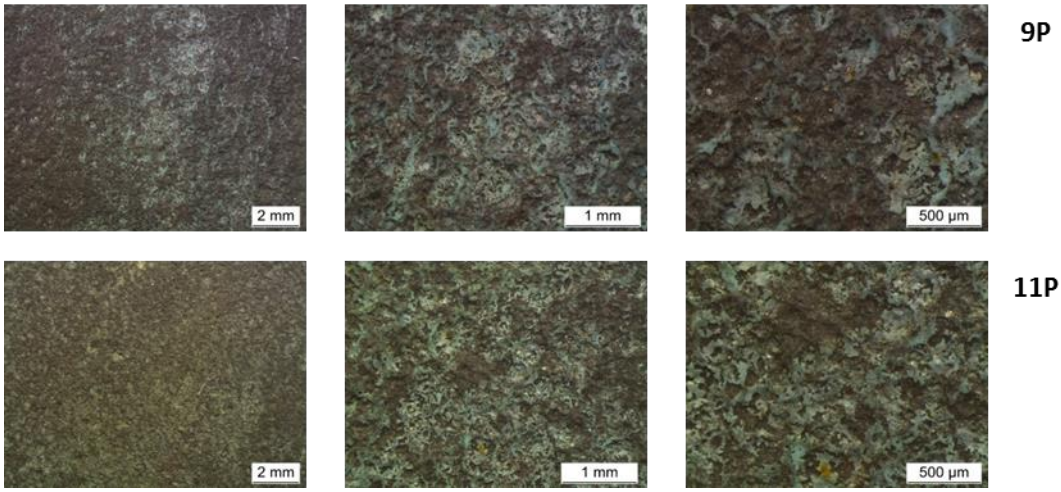

Figure 3.25 green corrosion products on patinated samples treated with Fluoline (upper image shows only Fluoline protective, lower images shows Fluoline + Mercaptobenzothiazole)

After exposure, the irregular aspect with stripes crossing the surface is still visible when double and triple layers are tested (**figure 3.26**).

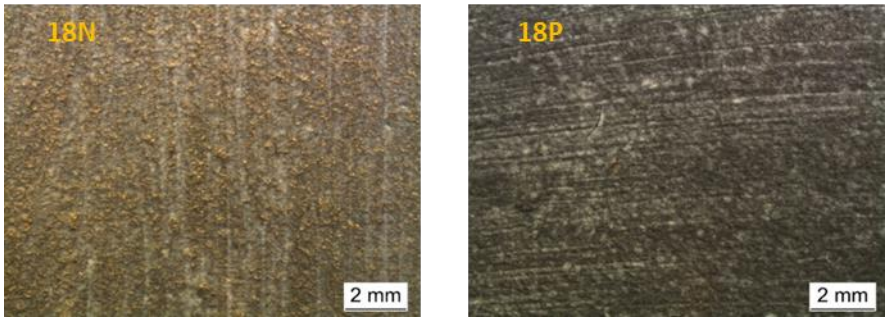

Figure 3.26 18N and 18P surfaces with a stripe-like pattern

Polysiloxane coating (13N, 13P, 14N and 14P) appears degraded on both patinated and not patinated samples (**figure 3.27**). It is not continuous after exposure due to the presence of diffused cracks. In some areas, cracks led to the detachment of the coating itself so that the bronze substrate is visible.

Protective coatings with similar composition have also been tested for the protection of a real artefact exposed to severe temperature and relative humidity conditions and they showed a similar behaviour with diffused cracking and a generally low durability (see the following paragraph for the case study of "Mi fuma il cervello (Autoritratto)" made by Alighiero Boetti).

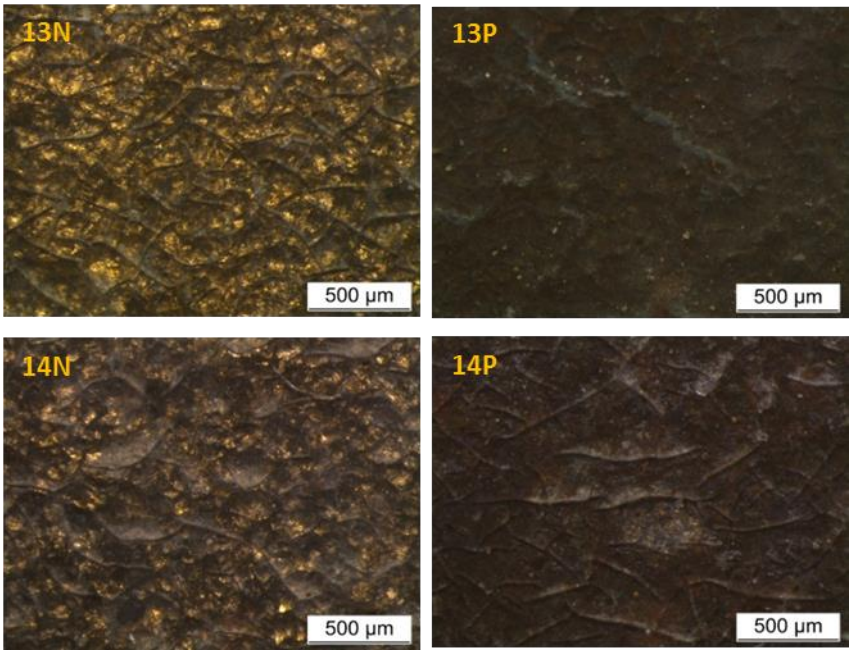

Figure 3.27 Polysiloxane on samples surface showing diffused cracking (not patinated specimens on the left, patinated specimens on the right)

SEM-EDX analysis has been used to study the surface morphology and to investigate the elemental composition of the samples, in order to assess the state of conservation of the protective coating and the presence of corrosion products. Analyses have been conducted on selected reference samples and on samples, which showed corroded surface condition already observed at stereomicroscope (i.e., samples with Fluoline treatments since they are rich in greenish corrosion products) or the presence of specific problems (i.e., samples with Polysiloxane treatments).

In **figure 3.28**, 1N and 1P are shown as reference samples of not protected patinated and not patinated surfaces. Corrosion products can be observed on their surfaces, as a result of the exposition.

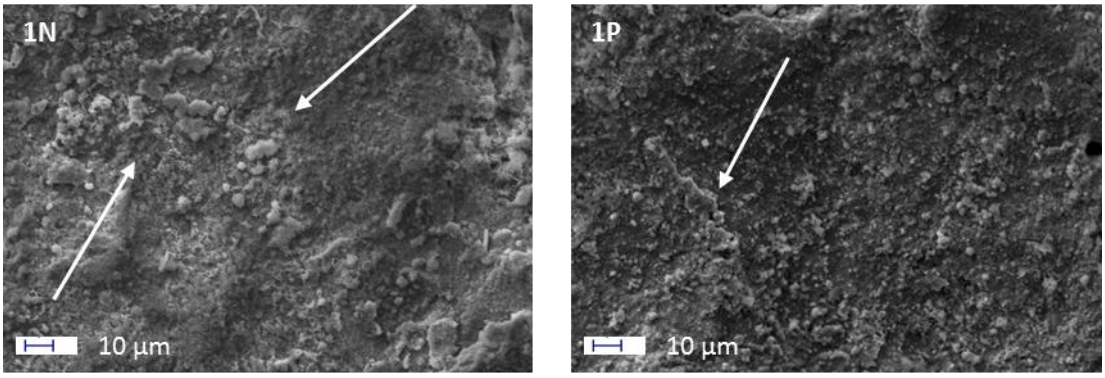

Figure 3.28 SEM images showing corrosion products on 1N and 1P, SE

They have similar morphology, as represented in **figure 3.29**. On both samples, it is possible to observe the presence of particulate matter and soil dust.

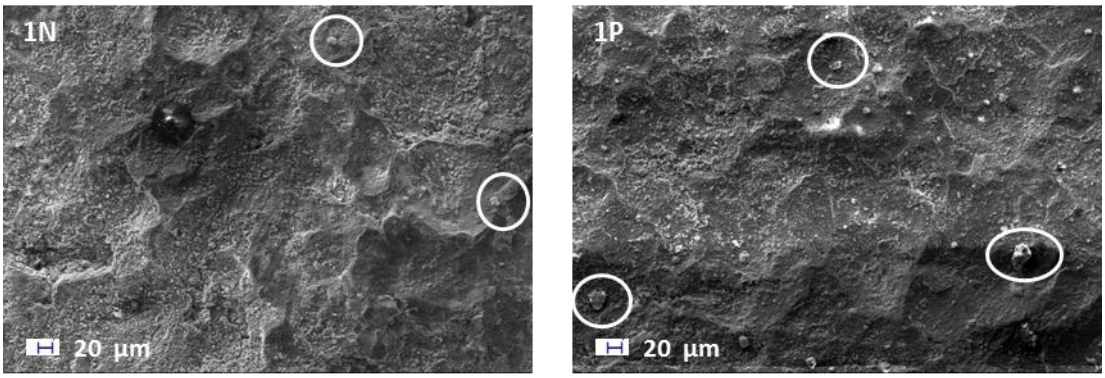

Figure 3.29 1N and 1P similar morphology, SE

The EDX analysis has been conducted in different areas of 1N and 1P reference samples and spectra representative of the average composition have been acquired. They show similar results for both samples with the main difference represented by the presence of Cl arising from the patina in the case of patinated sample (**figure 3.30**).

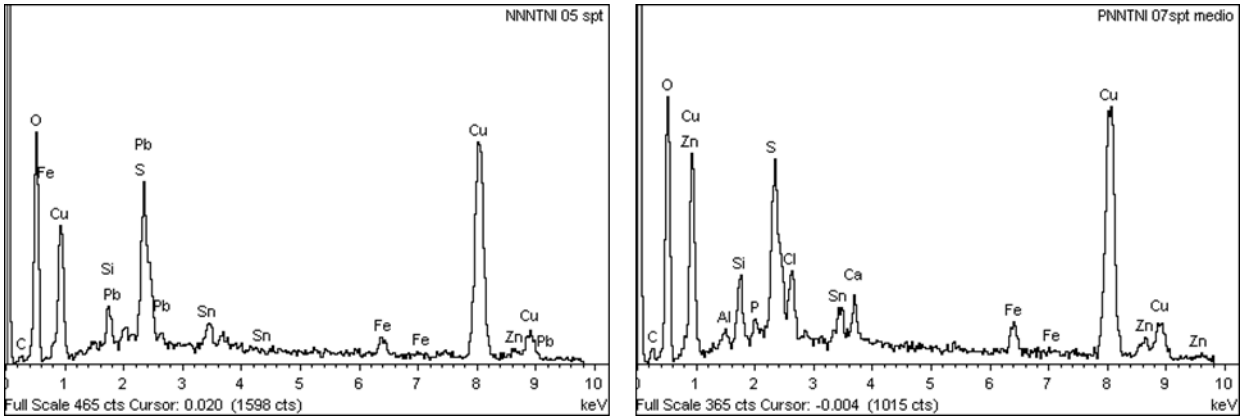

Figure 3.30 EDX of 1N (left) and 1P (right)

The presence of Si and Fe on not patinated sample and of Si, Al, Fe and P on patinated sample is related to the accumulation of soil dust and particulate matter as a result of the prolonged exposition. Other elements have been observed and they are the main component of the bronze substrates, according to the alloy composition previously discussed (see chapter 2). These are Sn, Pb, Zn and especially Cu.

As already mentioned, corrosion products are visible on the samples treated with Fluoline (**figure 3.22** and **3.25**). They are irregularly shaped and largely diffused on the observed patinated and not patinated surfaces. They tend to grow forming a discontinuous crust on patinated samples of such an extent that they can easily be observed even at naked eye. **Figure 3.31** shows the typical corrosion products that are formed on patinated surfaces protected with Fluoline (9P). Similar morphology has been observed also for 11P, when Fluoline is combined with inhibitor.

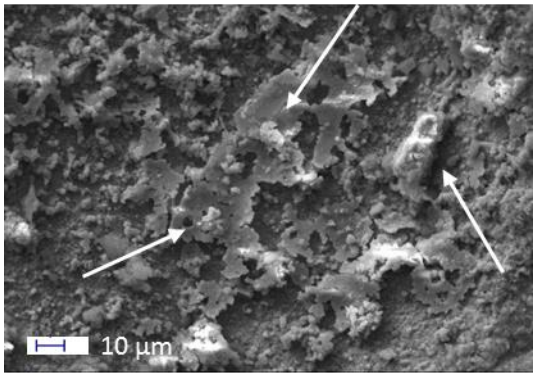

Figure 3.31 corrosion products on 9P, SE, visible as a discontinuous and irregularly shaped crust

Elements related to atmospheric contaminants (i.e., Si, Al and Ca) are accumulated on not patinated samples surfaces too. EDX spectra have been acquired in different areas of both samples 9N and 11N (**figure 3.32**). Traces of Fluoline protective are still present: indeed, F has been detected.

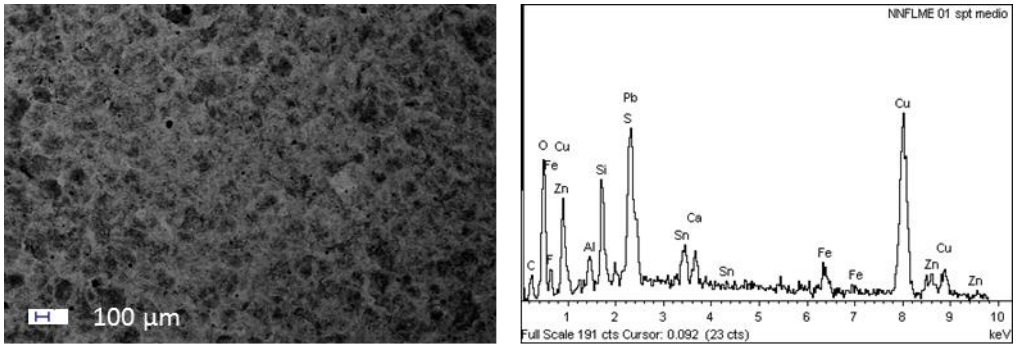

Figure 3.32 QBSD image (on the left), EDX of 11N (on the right)

The EDX analysis has been carried out in detailed areas of both 9P and 11P. It has been conducted in order to evaluate if the protective treatment is present on small area of the substrate, since F has been observed in the previous image. Three different spectra have been acquired (**figure 3.33**).

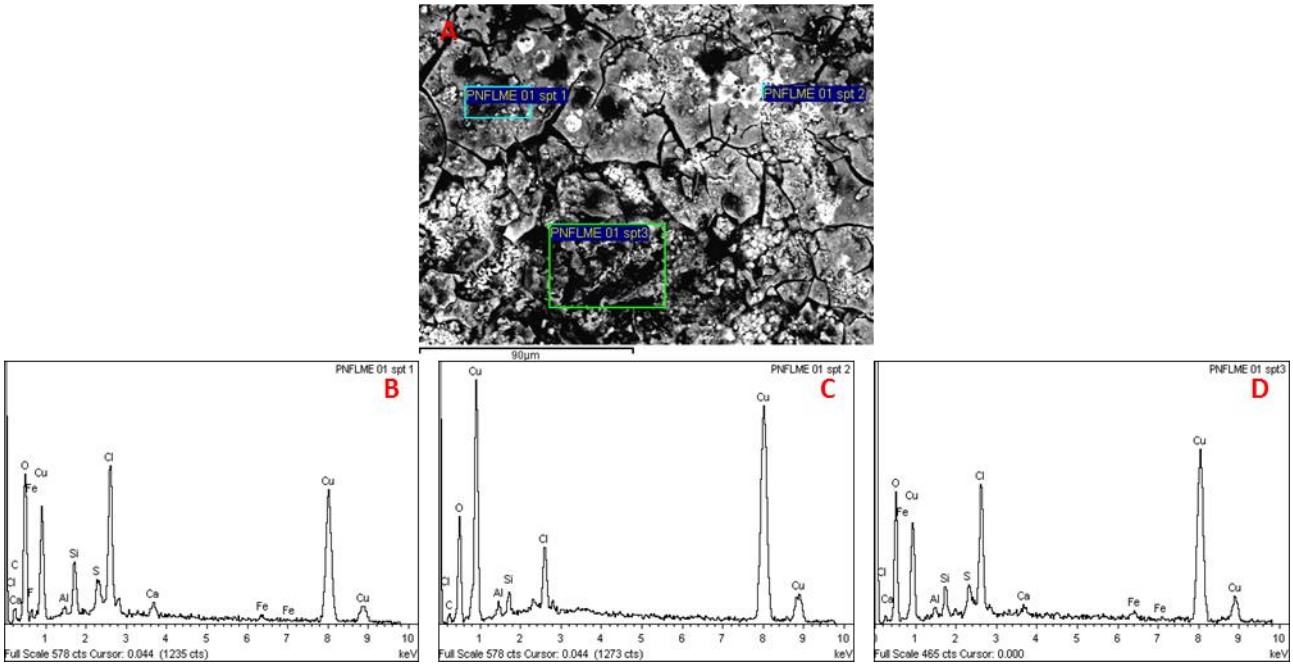

Figure 3.33 A reference SEM image showing the location of the EDX analysis (B, C, D)

The EDX analysis has been conducted in three different areas. The presence of F in B image is related to the protective treatment and it indicates that the protective coating is still present in small amount on the substrate after exposure. By observing C and D, Cu, O and Cl are the main elements and their concentration identifies the presence of corrosion products as result of prolonged exposition. The presence of Al, Si, Fe and Ca is ascribed to the accumulation of soil dust and particulate matter.

Figure 3.34 shows the superficial morphology of samples treated with Polysiloxane (13N, 13P, 14N and 14P): they confirm the presence of the coating, which main element is Si and which thickness is of the order of tens micron, and of small and lengthened cracks, already seen at stereomicroscope in **figure 3.27**. Cracks have quite different form on patinated and not patinated samples and they are more diffused on 13P and 14P: it is reasonable to think that the patina leads to a faster degradation of the coating.

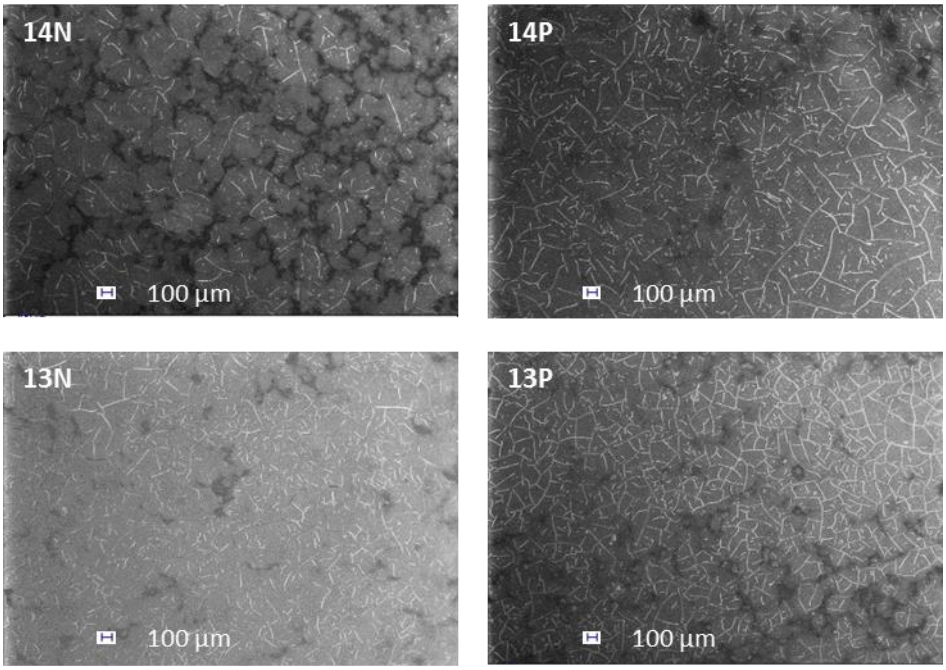

Figure 3.34 cracks on samples treated with Polysiloxane (not patinated specimens on the left, patinated specimens on the right)

The EDX analysis of 13N, 13P, 14N and 14P has been performed in different areas of the samples representative of the average composition with similar results. The element with higher concentration is Si, whose presence is associated to the composition of the applied coating (**figure 3.35**). In the area in which coating is damaged, Cu of the substrate emerges and is the only element traced.

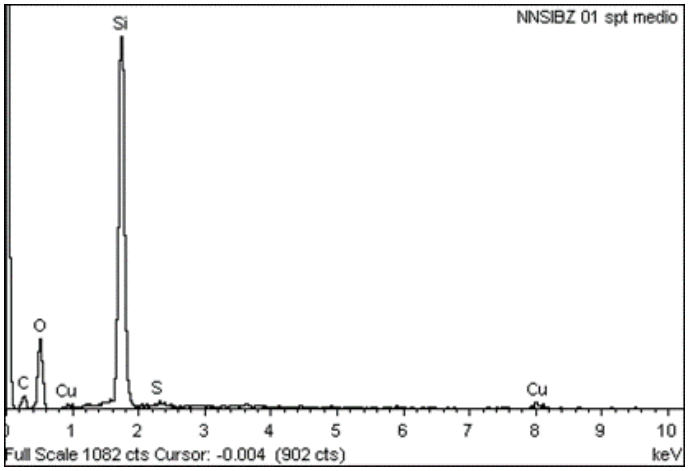

Figure 3.35 EDX of 14N showing high Si content

A similar situation can be observed in **figure 3.36** that represents a general crack where coating detachment occurs.

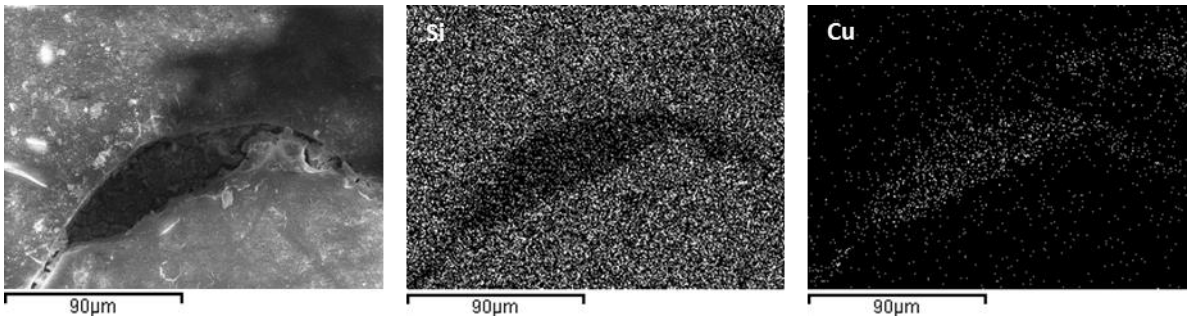

Figure 3.36 SEM image of an area of 14N containing cracks and SI and Cu distribution

Cu is the main element observed inside the crack and it correspond to substrate where protection is no longer present. Si is the prevailing element on the surface where the coating is still present after exposure.

As previously said, cracks morphology is influenced by the presence of the patina: indeed, cracks observed on patinated samples appear narrower and more extended with respect to the ones observed on not patinated samples (**figure 3.37**).

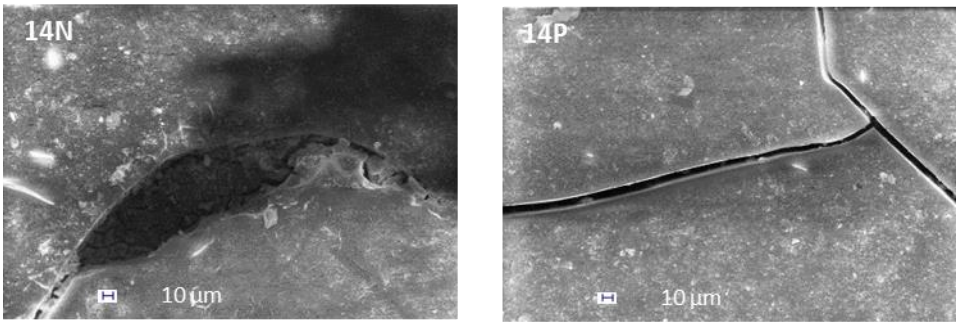

Figure 3.37 comparison between cracks on different samples (not patinated on the left, patinated on the right)

- *colorimetric measurements*

Average values of L*, a* and b* parameters calculated after exposure are compared with the same data collected with the same modality before exposure. The evaluation of colour variations and their comparison according to the different treatments is very important to classify protective performances in term of visual appearance.

L represents lightness while a* and b* are the chromatic coordinates of the CIE L*a*b* colour space. L* varies from dark (0) to light (100), a* varies between green (negative values) and red (positive values), b* varies between blue (negative values) and yellow (positive values).

In the following bubble charts, the bubbles diameter represents L* values and a* and b* chromatic coordinates vary respectively along X-axis and Y-axis.

In **figure 3.38**, not patinated samples are represented before and after exposure.

In **figure 3.39**, patinated samples are represented before and after exposure.

Table 3.7 shows chromatic colours variations (Δa and Δb) for both patinated and not patinated samples.

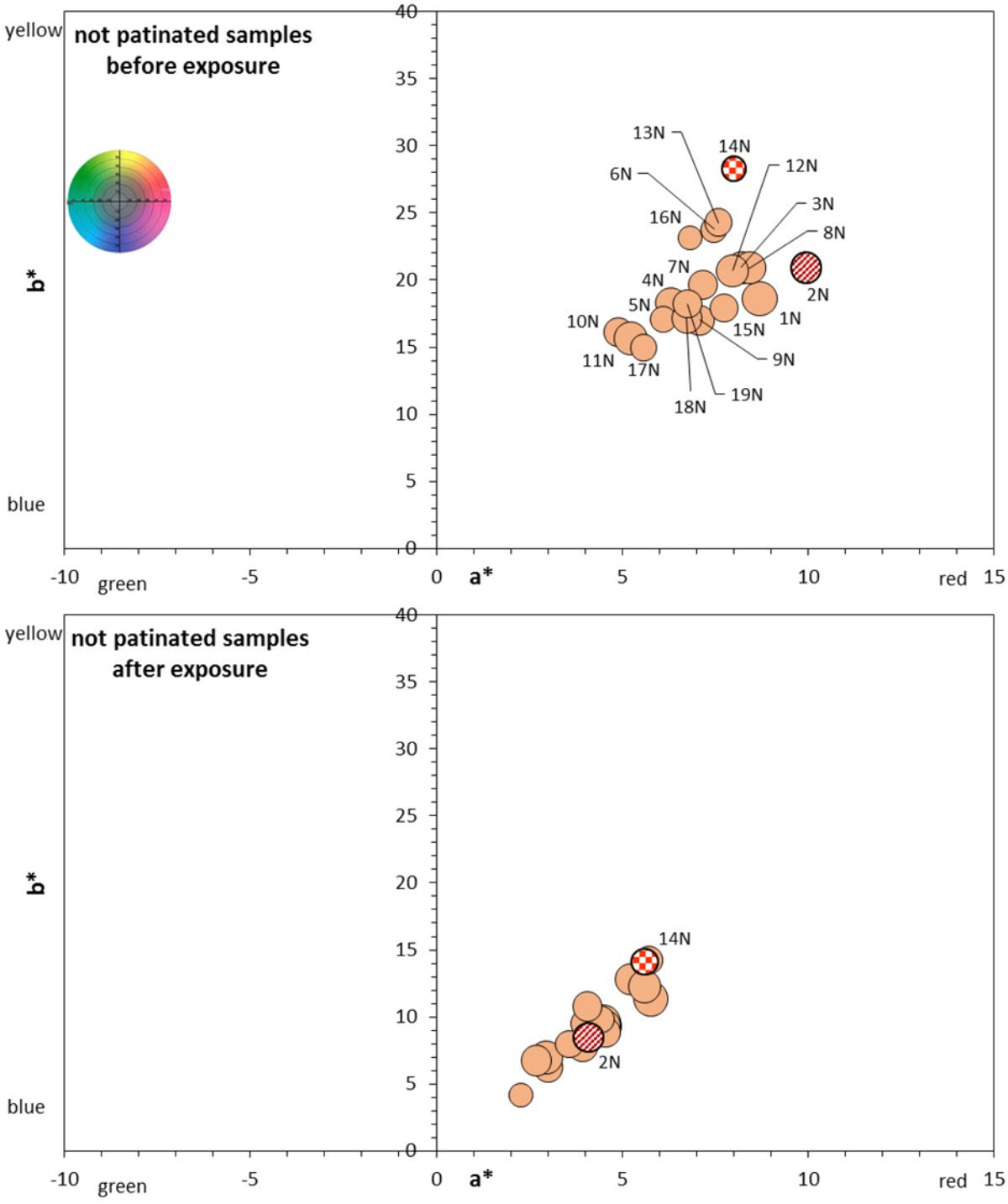

Figure 3.38 colorimetric characterization of not patinated samples before (above) and after (below) exposure

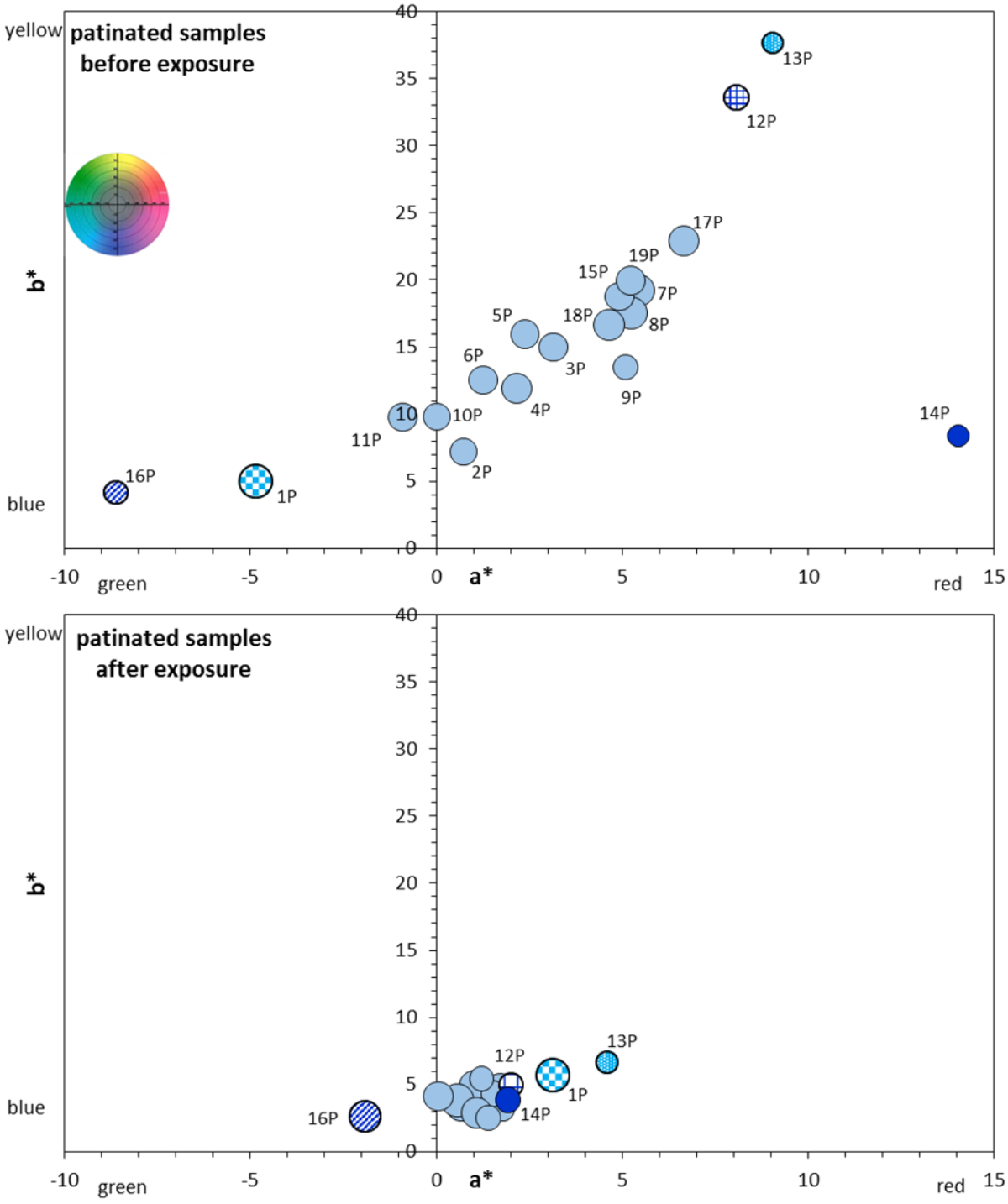

Figure 3.39 colorimetric characterization of patinated samples before (above) and after (below) exposure

Table 3.7 Δa and Δb values for all the samples

treatments	inhibitors	name	extended name	Δa	Δb	name	extended name	Δa	Δb
-	-	1N	NNNTNIA	-6.41	-14.47	1P	PNNTNIA	7.98	0.71
Resvax	-	2N	NNCRNIA	-6.02	-13.11	2P	PNCRNIA	-0.06	-3.83
	BTA	3N	NNCRBZA	-3.65	-11.65	3P	PNCRBZA	-1.47	-11.37
	Mercaptobenzothiazole	4N	NNCRMEA	-0.55	-6.93	4P	PNCRMEA	-0.45	-7.30
	Sodium Oleate	5N	NNCROLA	-3.10	-10.87	5P	PNCROLA	-1.29	-11.67
	Tolyltriazole	6N	NNCRTTA	-3.46	-14.27	6P	PNCRTTA	0.01	-7.96
Soter	-	7N	NNCSNIA	-4.20	-12.64	7P	PNCSNIA	-4.42	-14.31
	BTA	8N	NNCSBZA	-3.93	-11.27	8P	PNCSBZA	-4.66	-13.71
Fluoline	-	9N	NNFLNIA	-2.54	-7.65	9P	PNFLNIA	-3.30	-10.41
	BTA	10N	NNFLBZA	-2.20	-9.40	10P	PNFLBZA	1.53	-5.47
	Mercaptobenzothiazole	11N	NNFLMEA	-0.01	-2.82	11P	PNFLMEA	0.94	-5.64
	Sodium Oleate	12N	NNFLOLA	-2.37	-8.42	12P	PNFLOLA	-6.07	-28.63
Polysiloxane	-	13N	NNSINIA	-1.87	-10.06	13P	PNSINIA	-4.47	-31.02
	BTA	14N	NNSIBZA	-2.40	-14.18	14P	PNSIBZA	-11.95	-5.09
PA func.BTA	-	15N	NNPFNIA	-3.19	-9.07	15P	PNPFNIA	-2.99	-14.90
PA mix.BTA	-	16N	NNPMNIA	-2.39	-13.28	16P	PNPMNIA	6.69	-1.53
Double Layer	-	17N	NNDSNIA	-2.00	-6.97	17P	PNDSNIA	-5.56	-20.00
	BTA	18N	NNDSBZA	-2.64	-8.72	18P	PNDSBZA	-3.25	-14.13
Triple Layer	-	19N	NNTSNIA	-2.70	-7.47	19P	PNTSNIA	-4.01	-14.51

By observing **figure 3.38** that refers to not patinated samples, it is possible to note that protected substrates before exposure were rather comparable for all the samples in terms of chromatic

coordinates. Indeed, a* varies from 5 to 9 with a slightly higher value calculated for 2N; b* varies from 14 to 24 with a slightly higher values for 14N.

Colorimetric measurements after exposure confirm what has been noted from visual examination. Indeed, samples are rather comparable and the chromatic parameters show variations in very limited range of values (a* varies from 2 to 6 and b* from 4 and 14). Chromatic parameters distribution has not significantly changed after exposure, but the global effect of ageing is a reduction of a* and b* that tend to “colder” hues.

By observing **figure 3.39** that refers to patinated samples, it is possible to note a higher range of values variability for a* and b* parameters. Indeed, a* varies from -1 to 8 and b* from 7 to 23. Few exceptions are represented by 1P and 16P with negative a* values and similar b* about 5 and by 12P and 13P with high b* about 35 and a* almost 10. Finally, a* is about 15 and b* 7 for 14P sample.

In this case, it is possible to observe that protectives application on patinated bronze substrates led to a higher values dispersion before exposure, while, after ageing, the colour variability is significantly reduced: a* varies from 0 to 3 and b* from 2 to 5. The samples, which before exposure were the most dispersed with respect to average behaviour, show very limited differences yet after exposures (a* is lower with respect to homogeneous samples for 16P and a* is higher for 1P and 13P). 12P and 14P coordinates are similar to homogeneous samples ones.

As for not patinated samples, the global effect of ageing induced by exposure is a* and b* reduction since samples tend to “colder” hues.

By observing **table 3.7**, it is possible to note that exposure leads to a general reduction of a* parameter in all not patinated samples. Indeed, Δa values are negatives confirming the global effect of ageing of leading samples to “colder” hues. The highest variation has been calculated for the not protected sample 1N (Δa = -6.41) and the lowest one for 11N (Δa = -0.01). The most of the patinated samples shows negative values for Δa, but some exceptions can be observed (1P, 10P, 11P and 16P). Δa varies from -11.95 calculated for 14P to 7.98 evaluated for 1P.

After exposure, b* parameters decreases for both patinated and not patinated samples, with the only exception of 1P where small value has been calculated (Δb = 0.71). Among not patinated samples, Δb varies from -14.47 for 1N to -2.82 for 11N. Among patinated ones, it varies from -31.02 for 13P and -1.53 for 16P.

Among not patinated samples, the smallest colours variations are ascribed to 11N and the highest ones to not treated sample 1N. Among patinated samples, 1P represents the only sample in which both a* and b* increases after exposure.

In the following graphs (**figure 3.40** and **3.41**), ΔL variations are represented as absolute values for both not patinated and patinated samples. L* decreases after exposure: indeed, samples become darker due to the combined effect of formation of corrosion products and deposition of particulate matter.

It is possible to observe that lightness variations are generally more significant for patinated samples. Indeed, they are darker with respect to the corresponding not patinated samples. The only exception is represented by 1N: as previously discussed according to visual observation, it is the only not treated sample as dark as the corresponding patinated one.

Among not patinated samples, in **figure 3.40**, L* decreases with not significant values in case of 4N, 5N, 6N, 7N, 15N and 16N, while, among patinated samples, in **figure 3.41**, L* variation is negligible only in case of 16P. Samples treated with Polylactic Acid mixed with BTA show small L* reduction after exposure in both patinated and not patinated case.

Among not patinated samples, the highest lightness variation is calculated for 2N and 11N with similar values (ΔL = -10.95 for 2N and ΔL = -10.61 for 11N). Among patinated samples, the highest lightness variation is calculated for 14P (ΔL = -23.01).

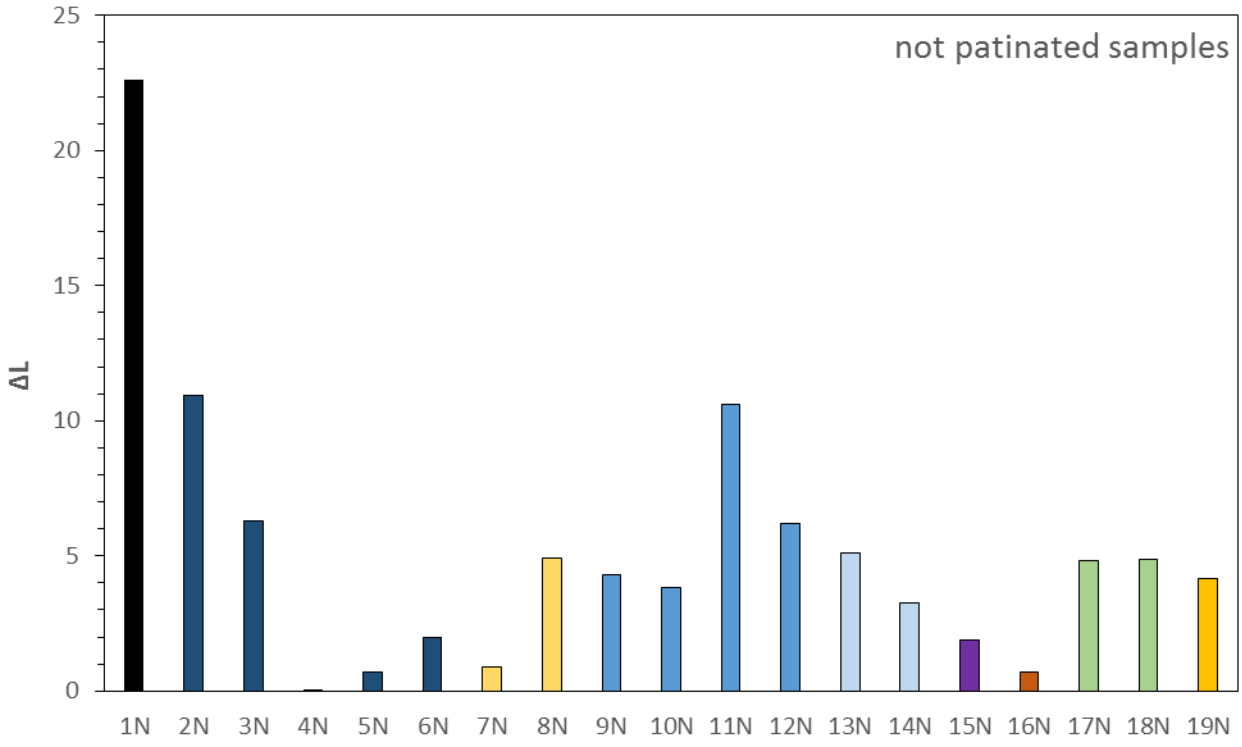

Figure 3.40 ΔL variations of not patinated samples

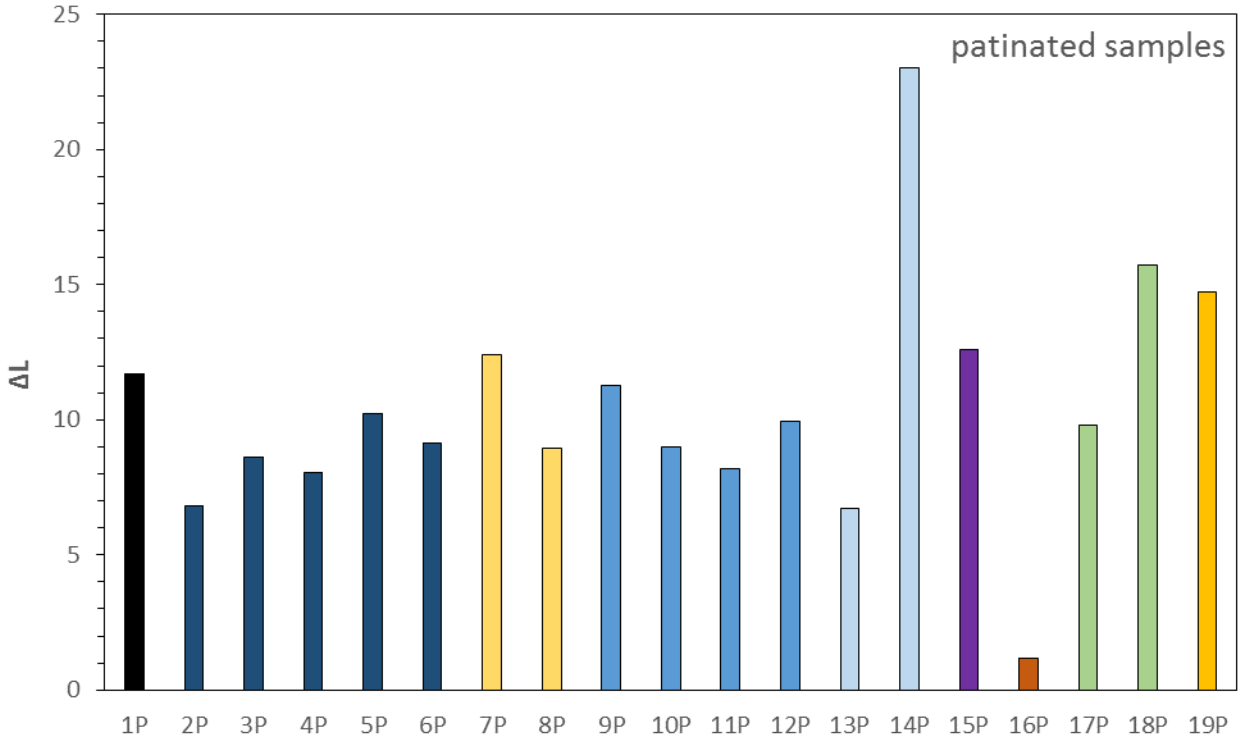

Figure 3.41 ΔL variations of patinated samples

ΔE is the total colour variation and it is calculated once ΔL, Δa and Δb are known.

ΔE are represented in the following graphs for patinated and not patinated samples (**figure 3.42** and **3.43**).

A ΔE > 3 variation is generally associated to an alteration perceivable by the naked eye (EN 2010). In this case, all the values are higher: indeed, exposure effect is relevant in altering global surface colour of the samples.

According to previously calculated chromatic and lightness alterations, among not patinated samples, in **figure 3.42**, 1N shows the highest global colour variation: ΔE = 27.57. ΔE usually varies from 9 to 15 for the most of not patinated samples, with few exceptions represented by the higher value calculated for 2N (ΔE = 18.11) and the lower one for 4N (ΔE = 6.95).

Among patinated samples, in **figure 3.43**, ΔE varies in a wider range of values. Indeed, protectives application on patinated bronze substrates leads to a more extended values distribution before exposure, while, after ageing, samples are almost similar, since they are rather comparable by exposure effect. The highest value is calculated for 13P (ΔE = 32.05) and the lowest one for 16P (ΔE = 6.97).

It is not possible to find a common colour variation trend associated to the application of the same protective treatment when different corrosion inhibitors are applied. In some cases, exposure may induce similar ΔE on specimens treated with the same protective even if in combination with different inhibitors. Indeed, inhibitors do not strongly affect global surface colour: it occurs when Soter wax and Fluoline are applied on not patinated samples. For example, when Fluoline is applied on not patinated samples, similar values have been calculated: ΔE = 9.14 for 9N, ΔE = 10.38 for 10N, ΔE = 10.97 for 11N and ΔE = 10.71 for 12N.

In general, significant colour variations may be ascribed to protectives yellowing after ageing, but in this work, yellowing effect has not been observed. According to aesthetic properties and colour variations calculated after two years exposure, 4N, 17N and 19N seem to be the best treatments with the lowest ΔE values, among not patinated samples. 2P, 11P and 16P lead to the lowest global colour alterations, among patinated samples.

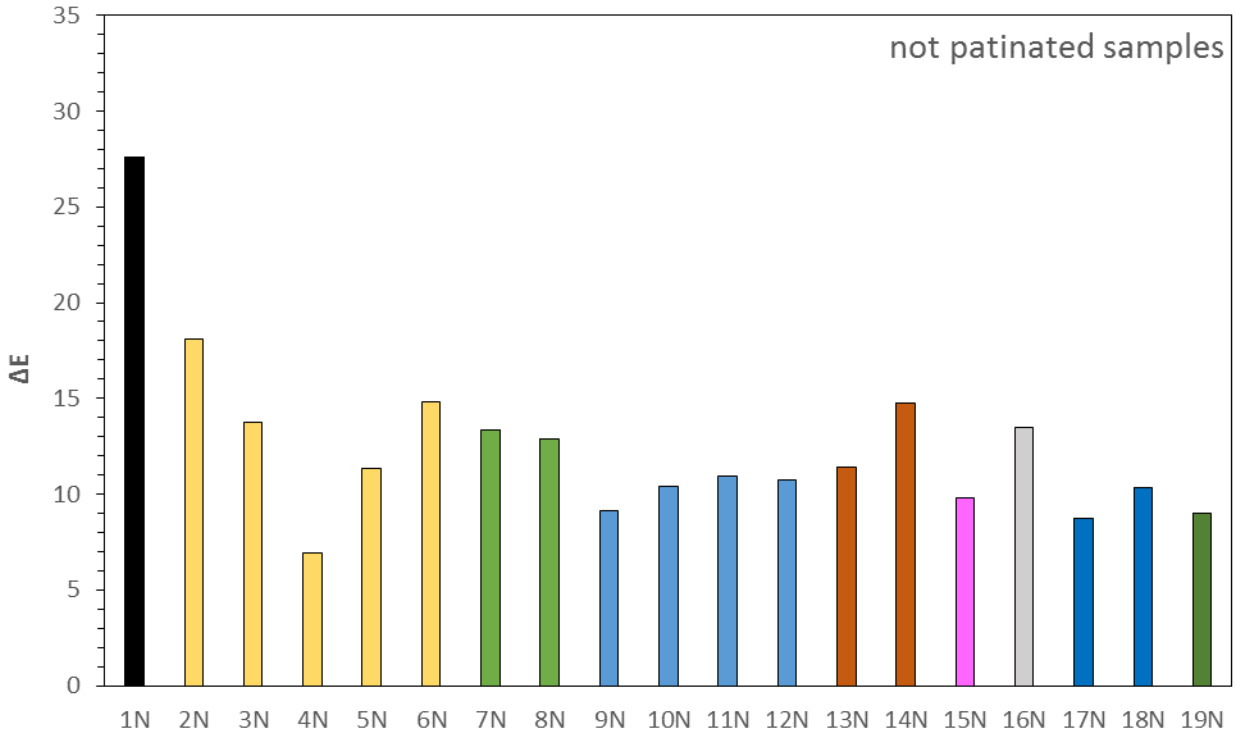

Figure 3.42 ΔE variations of not patinated samples

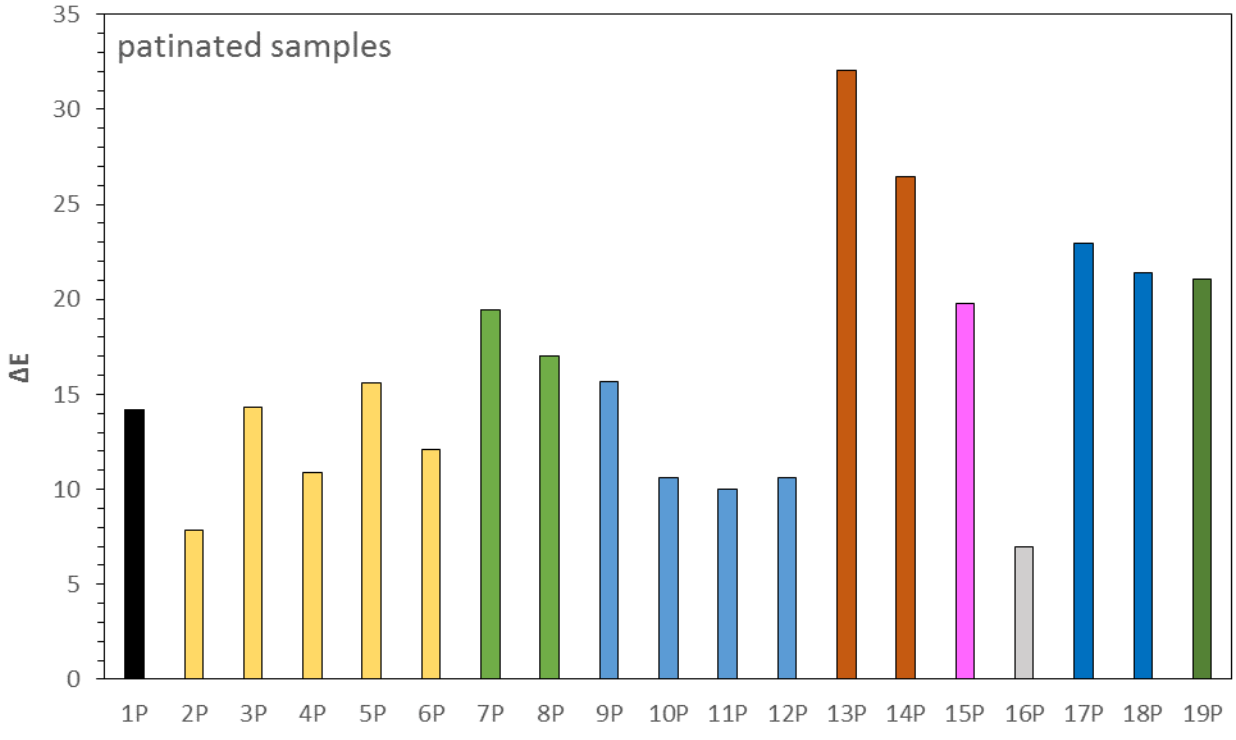

Figure 3.43 ΔE variations of patinated samples

- *electrochemical measurements*

Electrochemical measurements have been useful for protective performances evaluation. The Rp values calculated from LPR and EIS have been used in a direct and comparative manner. Indeed, polarization resistance values are very useful since they allow the estimation of the artefacts degradation and the evaluation of the efficacy of surface protectives and inhibitors.

As previously mentioned, the polarization resistance of a material calculated from LPR is defined as the slope of the potential – current density curve (**figure 3.44**).

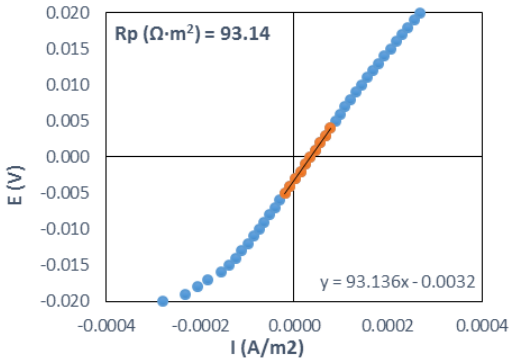

Figure 3.44 example of Rp evaluation from LPR data in the case of 2N (Resvax wax and no inhibitor) sample after exposure

Rp values from EIS are calculated from Bode plots, as mentioned in the previous paragraph. Indeed, at high frequencies, Bode plots contain information on the electrolyte resistance; while at low frequencies, they contain information on the corrosion processes on the metallic substrates. According to Zhang et al. studies, corrosion rates have been derived from the difference in EIS data of $|Z|$ between the low and high frequency ranges (**figure 3.45**). The higher $|Z|$, the lower corrosion rate (Zhang 2002; Cano, Bastidas et al. 2010; Cano, Lafuente et al. 2010; Pons, Lemaitre et al. 2013).

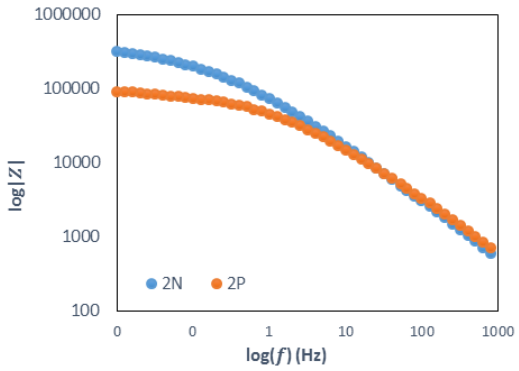

Figure 3.45 example of Bode plots trend for 2N and 2P (Resvax wax and no inhibitor)

LPR and EIS provide similar results, as already mentioned in the previous paragraph on the validation of electrochemical techniques. Indeed, it is possible to note that LPR and EIS give similar Rp trends, with usually slightly higher Rp values estimated through LPR technique. For this reason in the following graph Rp values from LPR and EIS are shown as an average values.

In this kind of comparative study, it should be better to repeat measurements on different areas of the same samples. In this work of thesis, only single measurement has been carried out for reason of time.

LPR and EIS have been used to evaluate Rp values for both patinated and not-patinated samples; all the values are shown in the following table (**table 3.8**).

Table 3.8 Rp values (Ω·m2) from LPR and EIS of all samples exposed in urban conditions

treatments	inhibitors	name	extended name	LPR	EIS	name	extended name	LPR	EIS
-	-	1N	NNNTNIA	37.4	21.4	1P	PNNTNIA	6.1	7.1
Resvax	-	2N	NNCRNIA	93.1	71.2	2P	PNCRNIA	24.1	20.8
	BTA	3N	NNCRBZA	118.2	76.2	3P	PNCRBZA	49.1	41.7
	Mercaptobenzothiazole	4N	NNCRMEA	117.7	81.3	4P	PNCRMEA	43.2	40.6
	Sodium Oleate	5N	NNCROLA	53.4	39.2	5P	PNCROLA	27.4	26.3
	Tolyltriazole	6N	NNCRTTA	28.4	26.0	6P	PNCRTTA	29.1	25.7
Soter	-	7N	NNCSNIA	28.1	27.1	7P	PNCSNIA	23.7	16.8
	BTA	8N	NNCSBZA	72.4	56.5	8P	PNCSBZA	122.4	142.6
Fluoline	-	9N	NNFLNIA	8.1	7.7	9P	PNFLNIA	12.5	6.4
	BTA	10N	NNFLBZA	0.8	6.4	10P	PNFLBZA	2.7	0.5
	Mercaptobenzothiazole	11N	NNFLMEA	8.8	7.7	11P	PNFLMEA	46.2	47.2
	Sodium Oleate	12N	NNFLOLA	40.4	32.3	12P	PNFLOLA	0.2	0.5
Polysiloxane	-	13N	NNSINIA	63.5	30.2	13P	PNSINIA	24.5	20.4
	BTA	14N	NNSIBZA	27.7	20.0	14P	PNSIBZA	33.0	19.7
PA func. BTA	-	15N	NNPFNIA	37.3	28.2	15P	PNPFNIA	34.2	31.0
PA mix. BTA	-	16N	NNPMNIA	65.6	56.5	16P	PNPMNIA	268.4	267.0
Double Layer	-	17N	NNDSNIA	158.1	106.7	17P	PNDSNIA	111.5	88.2
	BTA	18N	NNDSBZA	169.7	116.6	18P	PNDSBZA	72.1	53.1
Triple Layer	-	19N	NNTSNIA	676.5	564.6	19P	PNTSNIA	73.4	49.8

In **figure 3.46**, the average values and the corresponding standard deviations of Rp for all the samples are reported.

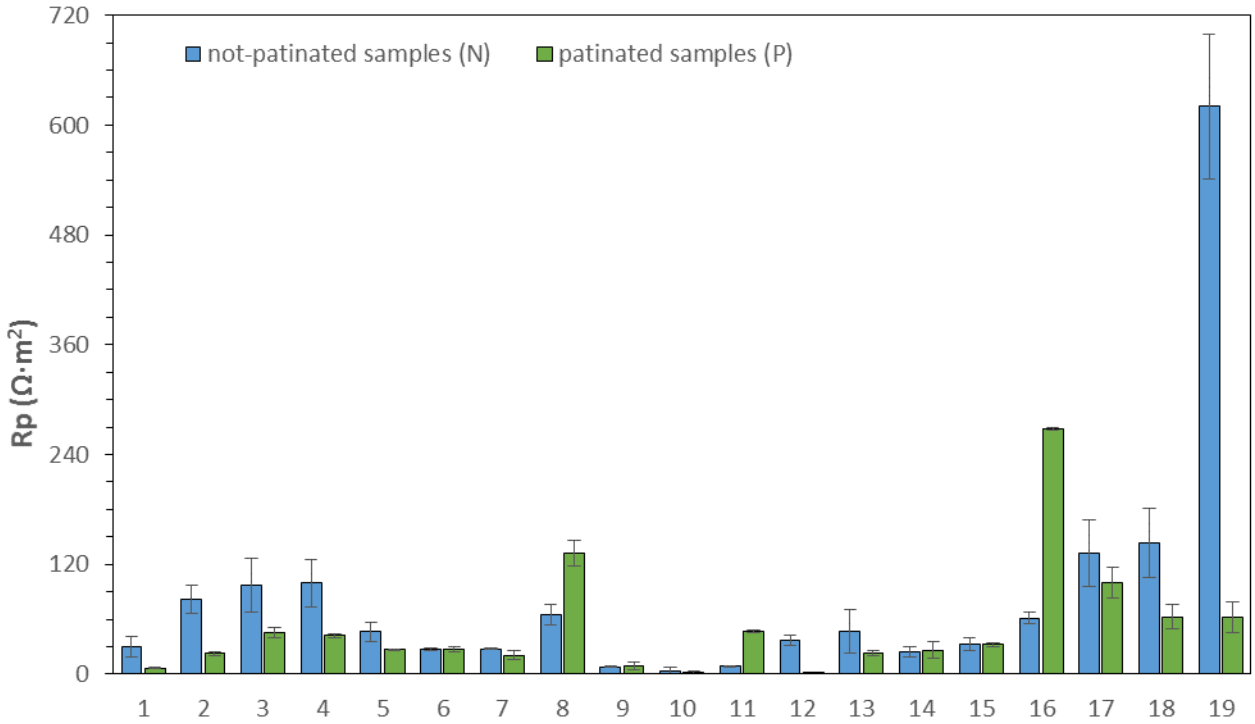

Figure 3.46 average values of Rp and standard deviations (Ω·m2)for all the samples exposed in urban condition

In some cases, the use of protective treatments and inhibitors does not guarantee a better electrochemical behaviour than the not protected samples. Among not patinated samples, it occurs for 9N, 10N, 11N and 12N treated with Fluoline and 7N treated with Soter wax in absence of inhibitors. Among patinated samples, it occurs for 10P and 12P treated with Fluoline in combination with BTA the former and Sodium Oleate the latter.

Most of the times, Rp is higher for the not patinated samples after two year of urban exposure. Significant exceptions are represented by 8P (Rp = 142.6 Ω·m^2 from EIS) and 8N (Rp = 56.5 Ω·m^2 from EIS) and 16P (Rp = 267.0 Ω·m^2 from EIS) and 16N (Rp = 56.5 Ω·m^2 from EIS). A possible interpretation is that protective treatments adhere better in the case of not patinated samples with more homogeneous and smooth surfaces.

It is confirmed, for example, by 2N and 2P samples and 13N and 13P samples. Indeed, Rp is 71.2 Ω·m^2 from EIS for the not patinated sample 2N, about three times higher than the patinated one 2P. In this case, Rp values before exposure were quite similar (Rp = 19.9 Ω·m^2 from EIS for 2N and Rp = 25.3 Ω·m^2 from EIS for 2P), while after exposure Rp values of 2N are higher than the starting ones. Many interpretations are possible. It is possible that the protective on 2N sample was already flawed when applied and that measurements before and after exposure have been carried

out in different areas of the same sample. It is also possible that the formation of corrosion products has caused the obstruction of superficial cracks already existing, leading to the increase of polarization resistance and to the decrease of corrosion rate.

In the case of Polysiloxane, Rp is 30.2 $\Omega \cdot m^2$ from EIS for the not patinated sample 13N, while Rp is 20.4 $\Omega \cdot m^2$ from EIS for the patinated sample 13P. In this case, the protective coating applied on 13P, before exposure, was more effective (Rp = 281676.6 $\Omega \cdot m^2$ from EIS) that the one applied on 13N (Rp = 651.2 $\Omega \cdot m^2$ from EIS). 13P was more promising before exposure but it has been degraded more than 13N, as it is confirmed by the superficial cracks observed at SEM. Indeed, cracks on 13P are more diffuse and they can be easily perceived at naked eye.

The Fluoline protective coating shows the worst behaviour of all, confirming the preliminary results before exposure (Beltrami 2011), even if the synergic effect with inhibitors may in same cases (12N and 11P) improve the treatment performances after exposure for both patinated and not patinated samples.

The synergic effect between treatment and inhibitor of increasing Rp values is represented in the following Nyquist and Bode plots both for not patinated specimens (2N and 4N) and patinated ones (2P and 4P) (**figure 3.47** and **3.48**).

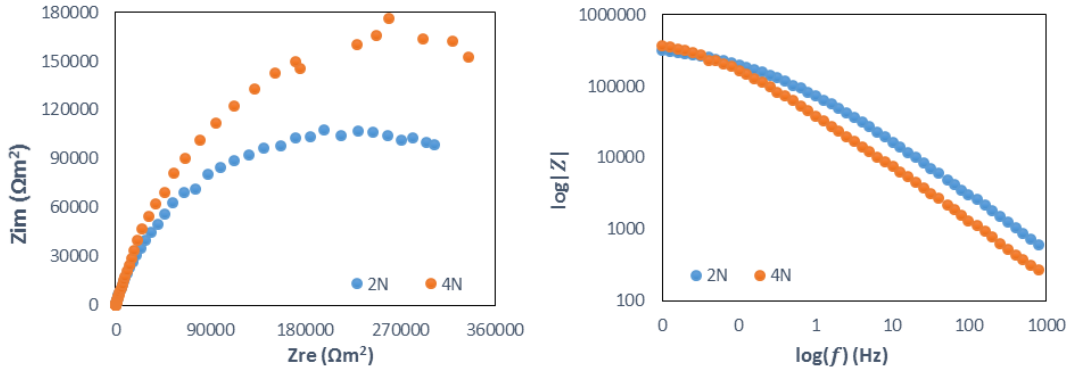

Figure 3.47 inhibitor effect for not patinated samples 2N and 4N: Nyquist (left) and Bode (right) plots

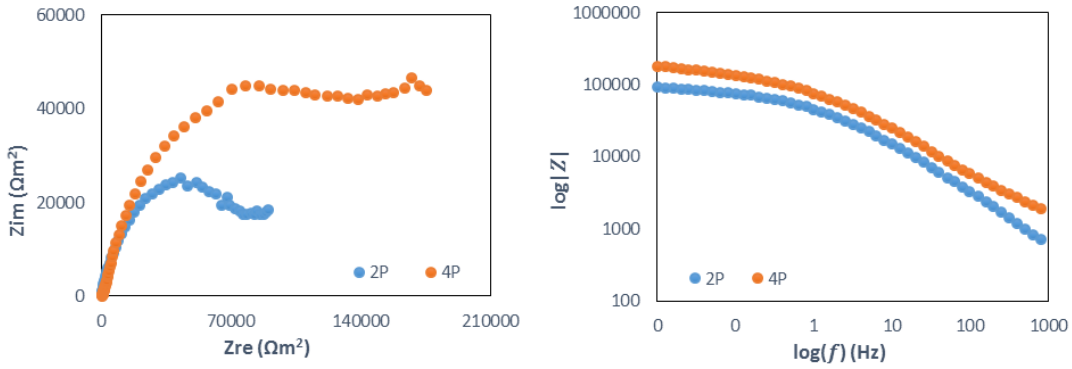

Figure 3.48 inhibitor effect for patinated samples 2P and 4P: Nyquist (left) and Bode (right) plots

As discussed in the previous paragraph, it is very important to provide to conservators also an approximate estimation of the actual corrosion rates, since the condition of the electrochemical measurements simulates a constantly wet surface, due to the continuous surface contact with the liquid electrolyte: this is not the real condition during outdoor exposure (Bartuli, Cigna et al. 1999; Schindelholz, Kellya et al. 2013). In order to estimate the corrosion rate of copper alloys exposed to the atmosphere, according to the previously discussed results, it is suggested to speculate an oxidation of bivalent copper (B = 60 mV/decade) and to multiply the result by the fraction of wetness. By using the meteorological data from Arpa Lombardia (www.arpalombardia.it), the fraction of wetness has been calculated about 0.38 for the city of Milan during the time exposure in orderto estimate corrosion rates (µm/y).

If the samples are not treated, corrosion rate is about 0.90 µm/y for 1N (not patinated, not treated, no inhibitor) and corrosion rate 4.0 µm/y for 1P (patinated, not treated, no inhibitor). In the worst cases, corrosion rate is estimated 7.4 µm/y for 10N (not patinated, Fluoline + BTA) and 88.8 µm/y for 12P (patinated, Fluoline + Sodium Oleate). Corrosion rates are two or three orders

of magnitude lower when protection is more effective, for example in case of 19N (not patinated, Triple layer, no inhibitor) that shows the lowest corrosion rate about 0.04 µm/y and 16P (patinated, Polylactic Acid mixed with BTA), which corrosion rate is about 0.10 µm/y.

- *electrochemical comparison*

Rp values have been compared to the ones collected before exposure in a previous research to test the durability of the protective coatings and their protection performances (Beltrami 2011; Bressan 2011).

The following graph shows the effect of urban exposure of reduction of the polarization resistance values obtained with EIS for patinated samples (**figure 3.49**). EIS values have been chosen instead of LPR ones, since this last technique was not able to characterize all the protectives before exposure, since they were too much insulating.

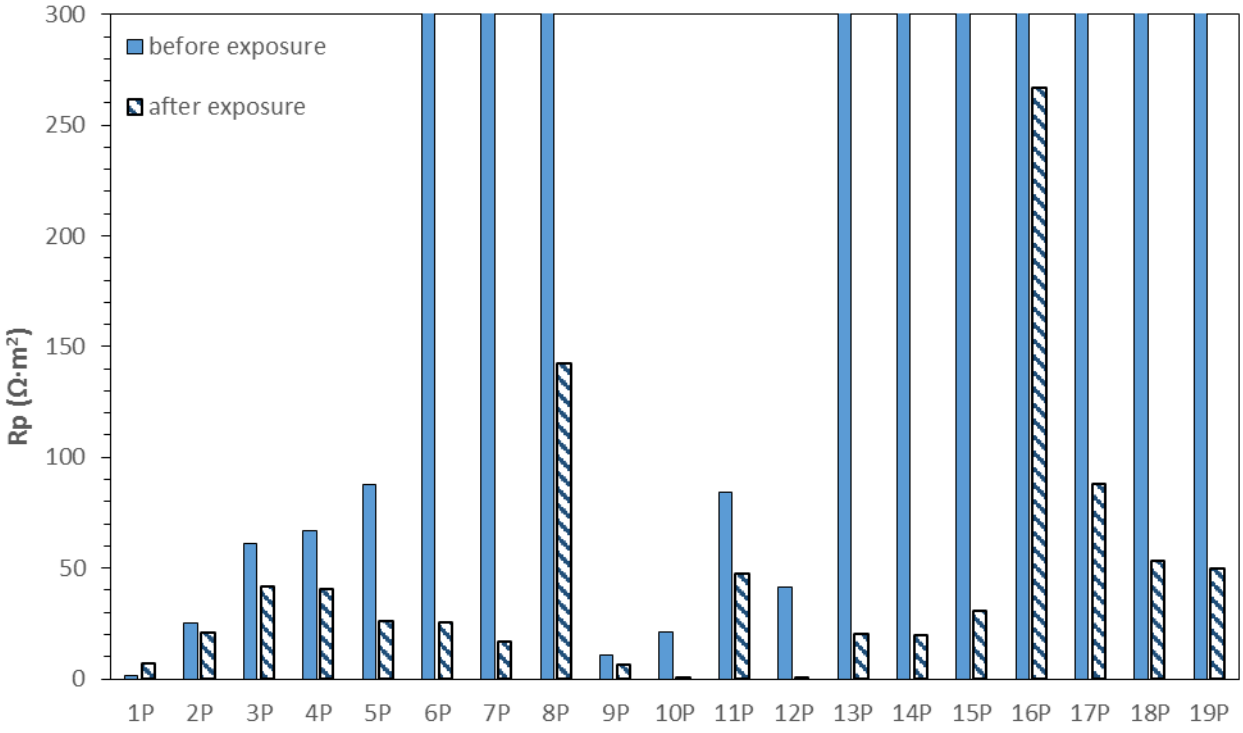

Figure 3.49 effect of urban environment on Rp values from EIS for all patinated samples

It is possible to note that the Rp values of all patinated samples decrease after exposure, since the interaction with the environment is responsible of the loss of efficiency and degradation of the protective coatings. The unique exception is represented by 1P: since this sample is not treated, it

can be ascribed to the fact that during exposure patina thickness increases, hindering corrosion process.

The same graph is represented for not patinated samples (**figure 3.50**).

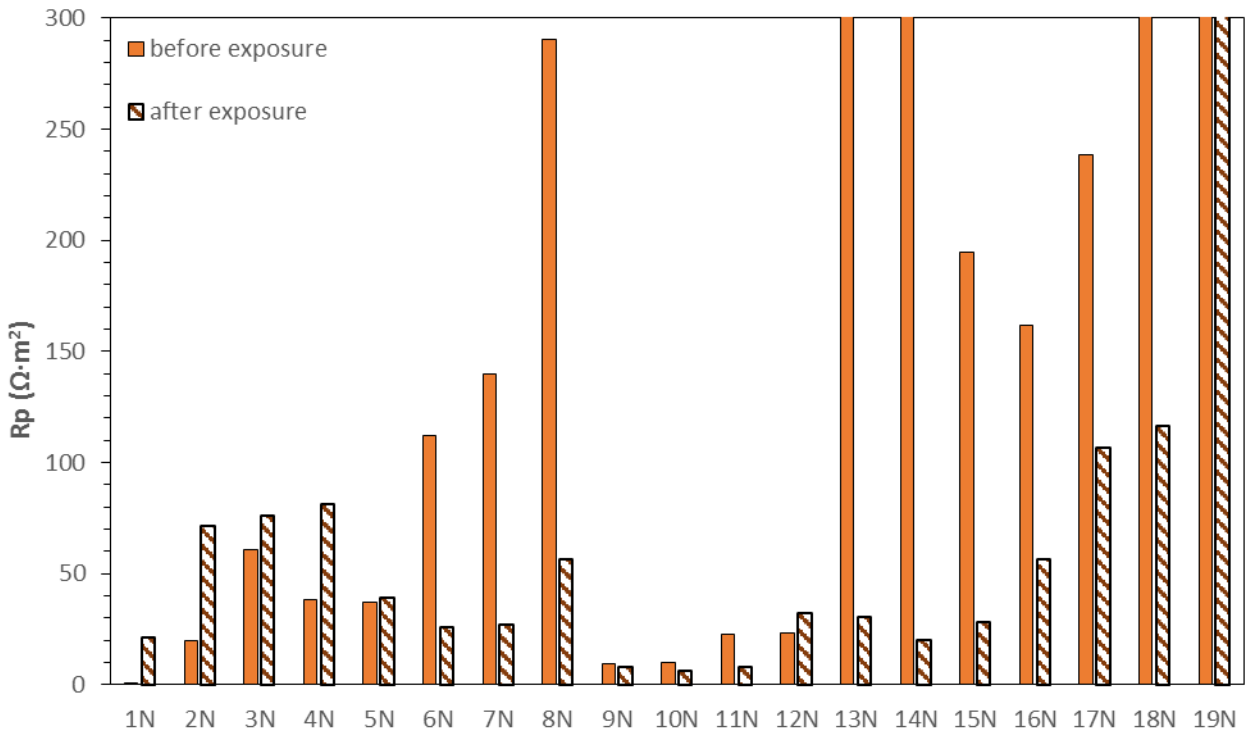

Figure 3.50 effect of urban environment on Rp values from EIS for all not patinated samples

In this case, it is possible to note that Rp values usually decrease after exposure with some exceptions, which are represented by those samples that show small Rp values before exposure, so for not very effective protective coatings. Many interpretations are possible. It is reasonable to think that the protectives were already flawed when applied or that measurements before and after exposure have been carried out in different areas of the samples surfaces. It is also possible to think that the formation of corrosion products has led to the obstruction of superficial cracks already existing or that during data collection some noises affect the measurements.

An important exception is represented by 1N: as in the case of 1P, since this sample is not treated, it is reasonable to think that during exposure corrosion products form a layer able to hinder corrosion process.

The Fluoline protective coating shows the worst behaviour of all, confirming the preliminary results before exposure (Beltrami 2011). Before exposure, the synergic effect with inhibitors in

some cases improved the treatment performances for both patinated and not patinated samples (**figure 3.51**). Indeed, before exposure, among not patinated samples 11N and 12N ensure a higher protection with respect to 9N in absence of inhibitor and 10N where BTA is combined with Fluoline. Among patinated samples, before exposure, Mercaptobenzothiazole on 11P and Sodium Oleate on 12P give a significant improvement of electrochemical behaviour; while BTA is responsible of a small increase of Rp values in the case of 10P.

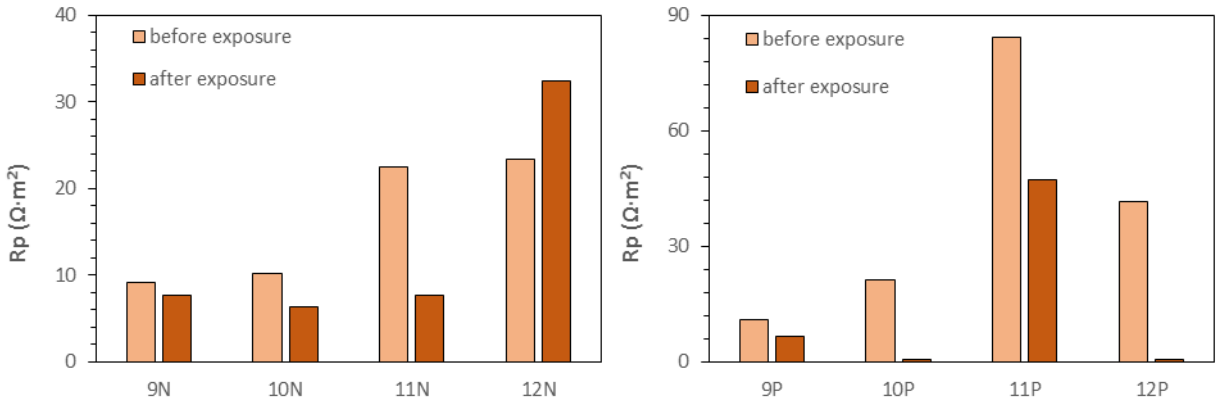

Figure 3.51 Fluoline performances for both not patinated (on the left) and patinated samples (on the right)

After exposure, all the Rp values are lower than the starting ones due to the degradation of the coatings, with exception for 12N. Indeed, the synergic effect of Fluoline and sodium oleate is responsible of good sample performances: Rp is one order of magnitude higher with respect to the others not patinated samples. In the case of patinated samples, although its Rp decreases after exposure, 11P that is treated with Fluoline combined with Mercaptobenzothiazole shows the best behaviour: Rp is one or two order of magnitudes higher with respect to the other samples.

Rp values for the treatments, which seemed to be very promising before exposure, drastically decrease, maybe to the degradation or to the lack of continuity of the coating itself. It has been very important to check the performances and the durability of protectives in order to evaluate which coating is the best after long lasting exposure. Indeed, treatments that guarantee the highest initial protection do not ensure the best protection after exposure. For example, the surface degradation and cracks observed on the protectives surface of 13N, 14N, 13P and 14P at previous stereomicroscope image (**figure 3.27**) and SEM images (**figure 3.34**, **3.36** and **3.37**) are responsible of a significant reduction in Rp values.

- *final considerations*

Among the patinated samples, 16P shows the best performances after two years exposure. It is treated with Polylactic Acid mixed with BTA. Indeed, it shows the highest Rp value (Rp = 267.05 $\Omega \cdot m^2$): even if Rp decreases after exposure, 16P ensures a good protection of the bronze substrate. It has also the lowest total colour variation (ΔE = 6.97). It means that the 27 months urban exposure do not alter too much the initial aesthetic appearance of the surface.

Among the not patinated samples, 19N is the best after two years exposure. It is treated with Triple layer protective coatings and no inhibitors are applied on the surface. It is very effective in protecting the bronze substrate from corrosion since it shows the highest Rp value (Rp = 564.60 $\Omega \cdot m^2$). It has also one of the smallest total colour variation among not patinated samples (ΔE = 8.97).

The objective of the analysis was also to test Polysiloxane coating, since it is commonly used for stone protection. It does not show good performances after exposure according to electrochemical behaviour: its protection was initially very promising in term of Rp values that significantly decreases after exposure. Degradation, detachments and surface cracks of the treatment, both with and without inhibitor, are also responsible of high global colour variations for 13N, 13P, 14N and 14P.

3.2.2 Stressed condition, the case study of "Mi fuma il cervello (Autoritratto)" by Alighiero Boetti

Fonderia Artistica Battaglia has provided all the bronze samples. They have been treated to create a patina made of ammonium sulfide, which simulates the one of the statue. The researches have been conducted in order to identify a protective commercial product that was able to create a resistant sacrificial layer, to ease the removal of the carbonate deposits and to preserve the aesthetic of the bronze substrate. One of the main problems is related to the fact that this restoration is not a definitive solution. Indeed, when the artwork is exposed again, carbonate crust will form once more, deteriorating the patina of bronze substrate.

The surveys have focused on three types of siliconic commercial paints (Talken, Dupli-Color, Saratoga), subjected to an accelerated ageing process of different duration (twenty-five hours, fifty hours and one-hundred hours) representative of the actual working condition.

The efficacy and durability of the protective coatings were evaluated by using non-destructive in-situ electrochemical techniques (LPR and EIS). The initial characterization and monitoring of the surface characteristics were performed by means of stereomicroscopy, scanning electron microscopy and colorimetric measurements.

The following table is a legend for the samples realized for the studies on the conservation of Alighiero Boetti statue (**table 3.9**).

Table 3.9 legend of specimens in stressed condition

Alighiero Boetti samples
P = Protective coating
R = Removed coating
PAXX = Protected sample, after XX hours Ageing
PAXX_C = Protected sample, after XX hours Ageing, after Cleaning
PAXX_CR = Protected sample, after XX hours Ageing, after Cleaning, after coating Removal

Two sets of samples have been made in order to analyze the siliconic paints used. The first set of samples has been subjected to an ageing procedure of twenty-five and fifty hours; the second set

of samples to a one-hundred hours ageing procedure, an amount of time more similar to the thermal stress of the statue during a real art exhibition.

Before use, the silicone paints need a heat-treatment, in order to have a proper cross-linking of the coating itself. This process has been applied only to the second set of samples, those exposed to the one-hundred ageing procedure. Indeed, before the protectives application, the second set has been processed by putting them in a stove for twenty hours at 50 °C before coating application in order to vouch for the complete superficial moisture evaporation that may be still present on the patinated surface and also by a further treatment of the same type in order to get the correct paint curing.

In the Cultural Heritage field, it is not always possible to subject an artwork to this kind of heat treatment in stove, due to the size of the piece or the location where the treatment has to be applied. For these reasons, it was important to verify the performances of these paints without thermal curing. The ageing time in this case was shorter because the coatings resulted already damaged after one hundred hours.

The coatings and the samples have been characterized before ageing by means of electrochemical measurements. LPR and EIS tests have been performed; the two techniques have provided similar trends and the results have been compared. The table below (**table 3.10**) reports the average Rp and the standard deviations obtained for all the samples before the ageing process by using electrochemical tests.

Table 3.10 initial Rp values for bronze samples without coatings

from LPR		**from EIS**	
average value ($\Omega \cdot m^2$)	**standard dev. ($\Omega \cdot m^2$)**	**average value ($\Omega \cdot m^2$)**	**standard dev. ($\Omega \cdot m^2$)**
1.34	0.64	0.87	0.50

The table below (**table 3.11**) reports Rp values obtained for all the samples after coatings application by using electrochemical tests.

Table 3.11 comparison of protectives Rp values

	protectives without curing		protectives with curing	
	Rp (Ω·m2) from LPR	**Rp (Ω·m2) from EIS**	**Rp (Ω·m2) from LPR**	**Rp (Ω·m2) from EIS**
Talken	20.56	17.18	-	2.34E+05
Dupli-Color	31.99	23.42	-	2.26E+05
Saratoga	310.90	275.85	-	2.37E+05

First two columns refer to protective treatments that have not been cured. As it can be observed, silicone paints are not able to adequately protect the metallic substrates from corrosion. If protective treatments are correctly cured at 50 °C for 20 hours, Rp values are three or four order of magnitude higher. It has been not possible to perform the LPR measurements on the cured protectives, because they are extremely insulating, as already mentioned in the previous paragraphs. The results of the three cured protectives are similar with regard to the order of magnitude and they have been analyzed by using EIS.

Referring to the approach used for the validation of electrochemical techniques, the fraction of wetness previously calculated around 0.28 for Milan can be used to estimate corrosion rates (µm/y) that are useful for conservators. The two electrochemical techniques provide similar results; only Rp values from EIS are taken into account. In order to estimate the corrosion rate of copper alloys exposed to the atmosphere, it is suggested to speculate an oxidation of bivalent copper (B = 60 mV/decade) and to multiply the result by the fraction of wetness. It is possible to estimate corrosion rate about 1.14 µm/y in the worst condition, when Talken paint is applied without curing. Corrosion rate is estimated 8.29E-05 µm/y in the best condition, if Saratoga paint is applied with proper curing. Without any protective treatment, corrosion rate will be higher and equal to 22.6 µm/y.

Colorimetric measurements have been performed; average values and standard deviations of L*, a* and b* parameters collected in SCI modality have been calculated before and after protective coatings application. Since only cured paints showed good protection from corrosion and better durability, only these samples are commented. They are showed in the following figure and they are collected by using stereomicroscope before and after protective application (**figure 3.52**). As it

is possible to see also by naked eye, protected samples appear brighter than the samples without protective coatings.

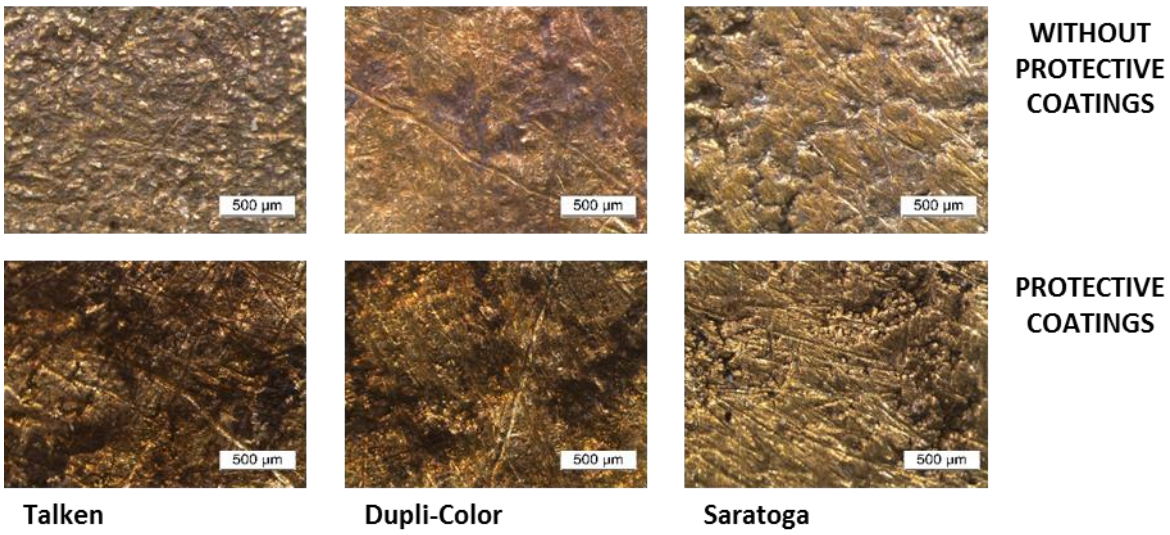

Figure 3.52 stereo microscope pictures showing protective application effect on samples with cured paints

The following figures (**figure 3.53**, **3.54** and **3.55**) represent the effect induced by the application of the protective treatments on the three colour parameters. Chromatic changes after protectives application are very small. Since L* decreases after application, ΔL values are negatives with the highest variation for Talken paint (ΔL = -2.43) and the smallest one for Saratoga paint (ΔL = -1.67). a* parameter increases after protective application for Talken paint (Δa = 0.80) and for Dupli-Color paint (Δa = 0.41). Δa = -0.08 for Saratoga paint, it is negligible. Since b* increases after coatings application, Δb values are positives with the highest variation for Dupli-Color paint (Δb = 1.90) and the smallest one for Talken paint (Δb = 1.36).

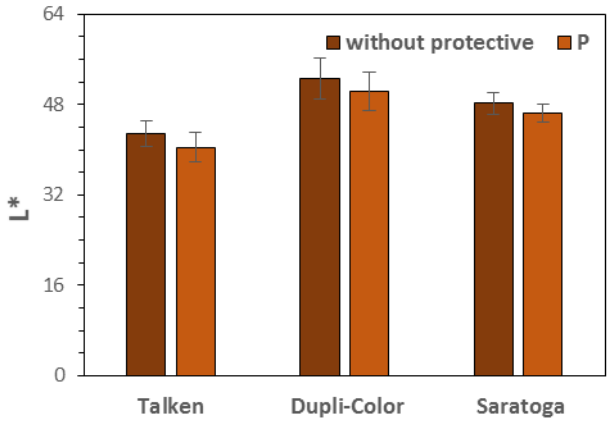

Figure 3.54 protective effect on L parameter*

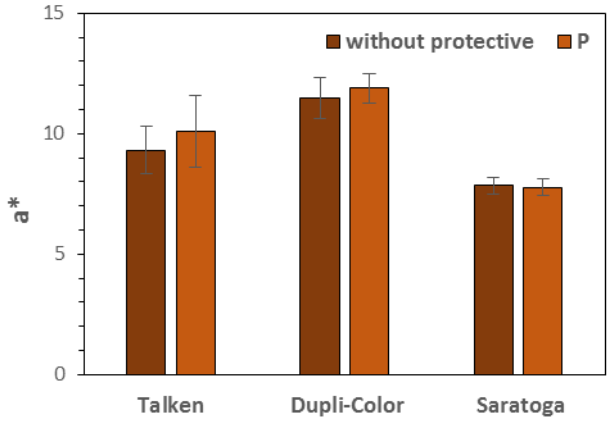

Figure 3.55 protective effect on a parameter*

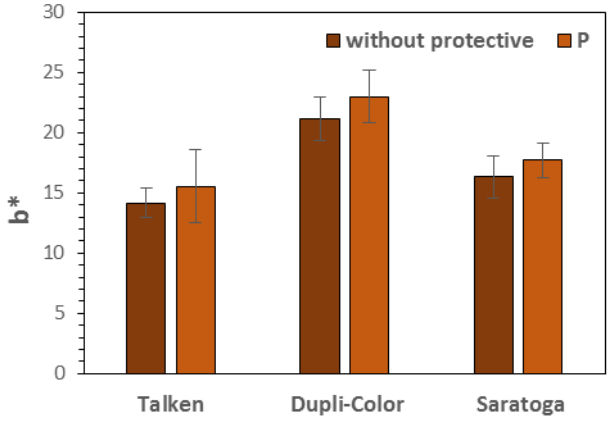

Figure 3.56 protective effect on b parameter*

ΔE values have been calculated too, according to the following formula:

$$\Delta E = \sqrt{(\Delta L^2 + \Delta a^2 + \Delta b^2)}$$

where ΔE is the total colour variation, ΔL the brightness variation, Δa and Δb the chromatic coordinates variation (**table 3.12**).

Table 3.12 global colour variation

	ΔE
Talken	2.90
Dupli-Color	2.93
Saratoga	2.17

Protectives application slightly changes chromatic characteristics of the surfaces. Indeed, ΔE values are below three, so they are not easily perceived by human eye: silicone paints are compatible with the aesthetical requirements for applications on the Cultural Heritage field. It means that coatings do not alter visual appearance. The best one is Saratoga that shows the lowest ΔE variation. Talken and Dupli-Color show very similar behavior.

Ageing process has been realized at three different duration: twenty-five hours, fifty hours and one-hundred hours. The samples have been exposed to similar conditions of the statue: pouring rain and heat (T = 400 °C for twenty-five and fifty hours ageing and T = 300 °C for one-hundred hours ageing). This ageing process leads to the formation of non-continuous carbonate deposits on the surface and to an alteration of surface appearance of the specimens, as in the statue. Indeed, surfaces are highly altered by thick and inhomogeneous superficial deposits. In the following figure (**figure 3.57**), samples with not cured paints are represented after twenty-five and fifty hours of ageing.

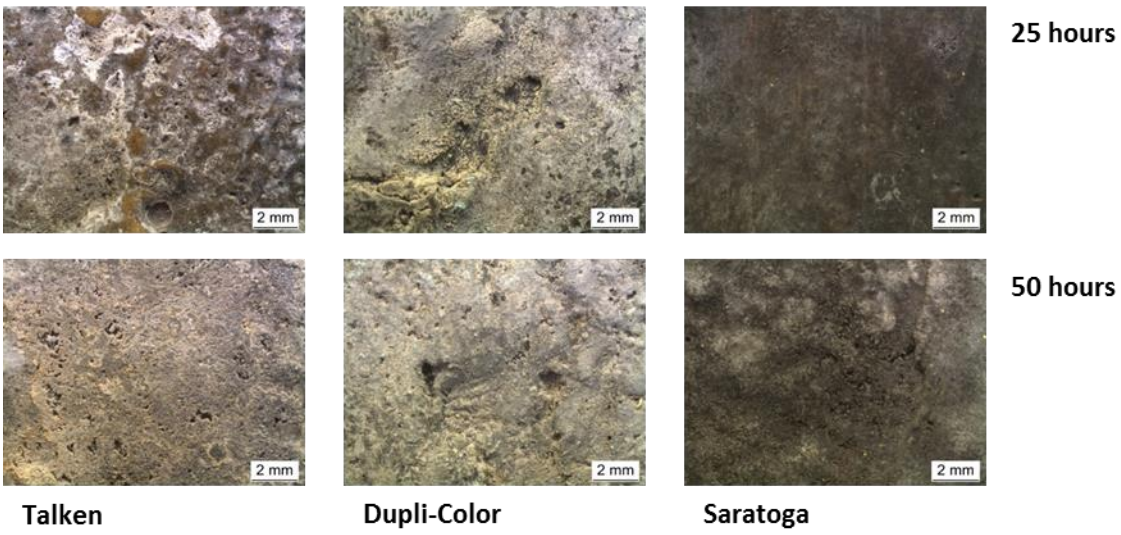

Figure 3.57 protective application effect on samples with cross-linked paints at 10x magnification

The following figure (**figure 3.58**) shows samples with different cured paints after one-hundred hours ageing.

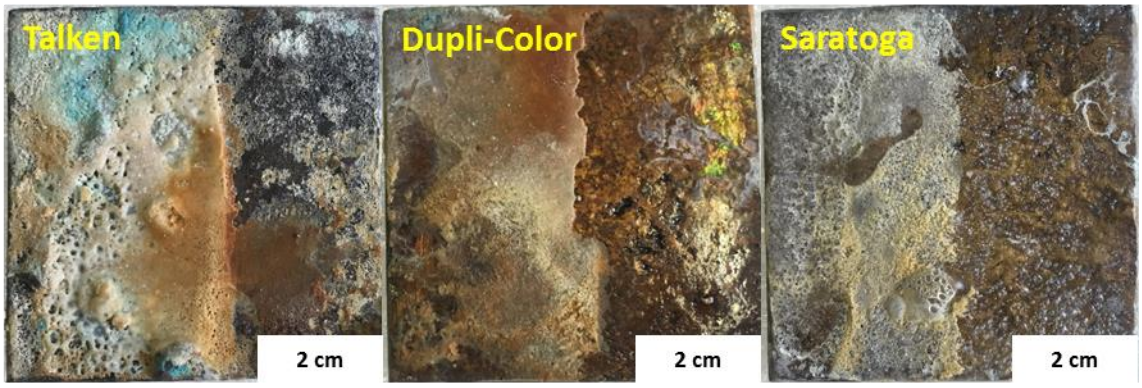

Figure 3.58 samples after one-hundred ageing and cleaning

This ageing process leads to the formation of a thick carbonate crust and to a fast degradation of silicon paints that suffer the same stressed condition in which the statue is. In the sample treated with Dupli-Color paint, carbonate deposits are not very adherent, in fact, they do not cover the entire surface and the crust is thinner. The sample treated with Talken paint shows the most adherent and thickest carbonate crust. Indeed, its removal is not complete.

Colorimetric measurements have been performed on one-hundred hours aged samples; average values and standard deviations of L*, a* and b* parameters collected in SCI modality have been calculated after ageing procedure and compared with the values before aging to evaluate colour

variations. The following graphs (**figure 3.59**, **3.60** and **3.61**) represent the effect induced by one-hundred hours ageing on the three colour parameters for the cured paints.

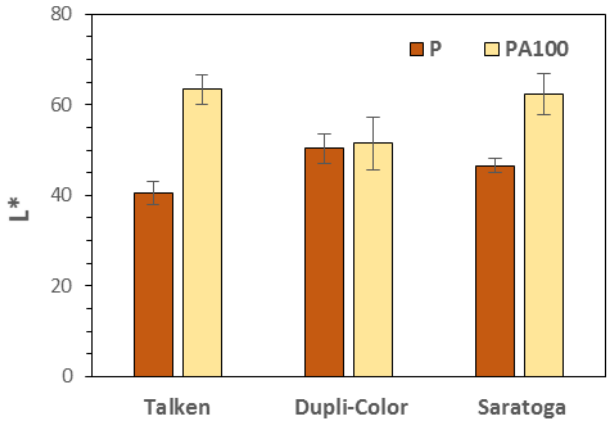

Figure 3.59 ageing effect on L parameter*

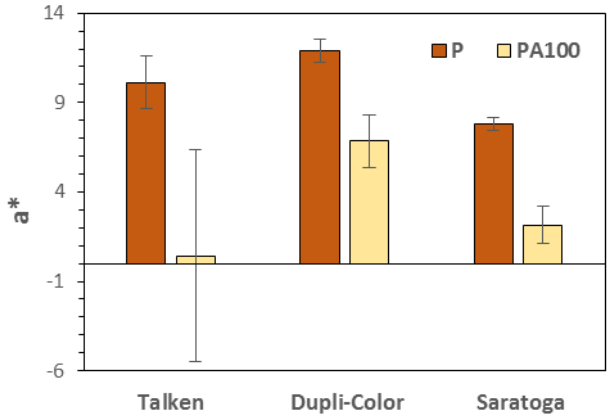

Figure 3.60 ageing effect on a parameter*

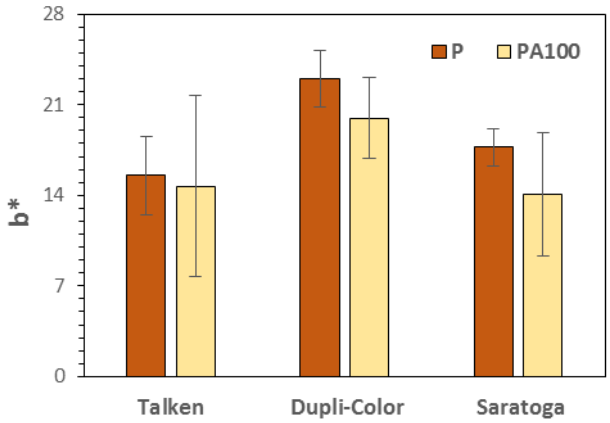

Figure 3.61 ageing effect on b parameter*

Standard deviations are significantly higher for the colorimetric parameters collected after ageing due to the inhomogeneity of the carbonate superficial deposits. Both b* and a* parameters decrease after ageing, while L* increases since the samples turn white. These effects can be ascribed to the formation of inhomogeneous superficial carbonate deposits. In the case of Talken paint, it seems that greenish corrosion products of copper form too.

ΔE values have been calculated too, according to the following formula:

$$\Delta E = \sqrt{(\Delta L^2 + \Delta a^2 + \Delta b^2)}$$

where ΔE is the total colour variation, ΔL the brightness variation, Δa and Δb the chromatic coordinates variation (**table 3.13**).

Table 3.13 global colour variation

	ΔE
Talken	24.92
Dupli-Color	5.98
Saratoga	17.15

Colour differences have been evaluated by considering aged (i.e., PA100) and protected samples (i.e., P) for each protective paint. Colorimetric measurements are in good agreement with visual observation. Indeed, Dupli-Color shows the smallest global colour variation, since carbonate deposits do not cover the entire surface and form a thin crust. A very high ΔE value has been calculated for Talken paint, since carbonate crust is very thick and greenish stains are visible on the surface.

The cleaning of the limescale has been realized using EDTA solution after the three different ageing processes in order to evaluate the removal efficacy and the durability of the paints. By observing stereomicroscope images, considering colorimetric measurements and comparing electrochemical results, it is possible to note that if the paint is not properly cured, it is not able to resist to the stressed condition of ageing. Indeed, the cleaning of limescale causes almost the complete removal of the protective layer (**figure 3.62**).

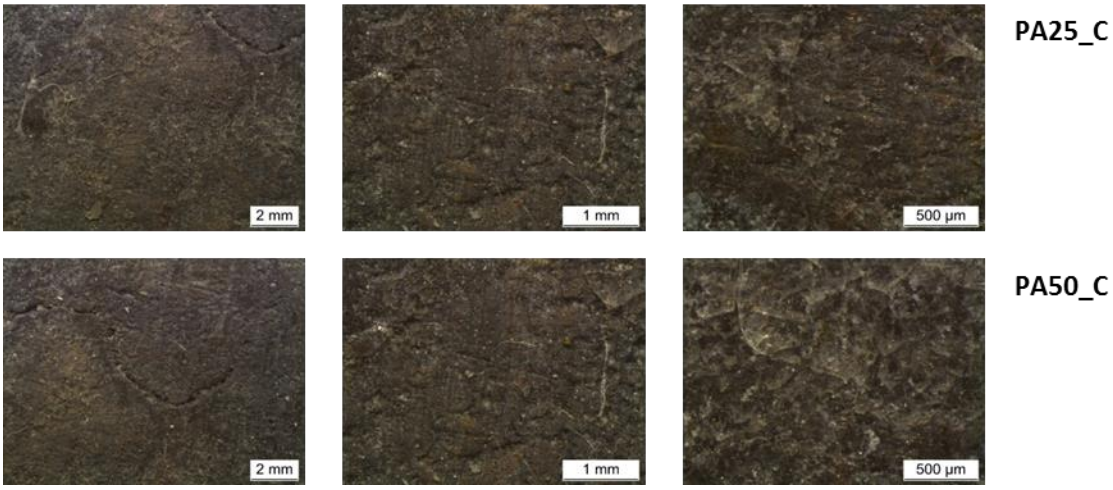

Figure 3.62 paint removal after calcareous crust cleaning after twenty-five and fifty hours ageing

In addition, the Rp values of the samples after limescale cleaning are very similar and close to the non-protected surface for all the samples (**figures 3.63**)**.** The fact that Rp values are of the same order of magnitude of the initial ones, confirms that the coatings have been heavily damaged by the ageing and do not provide anymore any protection against corrosion. As previously observed for validation of electrochemical techniques, when i_{corr} is high and Rp is low, LPR and EIS techniques give similar values.

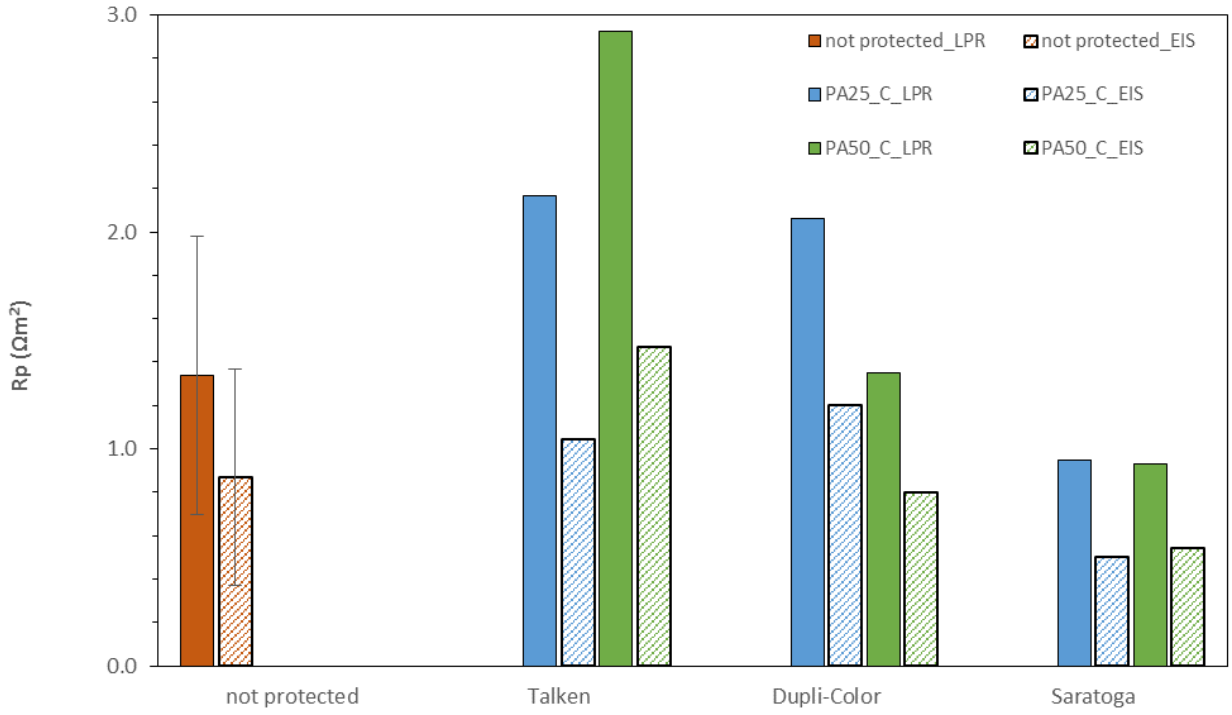

Figure 3.63 paint damaging after calcareous crust cleaning; Rp values from LPR and EIS

The behavior changes if the cured samples are considered after 100 hours ageing. Colorimetric measurements have been performed; average values and standard deviations of L*, a* and b* parameters collected in SCI modality have been calculated after limescale cleaning. In **table 3.14**, colour parameters after calcareous crust cleaning with EDTA solution are listed.

Table 3.14 colour parameters after cleaning

	average L*	standard deviation	average a*	standard deviation	average b*	standard deviation
Talken	42.48	5.77	4.69	2.88	13.89	5.84
Dupli-Color	41.55	4.62	8.39	1.26	11.71	3.41
Saratoga	45.89	3.05	5.47	0.85	12.00	1.81

These collected values have been compared to the initial ones of protected samples (i.e., P) to verify the protective alteration after cleaning of the carbonate layer and the ability of the sacrificial layer to help the removal of carbonates without modifying the bronze below. Colour variation are represented in the following table (**table 3.15**) and they are calculated between PA100_C and P samples.

Table 3.15 colour variations after cleaning

	ΔL	Δa	Δb	ΔE
Talken	2.73	-5.43	-1.64	6.02
Dupli-Color	-8.69	-3.50	-11.20	14.73
Saratoga	-0.66	-2.31	-5.71	6.19

By observing these chromatic variations, it is possible to note that the limescale cleaning does not allow a complete removal since the surface is altered even if protectives are applied.

SEM analysis shows that protectives are still present after ageing, but they are damaged and not continuous. **Figure 3.64** shows the three siliconic paints damaged after ageing procedure. It is possible to note the simultaneous presence of carbonate and paint in the sample treated with Talken paint. Superficial cracks are visible on sample treated with Dupli-Color paint. Bubbles formation is evident on sample treated with Saratoga paint.

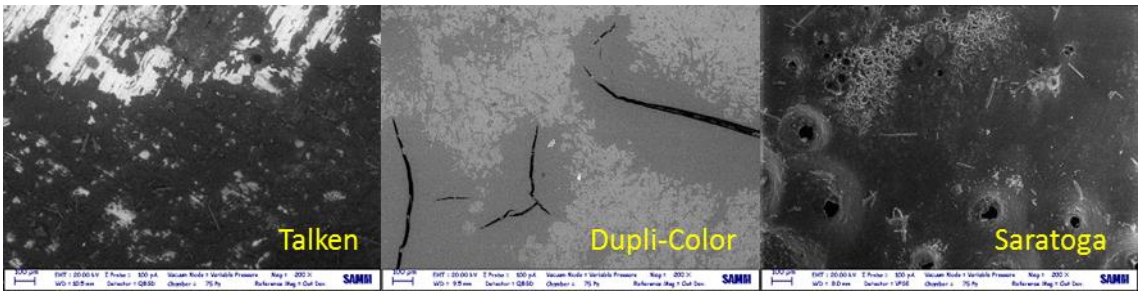

Figure 3.64 damaged and not continuous coatings after carbonate removal in SEM images

Descaling is much easier only when using Saratoga paint. The SEM images collected in VPSE and QBSD confirm that surface protected by Saratoga paint has very little residual of limescale crystals (**figure 3.65**).

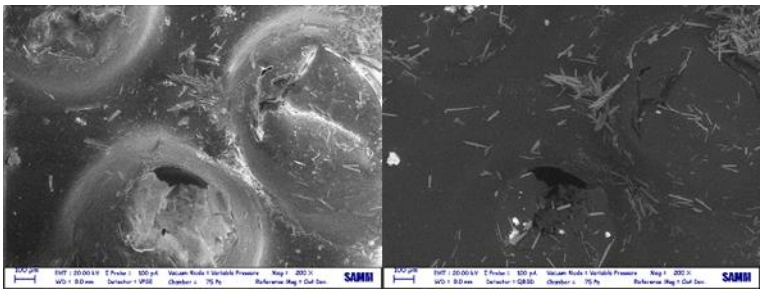

Figure 3.65 bubbles and residual calcareous crystals on bronze substrate treated with Saratoga

In the other two cases, the carbonate traces are more prominent after cleaning. The SEM images collected in QBSD show that the protective Dupli-Color film is not continuous due to the presence of cracks in different areas of the sample (**figure 3.66**).

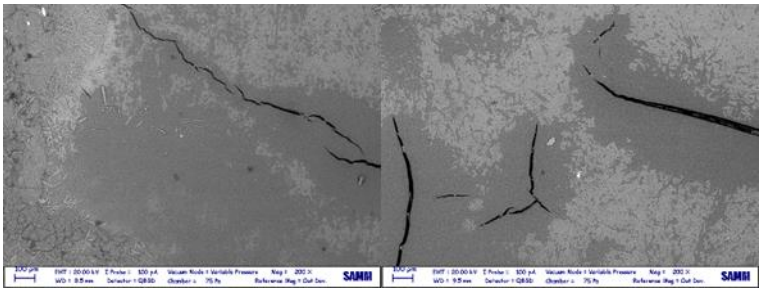

Figure 3.66 residual calcareous crust and protective cracks on bronze substrate treated with Saratoga

The presence of residual limescale is even more prominent on the sample when using Talken paint. The SEM images collected in VPSE and QBSD show that the limescale that can not be cleaned overlaps the protective layer (**figure 3.67**). The layer composition is highlighted in **figure 3.68**: the silicon that is the main element of the protective layers is spread overall examined area.

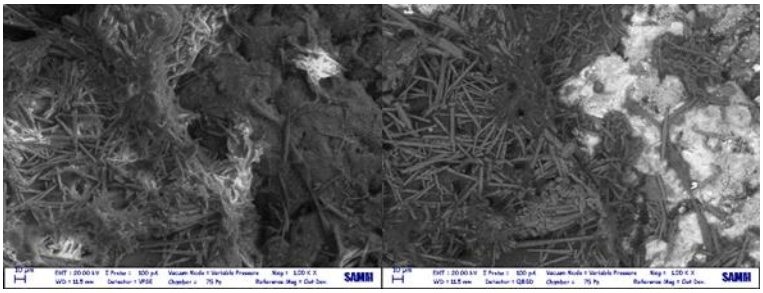

Figure 3.67 residual calcareous crust on bronze substrate treated with Talken

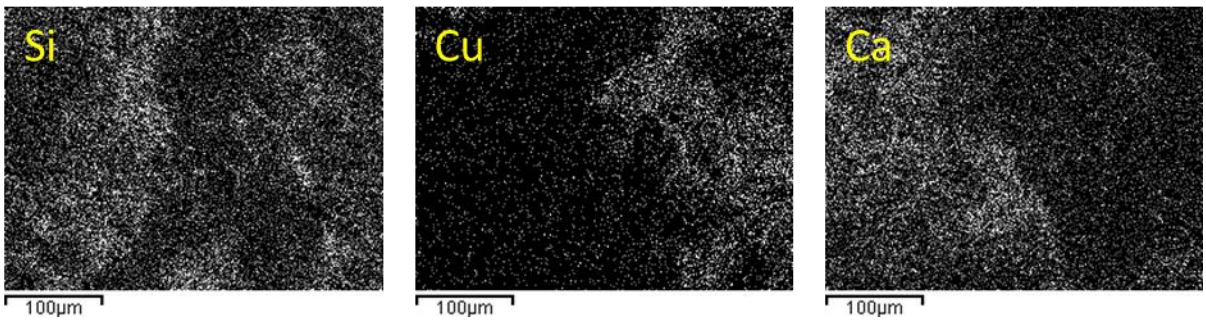

Figure 3.68 SEM-EDX of an area with residual calcareous crust

The ageing process reduces the protectiveness of the coatings, as demonstrated by electrochemical techniques. LPR and EIS show different durability of coatings after cleaning (**figure 3.69** and **3.70**). Saratoga paint shows the best performances after ageing, even if it is apparently the most damaged, indeed, superficial bubbles can be perceived at naked eye too.

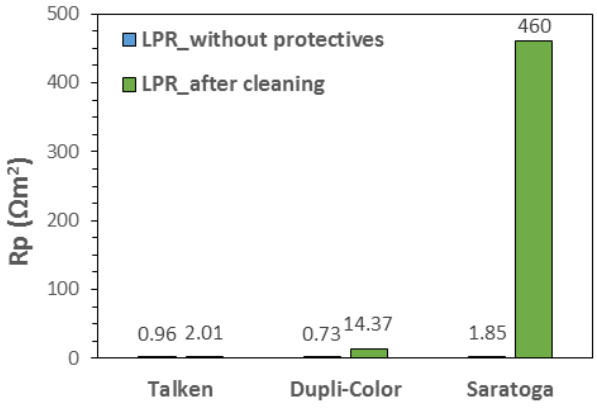

Figure 3.69 durability evaluation through LPR

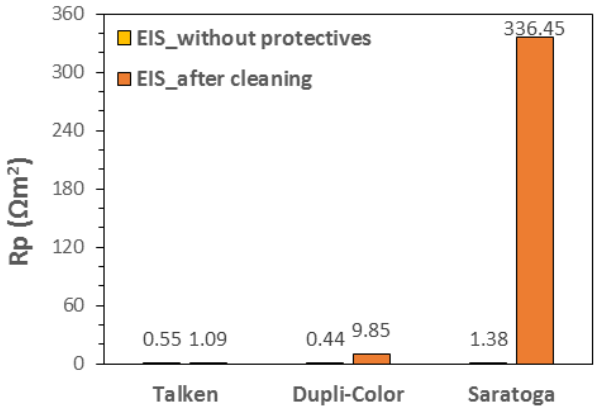

Figure 3.70 durability evaluation through EIS

The analysis suggests that the surface coatings are still present after the ageing procedure, although strongly deteriorated, as confirmed by the SEM images and Rp measurements. The electrochemical measurements claim that superficial coatings are not able to guarantee a protection of the substrate equal to the starting one. The surface coatings are thus mainly able to withstand high stress condition by forming a sacrificial layer that prevents the deterioration of bronze substrate, but do not guarantee a lasting protection against corrosion. However, in this specific case, corrosion was not the main issue, which was instead represented by the limescale deposits.

- *final considerations*

The purpose of this experimental work was to define an artwork preventive conservative methodology by individuating commercial paints able to facilitate carbonate layer removal, acting as a sacrificial layer, without altering the bronze below and to choose the one with the best performances in terms of removal ease, durability and protection against corrosion.
Results have shown that paints without a proper curing are not able to guarantee an adequate protection to the bronze substrate. These paints in fact show a deterioration due to the ageing procedure, so the carbonate cleaning leads to their removal. For this reason, it is necessary to use cured paints in these sorts of applications. In the case of “Mi fuma il cervello”, since the restoration has been directed in the Fonderia Artistica Battaglia laboratories, the cross-linking can be obtained with the use of infrared lamps (able to work up to 90 °C) on the specific points, like head and shoulders, that are the areas mostly affected by lime deposits.

This work, based on the use of electrochemical monitoring measurements and surface characterization techniques, allows identifying Saratoga paint as the best treatment in achieving the intended initial objectives. The first application of the protectives is not a discriminant factor, since the Rp values calculated from EIS are similar and none of the three coatings does not alter too much the surface aesthetic. By considering the one-hundred ageing procedure, Dupli-Color and Saratoga can be considered the best treatments, in fact their ΔE are lower than the Talken one. The limescale cleaning does not allow a complete removal and the smallest ΔE after cleaning have been calculated for Talken and Saratoga paints. SEM analysis shows that protectives are still present after ageing, but they are damaged and not continuous. Since Saratoga paint shows the

best electrochemical performances after ageing, even if it is apparently the most damaged due to the presence of superficial bubbles, it is considered as the best commercial paint. Indeed, descaling is much easier only when using Saratoga paint.

These results are very useful to define a preventive conservation of the bronze statue, by using a commercial product. As decided by laboratories of the Fonderia Artistica Battaglia, the protective treatment that is considered as the most adequate for this kind of application will be directly tested on the original artefact of Alighiero Boetti at the end of the actual art exhibition in which the statue is involved. Furthermore, the selected protective coating will be periodically monitored to understand the real effect of the ageing cycles on the paint performances and on the integrity of the substrate and to evaluate if it is necessary to reapply surface coatings in every future restoration.

CONCLUSIONS

CONCLUSIONS

The present analysis intended to achieve the following goals:

- validation of LPR and EIS techniques to verify their reliability to estimate corrosion rate
- realization of improved galvanic sensors, evaluation of their ability to estimate corrosion rate and of the possibility of using them also for the monitoring of patinated, but not gilded bronzes
- evaluation of the effectiveness of protectives and corrosion inhibitors applied on quaternary bronzes in two different condition (urban condition and stressed condition), using surface characterization and electrochemical monitoring techniques.

Environmental monitoring is extremely important for effective Cultural Heritage protection. The aim of in-situ non-destructive monitoring is to collect all the necessary data and information to allow conservators to decide accurate conservation strategies without altering surfaces integrity, to ensure the artwork condition to be stable in time and the speed of decay to be low or at least acceptable. Indeed, it is important to validate the methodology using gravimetric tests on samples exposed in the same condition.

In the first part of this work, monitoring techniques have been validated for two different situations.

For Cultural Heritage artefacts exposed in outdoor condition, LPR and EIS are commonly used. They have been compared in order to assess the effectiveness of in-situ measurements and provide an evaluation of the reliability of the results not only in terms of polarization resistance but also of corrosion rate.

LPR allows simple and fast measurements with higher reproducibility of results, but it cannot be applied on too much insulating coatings. EIS provides more information only if a proper equivalent circuit is individuated and it can be applied even with highly insulating coatings. Since it is difficult to find an equivalent circuit for the complex surfaces of metallic artefacts, its application is often limited to the Rp values calculation from the Bode curves.

Corrosion rate values obtained using electrochemical measurements are higher if compared to gravimetric measurements since the conditions of the electrochemical measurements simulate a constantly wet surface that does not represent the real condition for the outdoor exposed

samples that are subjected to T and RH variations. LPR and EIS provide similar results that are coherent with the mass losses by considering an oxidation of bivalent copper (B = 60 mV/decade, from literature) and the time of wetness (TOW), calculated using meteorological data.

LPR and EIS cannot be applied on gilded bronzes due to the difficulties on the interpretation of the results. By collecting the macro couple current flowing between the gold/bronze galvanic couple of the galvanic sensors that simulate real artefacts stratigraphy, it is possible to provide an estimation of the corrosion rate.

Galvanic sensors confirmed to be a powerful tool for monitoring corrosion rates on gilded bronzes. The new and improved sets of sensors seem to give reproducible and reliable signals.

Galvanic sensors have been validated in order to verify their ability to estimate corrosion rate and to try to apply them also on patinated, but not gilded bronzes. Mass losses have been calculated for both non-gilded and gilded samples. Since corrosion rates of gilded samples are slightly higher than not gilded ones, it will be possible to apply galvanic sensors also for the continuous monitoring of patinated or heavily corroded non-gilded bronzes without committing a significant error. Furthermore, normally it is very important to monitor variation on corrosion rate in order to detect immediately any change on the environment that may be harmful for the museum objects. The comparison between mass losses and galvanic current indicate that galvanic sensors underestimate the actual current density flowing between the gilding and the bronze. Further tests are required to evaluate better the entity of the underestimation.

Once the monitoring techniques have been validated, electrochemical tests in combination with surface characterization methods have been used to evaluate the efficiency of protective coatings and corrosion inhibitors in two different condition: urban condition and stressed condition.

The aim of the work was to test protectives effectiveness after exposure and identify the best treatment. The Fluoline protective coating shows the worst behaviour, confirming the preliminary results. In some cases, the synergic effect with inhibitors improved the treatment performances. Polylactic Acid mixed with BTA represents the best treatment among patinated samples; while the Triple layer protective coatings (Soter wax, Incral, Soter wax) applied without inhibitors is the best solution among not patinated samples.

In the present analysis, Polysiloxane coating has been tested too, since it is commonly used for stone protection. It does not show good performances after exposure: its protection was initially

very promising in term of Rp values that significantly decrease after exposure. The degradation of the treatment can be perceived at naked eye both in presence and in absence of inhibitor and it is responsible of high global colour variations.

The purpose of the experimental work on the Alighiero Boetti case study was to define an artwork preventive conservative methodology by individuating commercial paints able to facilitate carbonate layer removal, acting as a sacrificial layer, without altering the bronze below and to choose the one with the best performances in terms of removal ease, durability and protection against corrosion.

Results have shown that paints without a proper curing are not able to guarantee an adequate protection to the bronze substrate: indeed, they are deteriorated due to the ageing procedure, and so the carbonate cleaning leads to their removal.

Electrochemical monitoring measurements and surface characterization techniques allow identifying Saratoga paint as the best treatment in achieving the intended initial objectives. Indeed, after application, it does not alter the surface aesthetic. After the ageing procedure, it shows the best electrochemical performances. SEM analysis shows that protective is still present after ageing, even if it is damaged.

These results were very useful to define a preventive conservation commercial product that will be directly applied on the original artefact of Alighiero Boetti by Fonderia Artistica Battaglia conservators.

REFERENCES

REFERENCES

"<case of study - Rocca.pdf>."

8044, I. S. (1999). "ISO: Corrosion of metals and alloys-Basic terms and definitions."

Adriaens, A. and M. Dowsett (2008). "Time resolved spectroelectrochemistry studies for protection of heritage metals." Surface Engineering **24**(2): 84-89.

Afshari, V. and C. Dehghanian (2010). "Inhibitor effect of sodium benzoate on the corrosion behavior of nanocrystalline pure iron metal in near-neutral aqueous solutions." Journal of Solid State Electrochemistry **14**(10): 1855-1861.

Aldrovandi, A., C. Lalli, et al. (2005). "Ossevazione e documentazione delle alterazioni superficiali mediante microscopia ottica." impatto ambientale, monitoraggio sulle porte bronze del battistero di Firenze, workshop progetto battisero.

Angelini, E., S. Grassini, et al. (2006). "Potentialities of XRF and EIS portable instruments for the characterisation of ancient artefacts." Applied Physics A **83**(4): 643-649.

Bacci, M. (2005). "Indagini spettroscopiche non invasive per la valutazione delle alterazioni dei materiali." impatto ambientale, monitoraggio sulle porte bronze del battistero di Firenze, workshop progetto battisero.

Baer, N. S., C. Sabbioni, et al. (1989). "Science, Technology and European Cultural Heritage: Proceedings of the European Symposium." 198-200.

Balbo, A., C. Chiavari, et al. (2012). "Effectiveness of corrosion inhibitor films for the conservation of bronzes and gilded bronzes." Corrosion Science **59**: 204-212.

Bartuli, C., R. Cigna, et al. (1999). "Prediction of Durability for Outdoor Exposed Bronzes: Estimation of the Corrosivity of the Atmospheric Environment of the Capitoline Hill in Rome." Studies in Conservation **44**(4): 245-252.

Beltrami, R. (2011). "messa a punto e validazione di misure elettrochimiche in-situ su leghe di rame e valutazione dell'efficacia di protettivi."

Bracci, S. and L. Morassi Bonzi (2005). "Analisi elementale e documentazione morfologica delle superfici bronzee tramite ESEM." impatto ambientale, monitoraggio sulle porte bronze del battistero di Firenze, workshop progetto battisero.

Brambilla, L. (2011). Multianalytical approach for the study of bronze and gilded bronze artefacts. Dipartimento di Chimica Inorganica, Metallorganica e Analitica "L. Malatesta". Milan,

Università degli Studi di Milano, Facoltà di Scienze Matematiche, Fisiche e Naturali. **DOCTORATE SCHOOL IN CHEMICAL SCIENCES AND TECHNOLOGIES PhD course - CHEMICAL SCIENCES (XXIV cycle)**.

Bressan, E. (2011). "STUDIO DI UN SISTEMA ELETTROCHIMICO PER IL MONITORAGGIO DELL'EFFICACIA PROTETTIVA DI SOSTANZE COMMERCIALI PER LEGHE DI RAME."

Brunoro, G., A. Frignani, et al. (2003). "Organic films for protection of copper and bronze against acid rain corrosion." Corrosion Science **45**(10): 2219-2231.

Cagnini, A., S. Porcinai, et al. (2012). "Monitoraggio dello stato di conservazione all'interno della vetrina."

Cagnini, A., S. Porcinai, et al. (2012). "Sperimentazione per la protezione dei fattori ambientali."

Cano, E., D. M. Bastidas, et al. (2010). "Electrochemical characterization of organic coatings for protection of historic steel artefacts." Journal of Solid State Electrochemistry **14**(3): 453-463.

Cano, E. and D. Lafuente (2013). Corrosion inhibitors for the preservation of metallic heritage artifacts Corrosion and Conservation of Cultural Heritage Metallic Artefacts. P. Dillmann, D. Watkinson, E. Angelini and A. Adriaens, Elsevier Science. **65**.

Cano, E., D. Lafuente, et al. (2010). "Use of EIS for the evaluation of the protective properties of coatings for metallic cultural heritage: a review." Journal of Solid State Electrochemistry **14**(3): 381-391.

Casellato, U. (2005). "Determinazione di alcune alterazioni superficiali mediante metodi non invasivi: micro-FTIR e XRD per film sottili." impatto ambientale, monitoraggio sulle porte bronze del battistero di Firenze, workshop progetto battisero.

Colledan, A., A. Frignani, et al. (2005). INHIBITING TREATMENTS FOR OUTDOOR BRONZES. 10th European Symposium on Corrosion and Scale Inhibitors (10 SEIC), Ferrara, Italy.

Corvo, F., T. Pérez, et al. (2008). "Time of wetness in tropical climate: Considerations on the estimation of TOW according to ISO 9223 standard." Corrosion Science **50**(1): 206-219.

D'Orazio, M. and G. Cursio "Facciate in laterizio faccia a vista contro il bio-degrado: risultati analitici."

Degrigny, C. (2011). "Use of electrochemical techniques for the conservation of metal artefacts: a review ".

Degrigny, C., G. Guibert, et al. (2010). "Use of Ecorr vs time plots for the qualitative analysis of metallic elements from scientific and technical objects: the SPAMT Test Project."

Diamanti, M. V., Del Curto, B., Pedeferri, M. (2008). "Interference Colors of Thin Oxide Layers on Titanium." Wiley Periodicals, Inc. **33**(3): 221–228.

Dillmann, P., D. Watkinson, et al. (2013). Introduction: conservation versus laboratory investigation in the preservation of metallic heritage artefacts. Corrosion and Conservation of Cultural Heritage Metallic Artefacts. P. Dillmann, D. Watkinson, E. Angelini and A. Adriaens, Elsevier Science. **65**.

Doménech-Carbó, A., M. Lastras, et al. (2013). "Monitoring stabilizing procedures of archaeological iron using electrochemical impedance spectroscopy." Journal of Solid State Electrochemistry **18**(2): 399-409.

Ellingson, L. A., T. J. Shedlosky, et al. (2004). "The Use of Electrochemical Impedance Spectroscopy in the Evaluation of Coatings for Outdoor Bronze ".

EN, U. (2010). "UNI EN 15886."

Finsgar, M. and I. Milosev (2010). "Inhibition of copper corrosion by 1,2,3-benzotriazole: A review." Corrosion Science **52**(9): 2737-2749.

Finšgar, M. and I. Milošev (2010). "Inhibition of copper corrosion by 1,2,3-benzotriazole: A review." Corrosion Science **52**(9): 2737-2749.

Fiorentino, P. (1994). Restoration of the monument of Marcus Aurelius: facts and comments. Ancient and Historic Metals: Conservation and Scientific Research. D. A. Scott, J. Podany and B. B. Considine. Los Angeles, Getty Conservation Institute**:** 21-31.

Fiorentino, P. (2004). I problemi della manutenzione: quali sistemi di monitoraggio. Monumenti in bronzo all'aperto. Esperienze di conservazione a confronto. I. T. Paola Letardi, Giuseppe Cutugno. Firenze, Nardini Editore.

Fiorentino, P., M. Marabelli, et al. (1982). "The Condition of the 'Door of Paradise' by L. Ghiberti. Tests and Proposals for Cleaning." Studies in Conservation **27**(4): 145-153.

Gece, G. (2011). "Drugs: A review of promising novel corrosion inhibitors." Corrosion Science **53**(12): 3873-3898.

Goidanich, S., L. Brambilla, et al. (2011). "Galvanic sensors for monitoring corrosion rate of gilded bronzes."

Goidanich, S., D. Gulotta, et al. (2014). "Setup of Galvanic Sensors for the Monitoring of Gilded Bronzes." Sensors **14**(4): 7066-7083.

Goidanich, S., M. Ormellese, et al. (2006). Characterization and stability of artificial bronze patinas. VIII Convegno Nazionale AIMAT, Palermo, Italy.

Goidanich, S., S. Porcinai, et al. (2013). "LA CONSERVAZIONE DEI BRONZI DORATI, UNA VECCHIA PASSIONE DI PIETRO PEDEFERRI ".

Goidanich, S., L. Toniolo, et al. (2010). "Effects of wax-based anti-graffiti on copper patina composition and dissolution during four years of outdoor urban exposure." Journal of Cultural Heritage **11**(3): 288-296.

Goidanich, S., L. Toniolo, et al. (11-15 October 2010). Corrosion Evaluation of Ghiberti's "Porta Del Paradiso" in Three Display Environments. Metal 2010, International Conference on Metal Conservation, Interim meeting of the international council of museums committee for conservation metal working group, Charleston, South Carolina, USA, © 2010 Clemson University.

Grassini, S. (2013). Electrochemical impedance spectroscopy (EIS) for the in-situ analysis of metallic heritage artefacts Corrosion and Conservation of Cultural Heritage Metallic Artefacts. P. Dillmann, D. Watkinson, E. Angelini and A. Adriaens, Elsevier Science. **65**.

GUILMINOT, E., J.-J. RAMEAU, et al. (2000). "Benzotriazole as inhibitor for copper with and without corrosion products in aqueous polyethylene glycol." Journal of Applied Electrochemistry **30**: 21-28.

Hoffmann, G. (2009). "CIELab Color Space."

Hughes, R. and M. Rowe (1997). The colouring, bronzing and patination of metals, Thames and Hudson.

Hunter (2008). "Insight of Color: L, a, b versus CIE 1976 L*a*b." **13**(2).

Ingo, G. M., E. Angelini, et al. (2004). "Combined use of XPS and SEM+ EDS for the study of surface microchemical structure of archaeological bronze Roman mirrors." Surface and Interface Analysis **36**(8): 871-875.

Ingo, G. M., E. Angelini, et al. (2004). "Microchemical investigation of archaeological copper-based artefacts used for currency in ancient Italy before the coinage." Surface and Interface Analysis **36**(8): 866-870.

Ingo, G. M., I. Calliari, et al. (2000). "Microchemical study of the corrosion products on ancient bronzes by means of glow discharge optical emission spectrometry." SURFACE AND INTERFACE ANALYSIS **30**: 264-268.

ISO9223:2012(E) (2012). "Corrosion of metals and alloys - Corrosivity of atmospheres . Classification, determination and estimation."

Joseph, E., P. Letardi, et al. (2007). Innovative treatments for the protection of outdoor bronze monuments. Metal 07, Interim meeting of the ICOM-CC Metal WG, Amsterdam, ICOM.

Kiele, E., J. Lukseniene, et al. (2014). "Methyl–modified hybrid organic-inorganic coatings for the conservation of copper." Journal of Cultural Heritage **15**(3): 242-249.

Letardi, P. (2002). Outdoor bronze protective coatings: characterisation by a new contact-probe Electrochemical Impedance measurements technique The Science of Art. Padova, Edizioni Libreria Progetto di Padova**:** 173-178.

Letardi, P. (2004). Misure elettrochimiche per la caratterizzazione e il monitoraggio del potere protettivo di patine e rivestimenti: la tecnica EIS. Monumenti in bronzo all'aperto. Esperienze di conservazione a confronto. P. Letardi, I. Trentin and G. Cutugno. Firenze, Nardini Editore.

Letardi, P. (2013). Electrochemical measurements in the conservation of metallic heritage artefacts: an overview Corrosion and Conservation of Cultural Heritage Metallic Artefacts. P. Dillmann, D. Watkinson, E. Angelini and A. Adriaens, Elsevier Science. **65**.

Leyssens, K., A. Adriaens, et al. (2005). "Simultaneous in situ time resolved SR-XRD and corrosion potential analyses to monitor the corrosion on copper." Electrochemistry Communications **7**(12): 1265-1270.

Li, C., Y. Ma, et al. (2010). "EIS monitoring study of atmospheric corrosion under variable relative humidity." Corrosion Science **52**(11): 3677-3686.

Li, S., Y.-G. Kim, et al. (2007). "Application of steel thin film electrical resistance sensor for in situ corrosion monitoring." Sensors and Actuators B: Chemical **120**(2): 368-377.

M. Saheb, D. N., P. Dillmann, M. Descostes, H. Matthiesen (2013). Long-term anoxic corrosion of iron. Corrosion and Conservation of Cultural Heritage Metallic Artefacts. P. Dillmann, D. Watkinson, E. Angelini and A. Adriaens, Elsevier Science. **65**.

MacLeod, I. D. (2013). Monitoring, modelling and prediction of corrosion rates of historical iron shipwrecks Corrosion and Conservation of Cultural Heritage Metallic Artefacts. P. Dillmann, D. Watkinson, E. Angelini and A. Adriaens, Elsevier Science. **65**.

Marušić, K., H. O. Ćurković, et al. (2011). "Inhibiting effect of 4-methyl-1-p-tolylimidazole to the corrosion of bronze patinated in sulphate medium." Electrochimica Acta **56**(22): 7491-7502.

Mathis, F., J. Salomon, et al. (2013). Corrosion patina or intentional patina: contribution of non-destructive analysis to the surface study of copper-based archaeological objects Corrosion

of Metallic Heritage Artefacts. P. Dillmann, G. Beranger, P. Piccardo and H. Matthiesen, Woodhead Publishing Limited. **48**.

Matteini, M. (2005). "Monitoraggio dell'impatto ambientale sulle Porte bronze del Battistero di Firenze " Impatto ambientale, monitoraggio sulle porte bronze del battistero di Firenze, workshop progetto battisero.

Matthiesen, H. (2013). Oxygen monitoring in the corrosion and preservation of metallic heritage artefacts Corrosion and Conservation of Cultural Heritage Metallic Artefacts. P. Dillmann, D. Watkinson, E. Angelini and A. Adriaens, Elsevier Science. **65**.

Matthiesen, H., D. Gregory, et al. (2013). Long-term corrosion of iron at the waterlogged site of Nydam in Denmark: studies of environment, archaeological artefacts, and modern analogues Corrosion of Metallic Heritage Artefacts. P. Dillmann, G. Beranger, P. Piccardo and H. Matthiesen, Woodhead Publishing Limited. **48**.

Mazza, B., P. Pedeferri, et al. (15-19 September 1975). Effectiveness of Some Inhibitors on the Atmospheric Corrosion of Gold Plated Bronzes. 4th European Symposium on Corrosion Inhibitors, Ferrara.

Mazza, B., P. Pedeferri, et al. (1977). "Behaviour of a galvanic cell simulating the atmospheric corrosion conditions of gold plated bronzes " Corrosion Science **17**(6): 535-541.

Modrone, B. V. d. (2008). Fonderia Artistica Battaglia. I. G. S. s.r.l., Elsevier Science. **65**.

Monnier, J., I. Guillot, et al. (2013). Reactivity studies of atmospheric corrosion of heritage iron Corrosion and Conservation of Cultural Heritage Metallic Artefacts. P. Dillmann, D. Watkinson, E. Angelini and A. Adriaens, Elsevier Science. **65**.

Neff, D. R., S. Dillmann, P. (2013). Analytical techniques for the study of corrosion of metallic heritage artifacts: from micrometer to nanometer scales. Corrosion and Conservation of Cultural Heritage Metallic Artefacts. P. Dillmann, D. Watkinson, E. Angelini and A. Adriaens, Elsevier Science. **65**.

Norberg, P. (20012). "Surface Moisture and Time of Wetness Measurements." American Chemical Society: 23-36.

Oddy, A. (2000). A History of Gilding with Particular Reference to Statuary. GILDED METALS History, Technology and Conservation. T. Drayman-Weisser, Archetype Publications.

Odnevall Wallinder, I., S. Bertling, et al. (2004). "Environmental interaction of copper and zinc released from building materials as a result of atmospheric corrosion." Metall **58**(11): 717-720.

Odnevall Wallinder, I., S. Bertling, et al. (2004). "Predictive models of copper runoff from external structures." Journal of Environmental Monitoring **6**(8): 704-712.

Odnevall Wallinder, I., Y. Hedberg, et al. (2009). "Storm water runoff measurements of copper from a naturally patinated roof and from a parking space. Aspects on environmental fate and chemical speciation." Water Research **43**(20): 5031-5038.

Odnevall Wallinder, I., Korpinen, T., Sundberg, R , and Leygraf, C (2002). Atmospheric Corrosion of Naturally and Pre-Patinated Copper Roofs in Singapore and Stockholm - Runoff Rates and Corrosion Product Formation. Outdoor Atmospheric Corrosion, ASTM STP 1421**:** 230-244.

Odnevall Wallinder, I. and C. leygraf (1997). "A study of copper runoff in an urban atmosphere." Corrosion Science **39**(12): 2039-2052.

Otmacic, H. (2003). "Copper corrosion inhibitors in near neutral media." Electrochimica Acta **48**(8): 985-991.

Parvis, M. (2013). Issues in environmental monitoring of metallic heritage Corrosion and Conservation of Cultural Heritage Metallic Artefacts. P. Dillmann, D. Watkinson, E. Angelini and A. Adriaens, Elsevier Science. **65**.

Pedeferri, P. and A. Cigada (1993). Elementi di corrosione e protezione dei materiali metallici, CittàStudi.

Piccardo, P. (2013). istic patinas on ancient bronze statues Corrosion and Conservation of Cultural Heritage Metallic Artefacts. P. Dillmann, D. Watkinson, E. Angelini and A. Adriaens, Elsevier Science. **65**.

Pons, E., C. Lemaitre, et al. (2013). Electrochemical study of steel artifacts from Wolrd War I: contribution of AC impedance spectroscopy and chronoamperometry to describe the behaviour of the corrosion layers Corrosion of Metallic Heritage Artefacts. P. Dillmann, G. Beranger, P. Piccardo and H. Matthiesen, Woodhead Publishing Limited. **48**.

Prosek, T., M. Kouril, et al. (2013). "Real-time monitoring of indoor air corrosivity in cultural heritage institutions with metallic electrical resistance sensors." Studies in Conservation **58**(2): 117-128.

Reguer, S., P. Dillmann, et al. (2013). Contribution of local and structural characterization for studies of the corrosion mechanisms related to the presence of chlorine on archaeological ferrous artefacts Corrosion of Metallic Heritage Artefacts. P. Dillmann, G. Beranger, P. Piccardo and H. Matthiesen, Woodhead Publishing Limited. **48**.

Rocca, E. and F. Mirambet (2013). Corrosion inhibitors for metallic artefacts: temporary protection Corrosion of Metallic Heritage Artefacts. P. Dillmann, G. Beranger, P. Piccardo and H. Matthiesen, Woodhead Publishing Limited. **48**.

Sadat-Shojai, M. and A. Ershad-Langroudi (2009). "Polymeric Coatings for Protection of Historic Monuments: Opportunities and Challenges." Journal of Applied Polymer Science **112**(4): 2535-2551.

Said, M., N. Azura, et al. (2011). "Fabrication and Electrochemical Characterization of MicroandNanoelectrode Arrays for Sensor Applications ".

Scendo, M. (2007). "Inhibitive action of the purine and adenine for copper corrosion in sulphate solutions." Corrosion Science **49**(7): 2985-3000.

Scendo, M. (2008). "The influence of adenine on corrosion of copper in chloride solutions." Corrosion Science **50**(7): 2070-2077.

Schindelholz, Kellya, et al. (2013). "Comparability and accuracy of time of wetness sensing methods relevant for atmospheric corrosion." corrosion science **67**.

Scott, D. A. (2013). The use of metallographic and metallurgical investigation methods in the preservation of metallic heritage artefacts. Corrosion and Conservation of Cultural Heritage Metallic Artefacts. P. Dillmann, D. Watkinson, E. Angelini and A. Adriaens, Elsevier Science. **65**.

Sherif, E., A. Elshamy, et al. (2007). "5-(Phenyl)-4H-1,2,4-triazole-3-thiol as a corrosion inhibitor for copper in 3.5% NaCl solutions." Materials Chemistry and Physics **102**(2-3): 231-239.

Sherif, E. and S. Park (2006). "2-Amino-5-ethyl-1,3,4-thiadiazole as a corrosion inhibitor for copper in 3.0% NaCl solutions." Corrosion Science **48**(12): 4065-4079.

Sjogren, L. and N. Le Bozec (2013). On-line corrosion monitoring of indoor atmospheres. Corrosion of Metallic Heritage Artefacts. P. Dillmann, G. Beranger, P. Piccardo and H. Matthiesen, Woodhead Publishing Limited. **48**.

Squarcialupi, M. C. and F. Burrini (2005). "Stato di avanzamento del progetto." impatto ambientale, monitoraggio sulle porte bronze del battistero di Firenze, workshop progetto battisero.

Stern and Weisert "Experimental observations on the relation between Rp and corrosion rate."

Tidblad, J. (2013). Atmospheric corrosion of heritage metallic artefacts: processes and prevention. Corrosion and Conservation of Cultural Heritage Metallic Artefacts. P. Dillmann, D. Watkinson, E. Angelini and A. Adriaens, Elsevier Science. **65**.

Watkinson, D. (2013). Conservation, corrosion science and evidence-based preservation strategies for metallic heritage artefacts. Corrosion and Conservation of Cultural Heritage Metallic Artefacts. P. Dillmann, D. Watkinson, E. Angelini and A. Adriaens, Elsevier Science. **65**.

www.arpalombardia.it.

Zhang (2002). "Corrosion Science." 2131-2151.

Zhang, X. Y., W. L. He, et al. (2002). "Determination of instantaneous corrosion rates and runoff rates of copper from naturally patinated copper during continuous rain events." Corrosion Science **44**(9): 2131-2151.